

Fast Thermalization from the Eigenstate Thermalization Hypothesis

Chi-Fang Chen^{1,*} and Fernando G.S.L. Brandão^{1,2}

¹*Institute for Quantum Information and Matter,
California Institute of Technology, Pasadena, CA, USA*
²*AWS Center for Quantum Computing, Pasadena, CA*

The Eigenstate Thermalization Hypothesis (ETH) has played a major role in explaining thermodynamic phenomena in quantum systems. However, so far, no connection has been known between ETH and the timescale of thermalization. In this paper, we rigorously show that ETH indeed implies fast thermalization to the global Gibbs state.

We show fast convergence for two models of thermalization. In the first, the system is weakly coupled to a bath of (quasi)-free Fermions that we control. We derive a finitely-resolved version of Davies' generator, with explicit error bounds and resource estimates, that describes the joint evolution at finite times. The second is Quantum Metropolis Sampling, a quantum algorithm for preparing Gibbs states on a quantum computer. In both cases, no guarantee for fast convergence was previously known for non-commuting Hamiltonians, partly due to technical issues with a finite energy resolution.

The critical feature of ETH we exploit is that the Hamiltonian can be modeled by random matrix theory below a sufficiently small energy scale. We show this gives quantum expander at nearby eigenstates of the Hamiltonian. This then implies fast convergence to the global Gibbs state by mapping the problem to a one-dimensional classical random walk on the spectrum of the Hamiltonian. Our results explain finite-time thermalization in chaotic open quantum systems and suggest an alternative formulation of ETH in terms of quantum expanders, which we confirm numerically for small systems.

CONTENTS

I. Introduction	2
A. Main Results	3
1. Davies' Generator at Finite Resources (Section III)	3
2. ETH Implies Fast Convergence of the Finitely-Resolved Davies' Generator (Section V)	5
3. ETH Implies Fast Convergence of Quantum Metropolis Sampling (Section VII)	6
B. Discussion	6
1. Convergence to the Global Gibbs State	6
2. ETH Gives Quantum Expanders at Nearby Energies	7
3. Global Convergence From a Random Walk on the Spectrum	8
4. Implications to Quantum Algorithms	8
5. Open Questions	8
C. Acknowledgments	8
II. Davies' Generator	9
A. The Weak-Coupling Limit with Infinite Time and Bath	9
B. The Advertised Form of Finitely-resolved Davies' Generator	10
1. The fixed point	10
C. The Quasi-free Fermionic Bath	11
1. Choosing a bath	11
III. Main Result I: Implementing Davies with Finite Resources	13
A. Proof of Finitely-resolved Davies' Generator (Theorem III.1)	14
1. The interaction picture	15
2. From a finite to an infinite bath	16
3. Rounding the spectrum	17
4. Infinite time limit	17
5. The secular approximation	18
IV. Preliminaries for Proofs of Fast Convergence	20
A. Modified Log Sobolev Inequality	20
B. Assumptions for the Eigenstate Thermalization Hypothesis and the Density of States	21

* chifang@caltech.edu

1. ETH	21
2. The density of states	22
3. Example: Gaussian density of state	23
C. Properties of finite-resolved Davies' generator	24
D. Quantum expanders	26
 V. Main Result II: Finitely-resolved Davies Convergences to Approximate Gibbs State	26
A. Local Gap and MLSI Estimates: ETH Gives Quantum Expanders (block-diagonal Inputs)	27
1. The Expected Lindbladian	28
2. Concentration around the expectation	29
3. Proof of Lemma V.3	30
B. Local to Global	31
1. Calculations for the random walk gap λ_{RW}	33
C. Off-block-diagonal Inputs	33
D. Proof of Theorem V.1	34
E. Comments on Non-diagonal $\gamma_{ab}(\bar{\omega})$.	34
F. Resource estimates	35
G. Comments on Optimality	35
1. Resource costs	36
 VI. Quantum Metropolis Sampling	36
A. Warmup: Perfect Energy Resolution	36
B. Explicit CPTN Map with Realistic Phase Estimation	37
C. Approximate Detailed Balance.	38
 VII. Main Result III: ETH Implies Fast Convergence of Quantum Metropolis	41
A. Proof Outline	42
1. Convergence with approximate detailed balance	42
2. The gap of the trace-non-increasing CP map	42
B. Local Properties	43
1. The expectation	43
2. Concentration	43
C. The Global Gap of the Self-adjoint Component \mathcal{N}_H .	44
1. The choice of $p(\bar{\nu}_1)$	44
2. The second eigenvalue $\lambda_2(\mathcal{N}_{1,H})$	46
D. Proof of Theorem VII.1	47
1. Proof of Proposition VII.1.2	48
E. Resource Estimates	49
References	49
 A. Gaussian Calculations	50
 B. Conductance Calculation	52
1. The 1d Random Walk with Gaussian Density of state	53
a. The Markov chain from the Lindbladian	53
b. The Markov chain from Metropolis sampling	55
 C. Numerical tests of expander properties	56
1. The gap of the Lindbladian	56
2. The deviation	56

I. INTRODUCTION

Thermodynamic phenomena are ubiquitous in nature but highly non-obvious to analyze from first principles. Therefore, to make progress, we often make assumptions that have strong explanatory power. An influential one in quantum thermodynamics is the Eigenstate Thermalization Hypothesis (ETH) [1, 2]. It states that thermalization happens at the level of individual eigenstates of the Hamiltonian and that random matrix theory (RMT) can model well the Hamiltonian at sufficiently small energy intervals. The folklore suggests ETH is generically fulfilled in chaotic systems, although its justification has been primarily numerical in several systems (see, e.g., [2]).

In its various versions, ETH [1] transparently explains static properties (how a closed system appears thermal at equilibrium) and infinite-time properties (fluctuations around time-averaged expectations). However, on the dynamical side, ETH has not yet been connected to the *timescale* of thermalization. Consider a particular thermalization model

such as coupling the system weakly to a heat bath or implementing a Gibbs sampler [3] on a quantum computer. Does ETH imply rapid convergence, or do we need another hypothesis for that? More generally, do we expect chaotic open systems to always thermalize in a reasonable time?

This apparent lack of connection signifies the larger open challenge of understanding the approach to thermalization (and equilibration more generally). While there are general arguments for equilibration [4] and thermalization (under ETH) [1, 2] at infinite times for both closed and open system dynamics, little is known at finite times. Even classically the problem is intricate, as demonstrated by the existence of glassy dynamics. Yet, interesting progress was accomplished classically using Glauber dynamics, a family of stochastic processes that model the interaction of the system with a heat bath. There, the rapid convergence to thermality was linked to finite correlation length in the Gibbs measure [5]. These results also featured in the development of classical algorithms in areas ranging from approximate counting [6] to computer vision [7], where sampling of Gibbs measures (i.e. Markov random fields [8]) is an important primitive [9].

Addressing the timescale of thermalization for quantum systems is substantially more challenging. Some progress was achieved for local commuting models where the quantum versions of Glauber dynamics are local themselves [10, 11]. In contrast, very few general results [12, 13] are known in the non-commuting case since even defining a good thermalization model for quantum systems is non-trivial. Davies derived a Lindbladian that models a system interacting weakly with a heat bath [14, 15]. Unfortunately, the derivation requires an unphysical infinite-time and weak-coupling limit that the Lindbladian distinguishes arbitrarily close energies. It is still an open question to find a Lindbladian that faithfully models a system coupled weakly to a heat bath [16–18], under realistic assumptions, and that leads to thermalization.

Another class of processes modeling thermalization is known as quantum Gibbs samplers. These are quantum algorithms for preparing Gibbs states on a future quantum computer; the best-known example is Quantum Metropolis Sampling [3, 19]. Further, similarly to the classical setting, they have shown to be an interesting quantum algorithmic primitive for more general problems (e.g., quantum algorithms for semi-definite programming [20] and machine learning [21, 22]). While Quantum Metropolis should eventually converge to the (approximate) Gibbs state, the convergence at finite times for any non-commuting model has remained an open question.

A. Main Results

This work addresses the timescale of thermalization for systems satisfying ETH, considering coupling a system to a thermal bath and Quantum Metropolis Sampling. For the former, we first answer how finite run-time and resources come into error estimates without taking the unphysical weak-coupling limit. Then we show how ETH implies efficient convergence to a good approximation of the *global* Gibbs state. For Quantum Metropolis, we first introduce a notion of approximate detailed balance that allows us to handle the finite resolution of quantum phase estimation (QPE), which has been a hurdle in analyzing Quantum Metropolis and related quantum algorithms.¹ We then proceed to show how ETH also implies fast convergence in this case.

1. Davies' Generator at Finite Resources (Section III)

We formalize a version of Davies' generator under physically *realistic* assumptions. We do not take any weak-coupling limit and only allow finite resources, which is different from the Lindbladian literature [16–18]. This makes our results applicable to digital or analog quantum computers and modeling thermalization in nature at finite times. The Lindbladian we derive approximates the marginal of the joint-evolution with an explicit trade-off between resources and accuracy. One crucial technical assumption we make is that the state of the bath is routinely refreshed.² Practically, the refreshing can be engineered efficiently in a quantum computer. However, for thermalization that occurs in nature, it remains open whether refreshing the bath is a good model for the rapid decay of bath memory.

Let us begin with an intuitive argument that will lead us to a finite-time version of Davies' generator. Consider a system with Hamiltonian \mathbf{H}_S interacting weakly with a bath

$$\mathbf{H} = \mathbf{H}_S + \mathbf{H}_B + \mathbf{H}_{SB}, \quad \mathbf{H}_{SB} := \lambda \sum_a \mathbf{A}^a \otimes \mathbf{B}^a, \quad (1.1)$$

where λ is the strength of the interaction and \mathbf{A}^a (\mathbf{B}^a) are operators acting on the system (bath). The Davies' generator for this Hamiltonian is given by

$$\mathcal{D}_{WCL}[\mathbf{X}] = \sum_{\omega} \sum_{ab} \gamma_{ab}(\omega) \left(\mathbf{A}^{a\dagger}(\omega) \mathbf{X} \mathbf{A}^b(\omega) - \frac{1}{2} \{ \mathbf{A}^{a\dagger}(\omega) \mathbf{A}^b(\omega), \mathbf{X} \} \right), \quad \mathbf{A}^a(\omega) := \sum_{\nu_1 - \nu_2 = \omega} \mathbf{P}_{\nu_2} \mathbf{A}^a \mathbf{P}_{\nu_1}, \quad (1.2)$$

¹ Existing literature using coherent QPE either assumes perfect resolution or an additional “rounding promise” for the Hamiltonian [23, 24] that the spectrum is expelled whenever QPE is ambiguous.

² Qualitatively, routine refreshing avoids heating (or cooling) of the bath. Practically, this may not be necessary if the bath temperature changes only slightly, but we leave it for future work.

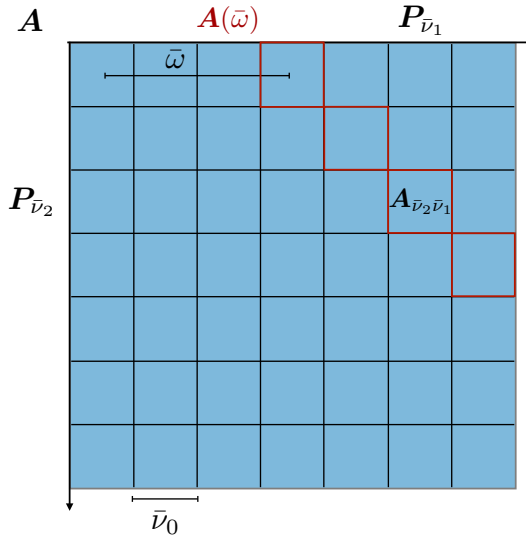


Figure 1. The operator $\mathbf{A}(\bar{\omega})$, dissected by projectors $\mathbf{P}_{\bar{\nu}_1}, \mathbf{P}_{\bar{\nu}_2}$. The conscious choice that $\bar{\nu}_1, \bar{\nu}_2$ are integer multiples of the base frequencies $\bar{\nu}_0$ implies that their difference $\bar{\omega}$ are also integer multiples.

where the scalar function $\gamma_{ab}(\omega)$ depends on the bath. Now, consider a *rounded* Hamiltonian with energies $\bar{\nu} = N \cdot \bar{\nu}_0$ being integer multiples of some resolution $\bar{\nu}_0$

$$\mathbf{H}_S \approx \bar{\mathbf{H}}_S = \sum_{\bar{\nu}} \bar{\nu} \mathbf{P}_{\bar{\nu}}, \quad (1.3)$$

which, at early times and for sufficiently small resolution $\bar{\nu}_0$, should be effectively equivalent to the original one. However, the Davies' generator of the rounded Hamiltonian is now³

$$\mathcal{D}[\mathbf{X}] = \sum_{\bar{\omega}} \sum_{ab} \gamma_{ab}(\bar{\omega}) \left(\mathbf{A}^{a\dagger}(\bar{\omega}) \mathbf{X} \mathbf{A}^b(\bar{\omega}) - \frac{1}{2} \{ \mathbf{A}^{a\dagger}(\bar{\omega}) \mathbf{A}^b(\bar{\omega}), \mathbf{X} \} \right), \quad \mathbf{A}^a(\bar{\omega}) := \sum_{\bar{\nu}_1 - \bar{\nu}_2 = \bar{\omega}} \mathbf{P}_{\bar{\nu}_2} \mathbf{A}^a \mathbf{P}_{\bar{\nu}_1}, \quad (1.4)$$

which is a drastic change to the original Davies' generator. The projector $\mathbf{P}_{\bar{\nu}}$ contains all the nearby energies and may have exponential rank $e^{\Omega(n)}$ (Figure 1). In other words, we see that the weak-coupling limit at infinite times (1.2) does not consistently capture the massive coherence between energies, which should be omnipresent at any reasonable run-time.

Our first main result formalizes the above intuition by showing that the above \mathcal{D} is the relevant finite-time object that approximates the marginal evolution

$$\mathcal{T}(t)[\rho] := \text{Tr}_B [e^{-i\mathbf{H}t} [\rho \otimes \sigma_B] e^{i\mathbf{H}t}]. \quad (1.5)$$

Theorem I.1 (Weak-coupling at finite times, informal). *For a system coupled to a quasi-free Fermionic bath as in Eq. (1.1), the finitely-resolved Davies' generator*

$$\bar{\mathcal{L}} := i[\mathbf{H}_S + \lambda^2 \mathbf{H}_{LS}, \cdot] + \lambda^2 \mathcal{D} \quad (1.6)$$

approximates the marginal evolution with ℓ refreshes, i.e.

$$\forall \rho, \quad \left\| \mathcal{T}(t/\ell)^\ell [\rho] - e^{\bar{\mathcal{L}}^\dagger t} [\rho] \right\|_1 \leq \epsilon, \quad (1.7)$$

whenever certain polynomial constraints are satisfied between t, τ, λ , the system size n , the energy resolution $\bar{\nu}_0$, the error ϵ , the number of refreshes of the bath ℓ , and the size of the bath.

See Theorem III.1 for the explicit trade-off between parameters. For example, one may set a desired effective time $\tau = \lambda^2 t$, and then estimate the required resources for implementation, which all scale polynomially with τ, λ , the system size n , and the desired accuracy ϵ . See Section II B for the non-dissipative term \mathbf{H}_{LS} , whose explicitly form we will never use.

Our finitely-resolved Davies' generator was inspired by [16], which (after taking several limits) presents the dissipative part \mathcal{D} that serves our purposes. What allows us to put together a finite resource estimate is due to refreshing the bath and controlling the secular approximation without taking limits.

³ In a slightly different context, [24] considers the Davies' generator for the rounded Hamiltonian, which turns out giving the same \mathcal{D} . We find this interpretation of \mathcal{D} an intuitive justification.

2. ETH Implies Fast Convergence of the Finitely-Resolved Davies' Generator (Section V)

Our next main result proves the convergence of the finitely-resolved Davies' generator (with any bath correlator such that $\gamma_{ab}(\bar{\omega}) = \delta_{ab}\gamma(\bar{\omega})$), with the crucial input from the following version of ETH.

Hypothesis I.1 (Eigenstate Thermalization Hypothesis, informal). *Consider a Hamiltonian \mathbf{H} and some operator \mathbf{A} . ETH asserts that for nearby energies $|\nu_i - \nu_j| \leq \Delta_{ETH}$ and the corresponding eigenstates $|\psi_i\rangle, |\psi_j\rangle$ of \mathbf{H} ,*

$$A_{ij} = \langle \psi_i | \mathbf{A} | \psi_j \rangle = O(\mu)\delta_{ij} + \frac{1}{\sqrt{\dim(\mathbf{H}) \cdot D(\mu)}} f_{\mathbf{A}}(\omega) g_{ij} \quad (1.8)$$

where $\mu = (\nu_i + \nu_j)/2$, $\omega = \nu_i - \nu_j$, $D(\cdot)$ is the normalized density of states, and g_{ij} are independent Gaussians $\mathbb{E}[g_{ij}] = 0, \mathbb{E}[g_{ij}^2] = 1$.

Intuitively, if one applies the operator \mathbf{A} to an energy eigenstate $|\psi\rangle$, the function $f_{\mathbf{A}}(\omega)$ governs the transition rate for an energy difference ω . Some formulations of ETH assume that the *diagonal* matrix elements $O(\mu)$ give the thermal expectation of \mathbf{A} at the energy μ , but it is irrelevant for our purposes. Instead, the crucial aspect of ETH we utilize is that below a certain energy scale Δ_{ETH} , the *off-diagonal* matrix elements of the observable \mathbf{A} in the energy eigenbasis follow random matrix theory (RMT).⁴ Note we have assumed the function $f_{\mathbf{A}}(\omega)$ to depend only on the energy difference ω , while in practice it may depend on μ and hence the temperature β . This simplification does not change the main argument of this work.

More carefully, there are many implicit assumptions behind ETH; let us briefly instantiate them. We assume that the density of states $D(\nu)$ is well-defined and that the density varies slowly such that for any $|\nu - \nu'| \leq \Delta_{ETH}$, the ratio of densities is bounded uniformly:

$$\frac{D(\nu)}{D(\nu')} \leq R. \quad (1.9)$$

Indeed, this is consistent with the existing assertions [2, 26] that the energy window Δ_{ETH} for which random matrix theory kicks in should be small (which also means that we assume nothing for the many entries outside Δ_{ETH}). Lastly, to be free of finite-sized effects, we truncate the Hamiltonian near the edge. See Section IVB for a review of ETH as well as the details in the assumptions. Now, let us show the above assumptions circling ETH suffice for thermalization at finite times.

Theorem I.2 (Convergence of the finitely-resolved Davies' generator, informal). *Consider an n -qubit Hamiltonian \mathbf{H}_S satisfying the above with $R = \mathcal{O}(1)$. Assume that each term \mathbf{A}^a satisfies ETH for energy differences below Δ_{ETH} and that $\beta\Delta_{ETH} = \mathcal{O}(1)$. Then, with high probability, (w.r.t to the randomness of ETH) with $|a| = \Omega(1)$ flips, running the finitely-resolved Davies' generator for effective time ($\tau = \lambda^2 t$)*

$$\tau \approx \frac{\ln(1/\epsilon)}{\lambda_{RW}} \frac{n^2}{|a| \int_0^{\Delta_{ETH}} \gamma(-\omega) |f_\omega|^2 d\omega} \quad \text{ensures} \quad \left\| e^{\tilde{\mathcal{L}}^\dagger t} [\rho] - \bar{\sigma} \right\|_1 \leq \epsilon, \quad (1.10)$$

where $\bar{\sigma} \propto e^{-\beta \bar{H}_S}$ is the rounded Gibbs state with energy resolution $\bar{\nu}_0 \leq \mathcal{O}(\Delta_{ETH})$, and λ_{RW} is the gap of a 1d classical random walk with the characteristic step size $\sim \Delta_{ETH}$ on the Gibbs distribution.

Note that τ is the natural time scale since the dissipative part \mathcal{D} is weighted by the weak-coupling strength squared λ^2 . We use \approx to drop parameters that are often small and see Theorem V.1 for completeness. Roughly, if the Gibbs state is a Gaussian with variance Δ_{spec} , then the random walk on the spectrum has gap $\lambda_{RW} = \Omega(\Delta_{ETH}^2 / \Delta_{spec}^2)$. The term $\int_0^{\Delta_{ETH}} \gamma(-\omega) |f_\omega|^2 d\omega$ is the rate of hopping given by ETH (and the bath) that reflects the size of the window Δ_{ETH} relative to the width of $|f_\omega|^2$; $|a|$ is the number of interaction terms reflecting the interaction strength $\sum_a \mathbf{A}^a \otimes \mathbf{B}^a$; the factors of $n = \log(\dim(\mathbf{H}))$ come from (potentially inefficient) conversions between norms. To obtain an altogether explicit resource estimate to sample Gibbs state via Davies' generator, see Section VF.

Roughly speaking, the Gibbs state of a Hamiltonian can be efficiently prepared (by a quantum computer or in Nature) for temperatures β where ETH holds; this justifies the Gibbs state as a meaningful thermodynamic notion. Note that at low-temperatures that $\beta \gg \Delta_{ETH}$, we would restrict to a smaller window $\Delta'_{ETH} = \mathcal{O}(\frac{1}{\beta})$, which only polynomially impacts the run time (analogously Δ'_{ETH} should ensure $R = \mathcal{O}(1)$). Of course, our results do not apply to systems in the glassy phase or many-body-localized phase (see, e.g., [27]); there, the thermal state is unphysical anyway.

⁴ This is reminiscent of Wigner's RMT model of heavy nuclei [25].

3. ETH Implies Fast Convergence of Quantum Metropolis Sampling (Section VII)

Let us quickly summarize the Metropolis CP map [3].⁵ It consists of the acceptance and rejection steps $\mathcal{N} = \mathcal{A} + \mathcal{R}$, and right now, we only sketch the former

$$\mathcal{A}[\rho] \approx \sum_{\bar{\nu}_2 \bar{\nu}_1} \sum_a \frac{1}{|a|} \mathbf{P}_{\bar{\nu}_2} \cdot \mathbf{A}^a (\mathbf{P}_{\bar{\nu}_1} \rho \mathbf{P}_{\bar{\nu}_1}) \mathbf{A}^{a\dagger} \cdot \mathbf{P}_{\bar{\nu}_2} \cdot \min(1, e^{-\beta(\bar{\nu}_2 - \bar{\nu}_1)}). \quad (1.11)$$

In other words, one iteration of Metropolis first estimates the energy $\bar{\nu}_1$ (again to certain resolution $\bar{\nu}_0$), applies some random "flip" operator \mathbf{A}^a (with uniform probability $\frac{1}{|a|}$), and then estimates the energy $\bar{\nu}_2$. With probability being the Metropolis weight $\min(1, e^{-\beta(\bar{\nu}_2 - \bar{\nu}_1)})$, this move is accepted, otherwise a complicated rejection procedure \mathcal{R} is initiated to return to the original energy. See Section VIB for more details.

QPE at a finite resolution poses a significant technical challenge. Indeed, energies nearby will be intelligible to QPE and remain entangled (1.11). Moreover, the same eigenstate may be probabilistically rounded to different discrete registers (which cannot be seen from (1.11); see Section VIB).

Our first step towards analyzing the Quantum Metropolis CP map is addressing how a finite resolution impacts the convergence and Gibbs state. We quantify an appropriate notion of *approximate* detailed balance (Section VIC)

$$\left\| \mathcal{N} - \sqrt{\sigma} \mathcal{N}^\dagger \left[\frac{1}{\sqrt{\sigma}} \cdot \frac{1}{\sqrt{\sigma}} \right] \sqrt{\sigma} \right\|_{1-1} \leq 2\epsilon_{DB}, \quad (1.12)$$

where ϵ_{DB} can be suppressed by better QPE resolution $\bar{\nu}_0$. At an infinite resolution, $\epsilon_{DB} = 0$, the exact Gibbs state would be a fixed point (if \mathcal{N} were also trace-preserving). At a finite resolution, this form of approximate detailed balance controls the accuracy of the prepared Gibbs state and reflects the rounding resolution needed. To reiterate, we do not need a rounding promise [23, 24] for the spectrum of the Hamiltonian. It is a follow-up question whether this applies to other Metropolis algorithms based on quantum walks [19]. Now that we know the fixed point is an approximate Gibbs state, we show ETH implies its convergence.

Theorem I.3 (ETH implies convergence of Quantum Metropolis, informal). *Consider a Hamiltonian \mathbf{H}_S with the same assumptions as in Theorem I.2. Assume each of the "flips" \mathbf{A}^a for energy differences below Δ_{ETH} is an i.i.d sample from the ETH Ansatz, and that $\beta\Delta_{ETH} = \mathcal{O}(1)$. Then with high probability (w.r.t to the randomness of ETH), applying ℓ iterations the Quantum Metropolis map \mathcal{N} with*

$$\ell \approx \frac{1}{\lambda_{RW}} \frac{\ln(1/\epsilon) + n}{\int_0^{\Delta_{ETH}} \gamma(-\omega) |f_\omega|^2 d\omega} \quad \text{ensures} \quad \|\mathcal{N}^\ell[\rho] - \sigma\|_1 \leq \epsilon, \quad (1.13)$$

using number of flips $|a|$ and run time per phase estimation t_{QPE} that depends polynomially with the random walk gap λ_{RW} , number of rounds ℓ , and accuracy ϵ , and inverse temperature β .

We see that ℓ is the analog of τ for Davies' generator (Theorem I.2). In addition, the total run time scales with both the number of iterations ℓ and the runtime per phase estimation t_{QPE} (which also needs to scale with ℓ). The difference from Davies' generator (Theorem I.2) is that we need quite a lot of flips $|a|$ (roughly the square of the random walk gap) that serve as i.i.d samples of the ETH Ansatz to choose from. This is due to the extra technicality involved with CP maps without exact detailed balance. See Theorem VII.1 for the complete statement and Section VII E for detailed resource estimates.

B. Discussion

We would like to discuss a few noteworthy points of our main results:

1. Convergence to the Global Gibbs State

One broader conceptual message is the strong notion of the convergence results: *every* initial state converges to a good approximation of the *global* Gibbs state, at reasonable times, if the Hamiltonian satisfies ETH (at the desired temperature). This justifies the notion of a Gibbs state (of "chaotic" systems) in quantum thermodynamics. Generally, the convergence of Lindbladians or CP maps, parameterized by the Hamiltonian \mathbf{H} and certain flips \mathbf{A}^a , seems to be a technically formidable task. While there are well-established tools and examples in the classical Markov chain literature (see, e.g., [29]), the quantum analogs are very much in their cradle.

⁵ Among the Quantum Metropolis proposals [19], we work with [3] since it worked out the low-level details.

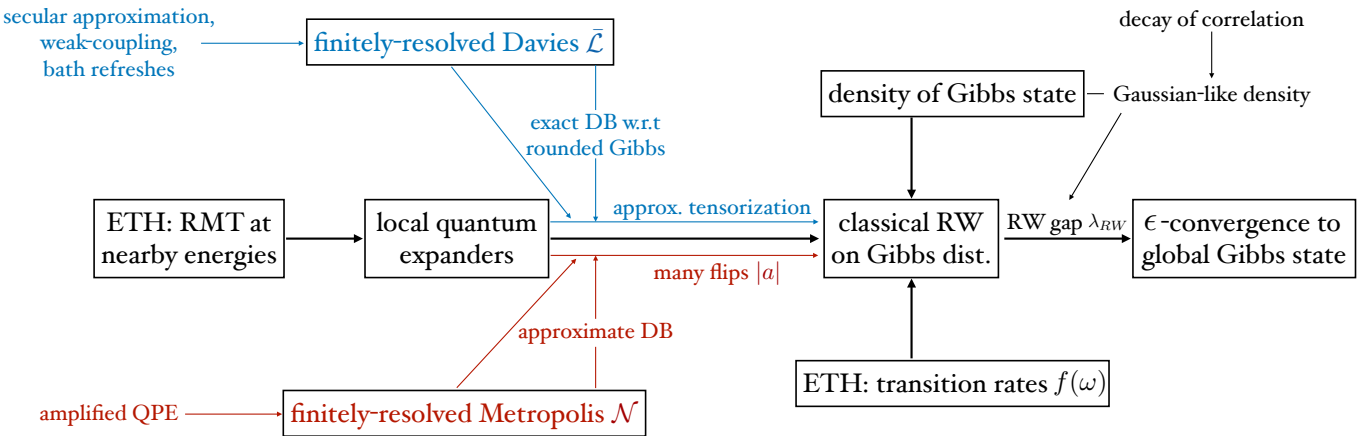


Figure 2. The interdependence of the concepts and the parameters in this work. The colored texts and arrows distinguish the notions for Davies' generator from that of Metropolis Sampling, and those in common are in black. This manifests the flexibility of the arguments presented. We need from ETH the RMT prescription, which gives quantum expanders at local energies, and from the density of Gibbs state that it has no bottlenecks. Interestingly, the decay of correlation in Gibbs state, which featured in the classical [5] and commuting Hamiltonian literature [10, 11], is now a replaceable component. It serves the only purpose that the density of states is Gaussian-like [28], which, through standard conductance calculation, implies the random walk on the Gibbs distribution mixes rapidly.

In quantum thermodynamics, it is unclear whether thermalization should refer to convergence to the global Gibbs state or just to another state that appears to be Gibbs (e.g., in terms of local marginals). People traditionally use ETH to explain the thermal behavior at very long times [1] and/or of small subsystems [30]. For isolated systems, indeed, thermalization of small subsystems is the best we could hope for. Our results extend the applicability of ETH to open quantum systems.

2. ETH Gives Quantum Expanders at Nearby Energies

Technically, the proof idea is the close link between the RMT prescription of ETH and the rapid, thorough decoherence at local energies: ETH gives *quantum expanders*. Historically, a quantum expander refers to an ensemble of unitaries that efficiently generate 1-designs with a gap between the largest (λ_1) and the second-largest (λ_2) eigenvalues; for expanders composed of $|a|$ Haar random unitaries and their adjoints, the gap is $1 - \mathcal{O}(\frac{1}{\sqrt{|a|}})$ [31, 32]⁶.

For Davies' generator, suppose our input has only two energy blocks $\mathbf{P}_{\bar{\nu}_1} \mathbf{X} \mathbf{P}_{\bar{\nu}_1} + \mathbf{P}_{\bar{\nu}_2} \mathbf{X} \mathbf{P}_{\bar{\nu}_2}$ (in the Heisenberg picture)

$$\mathcal{L}_{\bar{\nu}_1, \bar{\nu}_2} [\mathbf{X}_{\bar{\nu}_1 \bar{\nu}_1} + \mathbf{X}_{\bar{\nu}_2 \bar{\nu}_2}] := \sum_a \left[\frac{\gamma(\bar{\nu}_1 - \bar{\nu}_2)}{2} \left(\mathbf{A}_{\bar{\nu}_1 \bar{\nu}_2}^a \mathbf{X} \mathbf{A}_{\bar{\nu}_2 \bar{\nu}_1}^a - \frac{1}{2} \{ \mathbf{A}_{\bar{\nu}_1 \bar{\nu}_2}^a \mathbf{A}_{\bar{\nu}_2 \bar{\nu}_1}^a, \mathbf{X}_{\bar{\nu}_1 \bar{\nu}_1} \} \right) + (\bar{\nu}_1 \leftrightarrow \bar{\nu}_2) \right], \quad (1.14)$$

we show that the Lindbladian rapidly mixes the nearby energies.⁷ For all $\bar{\nu}_1, \bar{\nu}_2$, with high probability w.r.t to the randomness in ETH,

$$\lambda_2(\mathcal{L}_{\bar{\nu}_1, \bar{\nu}_2}) = -\Omega \left((1 - \mathcal{O}(\frac{1}{\sqrt{|a|}})) \cdot |a| \cdot \gamma(-\bar{\omega}) |f(\bar{\omega})|^2 \bar{\nu}_0 \right). \quad (1.15)$$

Roughly speaking, using $|a| = \Omega(1)$ flips ensures the Lindbladian converges quickly. See Section IV D for a formal definition that also considers the off-diagonal inputs.⁸ Our proof for quantum expanders relies on the ETH ansatz that the flips $\mathbf{A}_{\bar{\nu}_1 \bar{\nu}_2}^a$, for close enough energies $\bar{\nu}_1 - \bar{\nu}_2 \leq \Delta_{ETH}$, are Gaussian matrices. We then go through concentration inequalities for a sum of tensor product of Gaussian matrices $\sum_a \mathbf{G}_a \otimes \mathbf{G}_a^*$, which follows [34].

In short, being a quantum expander in the sense above is how ETH (open) systems thermalize; at the same time, quantum expanders may be an alternative definition of ETH that is more precise and checkable than invoking RMT at nearby energies as a black box. Indeed, the RHS (1.15) does not refer to any randomness, and that is all we needed for our proofs. In small-scale numerics (a chaotic spin chain on 12 qubits, Appendix C), we observe the expander behavior as predicted by ETH.

⁶ There are also notions of quantum tensor product expanders [32, 33] that generates t-designs.

⁷ Note that the leading eigenvalue on the diagonal block Lindbladian is zero $\lambda_1 = 0$.

⁸ As a technical note, the above definition for quantum expander is intended for the cases when the density ratio between $\bar{\nu}_1, \bar{\nu}_2$ and the Boltzmann factor $e^{\beta \Delta_{ETH}}$ are $\mathcal{O}(1)$.

3. Global Convergence From a Random Walk on the Spectrum

Interestingly, once we obtain local convergence (namely, the expander property) using ETH, global convergence is controlled by a *classical* random walk gap on the Gibbs distribution (Figure 2). This is consistent with the known results [13] for infinite run-time where coherence is not an issue.

For Davies' generator, the local-to-global lift is done via Modified-Log-Sobolev inequalities using a very recent development called *approximate tensorization* [35, 36]⁹. The fact that our finitely-resolved Davies' generator satisfies exact detailed balance (w.r.t. the rounded Gibbs state) has also saved us from potential issues with approximate detailed balance.

For the Metropolis CP map, the proof of global convergence is more ad-hoc because of QPE rounding errors (approximate detailed balance), chances of failure, and being less structured than a Lindbladian (each local Lindbladian generates a trace-preserving map). We have to use a large number of flips $|a|$ to ensure fluctuation of local terms $\mathcal{A}_{(\bar{\nu}_1 \bar{\nu}_2)}$ concentrates and does not close the tiny gap of the random walk. Also, we have to decompose the CP map into the self-adjoint component, which satisfies exact detailed balance, and the anti-self-adjoint component, which is small due to approximate detailed balance.

See Section V G for comments on the optimality of the Lindbladian results (Theorem I.1, Theorem I.2) and a comparison with the case of commuting Hamiltonian.

4. Implications to Quantum Algorithms

Simulating the thermal properties of physical systems is expected to be one important application of quantum computers. This paper shows that for the broad class of Hamiltonians satisfying ETH, we can prepare the associated quantum Gibbs states efficiently on a quantum computer (which is unexpected for classical methods). Our work suggests a class of physically relevant problems where we may expect a quantum advantage.

Quantum Gibbs sampling has been used as a primitive in many quantum algorithms (see, e.g., [20–22, 37]). As a concrete example, consider the task of solving semi-definite programs (SDPs) on a quantum computer [20, 37]. There, it was shown that one could solve SDPs in roughly the time required to prepare Gibbs states (of Hamiltonians given by linear combinations of the input matrices of the instance). Our work suggests a large class of instances for which this preparation, and hence the associated SDPs, can be solved in polylogarithmic time in the dimension of the input matrices: namely, whenever those matrices, treated as Hamiltonians, satisfy ETH (with suitable choices of flips). Again, we can expect large speed-ups in comparison with state-of-the-art classical methods.

In another connection to quantum algorithms, we hope our treatment of quantum phase estimation inspires further careful analysis of algorithms using coherent QPE at a finite resolution. Especially, it would be an interesting follow-up to understand how quantum walk methods are impacted by rounding errors, *without* a rounding promise for the Hamiltonian.

5. Open Questions

Even though we have shown ETH implies fast thermalization, many conceptual questions remain that point towards a better understanding of ETH itself. First, there is a big gap between the convergence rate we obtained and the convergence rates obtained for the commuting case (assuming a finite correlation length). Resolving it would require a re-examination of the ETH parameters as well as a more stringent analysis. Second, the proof methods for the commuting case, which uses the locality of Lindbladian, seem completely distinct from the random walk picture on the spectrum we employ in this work. It would be technically curious to make connections. Third, how can we describe ETH, and more broadly chaotic systems, without introducing artificial randomness? A potential answer we gave is in terms of quantum expanders. It would be interesting to ask which components of the traditional ETH it can replace and to carry out larger scale numerics for the validity of the expander property.

C. Acknowledgments

We thank Charles Xu for early discussions on the topic of this paper. We thank Robert (Hsin-Yuan) Huang for suggesting to check quantum expander properties numerically. We thank Cambaye Rouzé for discussions on approximate tensorization. CFC is supported by Caltech RA fellowship and the Eddleman Fellowship.

⁹ This was developed for tensor product Hilbert spaces, but we applied it to the energy spectrum, which is more like a single particle Hilbert space. It is possible that an elementary derivation without approximate tensorization exists. Indeed, we could have used a similar argument as in Metropolis, but that requires quantum expander to hold at a large number of flips $|a|$ that scales with the inverse random walk gap squared $1/\lambda_{RW}^2$.

II. DAVIES' GENERATOR

Consider our system of interest \mathbf{H}_S coupled to a heat bath. We can ask several basic questions: (1) when does the subsystem S permit an effective Markovian description (i.e., Lindbladians)? (2) Is its fixed point the Gibbs state? (3) How fast does it converge?

A. The Weak-Coupling Limit with Infinite Time and Bath

The general question is, of course, hard; however, a Lindbladian can be derived by taking the *weak-coupling limit* by inserting a small parameter λ

$$\mathbf{H} = \mathbf{H}_S + \mathbf{H}_B + \mathbf{H}_{SB}, \quad \mathbf{H}_{SB} := \lambda \sum_a \mathbf{A}^a \otimes \mathbf{B}^a, \quad (2.1)$$

and setting $\lambda \rightarrow 0, \lambda^2 t = \tau < \infty$. Technically, we also assume we start with a state tensored with the bath Gibbs state $\rho_S \otimes \sigma_B$, and that the bath are quasi-free Fermions (Section II C). Then, Davies showed that the marginal of the joint-evolution is effectively described by a Lindbladian acting only on system S

$$\text{Tr}_B[e^{-i\mathbf{H}t}(\rho_S \otimes \sigma_B)e^{i\mathbf{H}t}] \xrightarrow{\lambda \rightarrow 0} e^{\mathcal{L}^\dagger t}[\rho_S]. \quad (2.2)$$

And the Lindbladian, *the Davies generators*, [15, 38] in the Heisenberg picture has the following form

$$\mathcal{L}[\mathbf{X}] = i[\mathbf{H} + \mathbf{H}_{LS}, \mathbf{X}] + \lambda^2 \sum_{\omega, a} \mathcal{L}_\omega[\mathbf{X}], \quad (2.3)$$

where the summands labeled by energy ω take the form

$$\mathcal{L}_\omega[\mathbf{X}] = \sum_{ab} \gamma_{ab}(\omega) \left(\mathbf{A}^{a\dagger}(\omega) \mathbf{X} \mathbf{A}^b(\omega) - \frac{1}{2} \{ \mathbf{A}^{a\dagger}(\omega) \mathbf{A}^b(\omega), \mathbf{X} \} \right). \quad (2.4)$$

Remarkably, all we need to remember for the bath is the function $\gamma_{ab}(\omega)$. The $\mathbf{A}^a(\omega)$, entirely independent of the bath, are Fourier transforms labeled by Bohr frequencies $e^{i\mathbf{H}t} \mathbf{A}^a e^{-i\mathbf{H}t} = \sum_\omega \mathbf{A}^a(\omega) e^{i\omega t}$, or equivalently

$$\mathbf{A}^a(\omega) = \sum_{\nu_1 - \nu_2 = \omega} \mathbf{P}_{\nu_2} \mathbf{A}^a \mathbf{P}_{\nu_1}. \quad (2.5)$$

The remaining variables are

$$\mathbf{H}_{LS} = \sum_\omega \sum_{ab} S_{ab}(\omega) \mathbf{A}^{a\dagger}(\omega) \mathbf{A}^b(\omega) \quad (2.6)$$

$$\gamma_{ab}(\omega) = \Gamma_{ab}(\omega) + \Gamma_{ba}^*(\omega) \quad (2.7)$$

$$S_{ab}(\omega) = \frac{1}{2i} (\Gamma_{ab}(\omega) + \Gamma_{ba}^*(\omega)) \quad (2.8)$$

$$\Gamma_{ab} = \int_0^\infty ds e^{i\omega s} \text{Tr} [e^{i\mathbf{H}_B s} \mathbf{B}^{a\dagger} e^{-i\mathbf{H}_B s} \mathbf{B}^b \sigma] \quad (2.9)$$

$$:= \int_0^\infty ds e^{i\omega s} \langle \mathbf{B}^{a\dagger}(s) \mathbf{B}^b \rangle_{\sigma_B} \quad (2.10)$$

While \mathbf{A} depends on the particular choices, let us emphasize the unconditional facts for any Lindbladian of this form: (a) The first is the *KMS condition*

$$\gamma_{ba}(-\omega) = e^{-\beta\omega} \gamma_{ab}(\omega) \quad (2.11)$$

(b) The second is that $\gamma_{ab}(\omega)$ is a positive-semidefinite matrix.

Fact II.1. *The KMS condition (a) and $\gamma_{ab}(\omega)$ being a PSD matrix (b) implies that (A) \mathcal{L}^\dagger is indeed a generator of CPTP map*

$$\mathcal{L}[\mathbf{I}] = 0, \text{Tr}[e^{\mathcal{L}^\dagger t}[\rho]] = \text{Tr}[\rho]$$

and (B) for each frequency ω , $\mathcal{L}_\omega + \mathcal{L}_{-\omega}$ satisfies the detailed balance condition

$$\sqrt{\sigma}(\mathcal{L}_\omega + \mathcal{L}_{-\omega})[\mathbf{X}] \sqrt{\sigma} = (\mathcal{L}_\omega + \mathcal{L}_{-\omega})^\dagger[\sqrt{\sigma} \mathbf{X} \sqrt{\sigma}].$$

Note that (B) further implies the Gibbs state $\sigma \propto e^{-\beta\mathbf{H}}$ is stationary $(\mathcal{L}_\omega + \mathcal{L}_{-\omega})[\sigma] = 0$.

Given the above form (and setting $\gamma_{ab}(\omega) = \delta_{ab} \gamma_\omega$), [13] has shown the gap can be calculated given the description of \mathbf{A} . However, it is not clear whether Davies' generator provides an accurate description of finite-time physics since the weak-coupling limit requires (1) an (unphysical) infinite time limit and (2) the bath to have a continuous spectrum is thus infinite-dimensional.

B. The Advertised Form of Finitely-resolved Davies' Generator

Our finite-time discussion highlights the following form of the *finitely-resolved Davies' generator* $\bar{\mathcal{L}}$, parameterized by some energy resolution $\bar{\nu}_0$. There are several recent related proposals [24], and the arguments in [16] is a prototype of our finite-times results, although we focus on a strict finite-resource mindset.

$$\bar{\mathcal{L}} := \mathcal{L}_S + \lambda^2(\mathcal{L}_{LS} + \mathcal{D}), \quad (2.12)$$

$$\mathcal{L}_{LS} := i[\mathbf{H}_{LS}, \cdot], \mathbf{H}_{LS} := \sum_{\bar{\omega}:\bar{\nu}_0|\bar{\omega}} \sum_{ab} S_{ab}(\bar{\omega}) \mathbf{A}^{a\dagger}(\bar{\omega}) \mathbf{A}^b(\bar{\omega}) \quad (2.13)$$

$$\mathcal{D}[\mathbf{X}] := \sum_{\bar{\omega}:\bar{\nu}_0|\bar{\omega}} \mathcal{L}_{\bar{\omega}}[\mathbf{X}] = \sum_{\bar{\omega}} \sum_{ab} \gamma_{ab}(\bar{\omega}) \left(\mathbf{A}^{a\dagger}(\bar{\omega}) \mathbf{X} \mathbf{A}^b(\bar{\omega}) - \frac{1}{2} \{ \mathbf{A}^{a\dagger}(\bar{\omega}) \mathbf{A}^b(\bar{\omega}), \mathbf{X} \} \right), \quad (2.14)$$

where the discrete frequencies $\{\bar{\nu}\}, \{\bar{\omega}\} = \{N \cdot \bar{\nu}_0\}$ are multiples of resolution $\bar{\nu}_0$

$$\mathbf{A}^a(\bar{\omega}) = \sum_{\bar{\nu}_1 - \bar{\nu}_2 = \bar{\omega}} \mathbf{P}_{\bar{\nu}_2} \mathbf{A}^a \mathbf{P}_{\bar{\nu}_1} =: \sum_{\bar{\nu}_1 - \bar{\nu}_2 = \bar{\omega}} A_{\bar{\nu}_2 \bar{\nu}_1}^a, \quad (2.15)$$

and $S_{ab}(\bar{\omega}), \gamma_{ab}(\bar{\omega})$ are defined as in the original Davies' generator (2.8), (2.7). Among the many other candidates for approximating the evolution at finite times[17, 18], this is the ultimate one that is nice both conceptually and technically. Conceptually, as we mentioned earlier, it coincides with the original Davies' generator for the Hamiltonian rounded at the resolution $\bar{\nu}_0$

$$\bar{\mathbf{H}}_S = \sum_{\bar{\nu}} \bar{\nu} \mathbf{P}_{\bar{\nu}}, \quad (2.16)$$

which differs slightly from the original Hamiltonian $\|\mathbf{H}_S - \bar{\mathbf{H}}_S\| \leq \bar{\nu}_0/2$. Comparing with the original Davies' generator, at a finite resolution $\bar{\nu}_0$, the energies are labeled by their rounded value $\bar{\omega}, \bar{\nu}$ and form a massive superposition. The different energy blocks $\mathbf{A}^{a\dagger}(\bar{\omega}), \mathbf{A}^{a\dagger}(\bar{\omega}')$ are “incoherent” since we do not have the cross term $\mathbf{A}^{a\dagger}(\bar{\omega}) \mathbf{X} \mathbf{A}^b(\bar{\omega}')$.

Technically, it is a generator of CPTP map and satisfies exact detailed balance (see below); it is also free of potential factors of $e^{i(\omega-\bar{\omega})t}$; the rounding into integer multiples gives the convenient labeling of input by discrete energies $\mathbf{P}_{\bar{\nu}'} \mathbf{X} \mathbf{P}_{\bar{\nu}}$, which simplifies the proof (postponed to Section IV C).

1. The fixed point

The immediate question before diving into the proof is about the fixed point. The finitely-resolved Lindbladian is nice in the sense that it satisfies detailed balance for the *finitely-resolved* Gibbs state. This brings about many technical conveniences (which Quantum Metropolis does not enjoy).

Fact II.2 (Exact detailed balance for each $\bar{\omega}$). *For the finitely-resolved Gibbs state $\sigma \propto e^{-\beta \bar{H}} = \sum_{\bar{\nu}} e^{-\beta \bar{\nu}} \mathbf{P}_{\bar{\nu}}$,*

$$\sqrt{\sigma}(\mathcal{L}_{\bar{\omega}} + \mathcal{L}_{-\bar{\omega}})[\mathbf{X}] \sqrt{\sigma} = (\mathcal{L}_{\bar{\omega}} + \mathcal{L}_{-\bar{\omega}})^\dagger[\sqrt{\sigma} \mathbf{X} \sqrt{\sigma}].$$

Proof. Observe

$$\begin{aligned} \sqrt{\sigma} \mathbf{A}^{a\dagger}(\bar{\omega}) &= e^{-\beta \bar{H}/2} \mathbf{A}^{a\dagger}(\bar{\omega}) = e^{-\beta \bar{\omega}/2} \mathbf{A}^{a\dagger}(\bar{\omega}) e^{-\beta \bar{H}/2} \\ &= e^{-\beta \bar{\omega}/2} \mathbf{A}^{a\dagger}(\bar{\omega}) \sqrt{\sigma} \end{aligned}$$

And similarly for $\mathbf{A}^a(\bar{\omega}) \sqrt{\sigma} = e^{-\beta \bar{\omega}/2} \sqrt{\sigma} \mathbf{A}^a(\bar{\omega})$. Hence, for the first term $\mathcal{L}_{\bar{\omega},1} := \sum_{ab} \gamma_{ab}(\bar{\omega}) \mathbf{A}^{a\dagger}(\bar{\omega}) \mathbf{X} \mathbf{A}^b(\bar{\omega})$,

$$\begin{aligned} \sqrt{\sigma} \mathcal{L}_{\bar{\omega},1}[\mathbf{X}] \sqrt{\sigma} &= \sum_{ab} \gamma_{ab}(\bar{\omega}) \sqrt{\sigma} \mathbf{A}^{a\dagger}(\bar{\omega}) \mathbf{X} \mathbf{A}^b(\bar{\omega}) \sqrt{\sigma} \\ &= \sum_{ab} \gamma_{ab}(\bar{\omega}) e^{-\beta \bar{\omega}} \mathbf{A}^{a\dagger}(\bar{\omega}) \sqrt{\sigma} \mathbf{X} \sqrt{\sigma} \mathbf{A}^b(\bar{\omega}) \\ &= \sum_{ab} \gamma_{ba}(-\bar{\omega}) \mathbf{A}^a(-\bar{\omega}) \sqrt{\sigma} \mathbf{X} \sqrt{\sigma} \mathbf{A}^{b\dagger}(-\bar{\omega}) \\ &= \mathcal{L}_{-\bar{\omega},1}^\dagger[\sqrt{\sigma} \mathbf{X} \sqrt{\sigma}]. \end{aligned}$$

In the second equality we commute $\sqrt{\sigma}$ through A and in the third we used the KMS condition (2.11) for $\gamma_{ab}(\bar{\omega})$. For the second term $\mathcal{L}_{\bar{\omega},2} := \sum_{ab} \gamma_{ab}(\bar{\omega}) \frac{1}{2} \{ \mathbf{A}^{a\dagger}(\bar{\omega}) \mathbf{A}^b(\bar{\omega}), \mathbf{X} \}$

$$\begin{aligned} \sqrt{\sigma} \mathcal{L}_{\bar{\omega},2}[\mathbf{X}] \sqrt{\sigma} &= \sum_{ab} \gamma_{ab}(\bar{\omega}) \sqrt{\sigma} \frac{-1}{2} \{ \mathbf{A}^{a\dagger}(\bar{\omega}) \mathbf{A}^b(\bar{\omega}), \mathbf{X} \} \sqrt{\sigma} \\ &= \sum_{ab} \gamma_{ab}(\bar{\omega}) \frac{1}{2} \{ \mathbf{A}^{a\dagger}(\bar{\omega}) \mathbf{A}^b(\bar{\omega}), \sqrt{\sigma} \mathbf{X} \sqrt{\sigma} \} \\ &= \mathcal{L}_{\bar{\omega},2}^\dagger[\sqrt{\sigma} \mathbf{X} \sqrt{\sigma}]. \end{aligned}$$

In the last equality we used self-adjointness $\mathcal{L}_{\bar{\omega},2} = \mathcal{L}_{\bar{\omega},2}^\dagger$. Finally, combine with the analogous calculation for $\mathcal{L}_{-\bar{\omega},1}, \mathcal{L}_{-\bar{\omega},2}$ to yield the advertised result. \square

C. The Quasi-free Fermionic Bath

In the finite resource mindset, one must also choose a bath. Here, we collect the specifications, finite or infinite, completing the missing details in Section II A. Again, consider the total Hamiltonian

$$\mathbf{H} = \mathbf{H}_0 + \mathbf{H}_I \quad (2.17)$$

$$= (\mathbf{H}_S + \mathbf{H}_B) + \lambda \sum_a \mathbf{A}^a \otimes \mathbf{B}^a \quad (2.18)$$

where system B consists of a direct sum of quasi-free Fermions with Hamiltonian

$$\mathbf{H}_B = \sum_p^{n_B} \omega(p) \mathbf{a}_p^\dagger \mathbf{a}_p, \quad (2.19)$$

where n_B is the dimension of *single-particle* Hilbert space and note that p may have energy degeneracy. Quasi-free refers to the (Wick-like) factorization of multipoint correlation into two-point correlation and is a consequence of the Hamiltonian \mathbf{H}_B being quadratic.

$$\langle \mathbf{a}^\dagger(g_m) \cdots \mathbf{a}^\dagger(g_1) \mathbf{a}(f_1) \cdots \mathbf{a}(f_n) \rangle_{\sigma} = \delta_{mn} \det(\langle \mathbf{a}(f_i) \mathbf{a}^\dagger(g_j) \rangle_{\sigma}) = \delta_{mn} \sum \epsilon_{ij} \prod \langle f_{ik} | g_{jk} \rangle \quad (2.20)$$

where $\epsilon_{ij} = \pm 1$ accounts for the signs (which thankfully we do not need to keep track of)

$$\mathbf{a}(f) := \sum_p^{n_B} f^*(p) \mathbf{a}_p, \quad \mathbf{a}^\dagger(g) := \sum_p^{n_B} g(p) \mathbf{a}_p^\dagger. \quad (2.21)$$

$$e^{i\mathbf{H}_B t} \mathbf{a}(f) e^{-i\mathbf{H}_B t} = \mathbf{a}(e^{iht} f) = \sum_p^{n_B} e^{-i\omega(p)t} f^*(p) \mathbf{a}_p. \quad (2.22)$$

1. Choosing a bath

In this section, we will make a simple choice of bath(s). The finite-sized bath is what we can implement, while the infinite limit will simplify the calculation. Label the single Fermion Hilbert space by

$$p = \{\bar{u}\} \times \{a\} \xrightarrow{n_B=\infty} p = \{u\} \times \{a\}$$

which means the Hamiltonian takes the form

$$\mathbf{H}_B = \sum_{a,\bar{u}} \bar{u} \mathbf{a}_{\bar{u},a}^\dagger \mathbf{a}_{\bar{u},a} \xrightarrow{n_B=\infty} \mathbf{H}_B = \sum_a \int u \mathbf{a}_{u,a}^\dagger \mathbf{a}_{u,a} du. \quad (2.23)$$

In other words, for each discrete energy \bar{u} we introduce degeneracies per interaction term $\mathbf{A}^a \otimes \mathbf{B}^a$. Correspondingly, each slot a is allocated for modes \mathbf{B}^a

$$\mathbf{B}_a = \sum_{\bar{u}} f^*(\bar{u}) \mathbf{a}_{\bar{u},a} + \sum_{\bar{u}} f(\bar{u}) \mathbf{a}_{\bar{u},a}^\dagger \xrightarrow{n_B=\infty} \mathbf{B}_a = \int f(u) \mathbf{a}_{u,a} du + \int f^*(u) \mathbf{a}_{u,a}^\dagger du. \quad (2.24)$$

We obtain correlation functions

$$\langle \mathbf{B}^a(t) \rangle_{\sigma_B} = 0 \quad (2.25)$$

$$\begin{aligned} \langle \mathbf{B}^a(t') \mathbf{B}^b \rangle_{\sigma_B} &= \delta_{ab} \sum_{\bar{u}} \text{Tr} \left[(\text{e}^{i\bar{u}t} \mathbf{a}_{\bar{u},a}^\dagger \mathbf{a}_{\bar{u}} + \text{e}^{-i\bar{u}t} \mathbf{a}_{\bar{u}} \mathbf{a}_{\bar{u},a}^\dagger) |f_{\bar{u}}|^2 \frac{\exp(-\beta\bar{u}\mathbf{a}_{\bar{u},a}^\dagger \mathbf{a}_{\bar{u},a})}{1 + \text{e}^{-\beta\bar{u}}} \right] \\ &= \delta_{ab} \sum_{\bar{u}} (\text{e}^{i\bar{u}t - \beta\bar{u}/2} + \text{e}^{-i\bar{u}t + \beta\bar{u}/2}) |f_{\bar{u}}|^2 \frac{\exp(-\beta\bar{u}/2)}{1 + \text{e}^{-\beta\bar{u}}} \end{aligned} \quad (2.26)$$

$$\stackrel{n_B \rightarrow \infty}{\rightarrow} \langle \mathbf{B}^a(t') \mathbf{B}^b \rangle_{\sigma_B} = \delta_{ab} \int (\text{e}^{iut - \beta u/2} + \text{e}^{-iut + \beta u/2}) |f_u|^2 \frac{\exp(-\beta u/2)}{1 + \text{e}^{-\beta u}} du. \quad (2.27)$$

where the cross term vanishes because different $\mathbf{B}^a \mathbf{B}^b$ acts on factorized Hilbert spaces and each single term correlator vanishes. We also recalled the free Fermionic Gibbs state

$$\sigma_B = \prod_{\bar{u},a} \frac{\exp(-\beta\bar{u}\mathbf{a}_{\bar{u},a}^\dagger \mathbf{a}_{\bar{u},a})}{1 + \text{e}^{-\beta\bar{u}}}. \quad (2.28)$$

The remaining parameters of bath are the functions $f_{\bar{u}}, f'_u$:

$$|f'_u|^2 \frac{\exp(-\frac{\beta u}{2})}{1 + \text{e}^{-\beta u}} := \frac{\text{e}^{-\frac{\beta^2 \Delta_B^2}{8}}}{\sqrt{2\pi \Delta_B^2}} \exp\left(\frac{-u^2}{2\Delta_B^2}\right) \quad (2.29)$$

$$|f_{\bar{u}}|^2 \frac{\exp(-\frac{\beta u}{2})}{1 + \text{e}^{-\beta u}} := \begin{cases} 0 & \text{if } |\bar{u}| \geq \bar{u}_{max} \\ \int_{\bar{u}_-}^{\bar{u}_+} |f'_u|^2 \frac{\exp(-\frac{\beta u}{2})}{1 + \text{e}^{-\beta u}} du. & \text{else.} \end{cases} \quad (2.30)$$

The scale Δ_B is the variation of the energy of the bath, and through Fourier transform implies a timescale $\sim 1/\Delta_B$ of bath decay of correlation.

Proposition II.2.1 (Correlators).

$$\langle \mathbf{B}^{a\dagger}(t') \mathbf{B}^a \rangle_{\sigma_{B'}} = \exp\left(\frac{i\beta\Delta_{B,a}^2 t}{2}\right) \exp\left(-\frac{\Delta_B^2 t^2}{2}\right) + (\text{h.c.}).$$

Proof.

$$\begin{aligned} \langle \mathbf{B}^{a\dagger}(t') \mathbf{B}^a \rangle_{\sigma_{B'}} &= \frac{\text{e}^{-\frac{\beta^2 \Delta_B^2}{8}}}{\sqrt{2\pi \Delta_B^2}} \int_{-\infty}^{\infty} \exp\left(\frac{-u^2}{2\Delta_B^2} - \frac{\beta u}{2} + iut\right) du + \frac{\text{e}^{-\frac{\beta^2 \Delta_B^2}{8}}}{\sqrt{2\pi \Delta_B^2}} \int_{-\infty}^{\infty} \exp\left(\frac{-u^2}{2\Delta_B^2} + \frac{\beta u}{2} - iut\right) du \\ &= \text{e}^{-\frac{\beta^2 \Delta_B^2}{8}} \exp\left(\frac{\beta\Delta_B^2 + i\Delta_B^2 t}{2\Delta_B^2}\right) + (\text{h.c.}). \end{aligned} \quad (2.31)$$

In the first line, the terms correspond to $\mathbf{a}_{\bar{u},a}^\dagger \mathbf{a}_{\bar{u},a}$ and $\mathbf{a}_{\bar{u},a} \mathbf{a}_{\bar{u},a}^\dagger$, respectively. The second equality is a Gaussian integral by completing the square, and our choice of normalization precisely cancels out the $\text{e}^{\beta^2 \Delta_B^2/8}$ term. This is the advertised result. \square

We will also need the integral of the (absolute) two-point correlator.

Proposition II.2.2.

$$\begin{aligned} c' &:= \int_0^\infty \sum_a \|\mathbf{A}^a\|^2 \left| \langle \mathbf{B}^{a\dagger}(t') \mathbf{B}^a \rangle_{\sigma_{B'}} \right| dt' \leq |a| \mathcal{O}\left(\frac{1}{\Delta_B}\right) \\ c(t) &:= \int_0^t \sum_a \|\mathbf{A}^a\|^2 \left| \langle \mathbf{B}^{a\dagger}(t') \mathbf{B}^a \rangle_{\sigma_B} \right| dt' \leq |a| \mathcal{O}\left(\frac{t(t + \beta)\bar{u}_{max}|a|}{n_B} + t \exp\left(-\frac{(\bar{u}_{max} - \beta V/2)^2}{2V}\right) + \frac{1}{\Delta_B}\right). \end{aligned}$$

The correlator with finite bath is actually dominated by $\frac{|a|}{\Delta_B}$ for all our purposes, and the reader should not be distracted by other terms.

Proof. We first evaluate the Fourier transform at an infinite system size limit

$$\int_0^\infty \exp\left(-\frac{\Delta_B^2 t^2}{2}\right) dt = \mathcal{O}\left(\frac{1}{\Delta_B}\right). \quad (2.32)$$

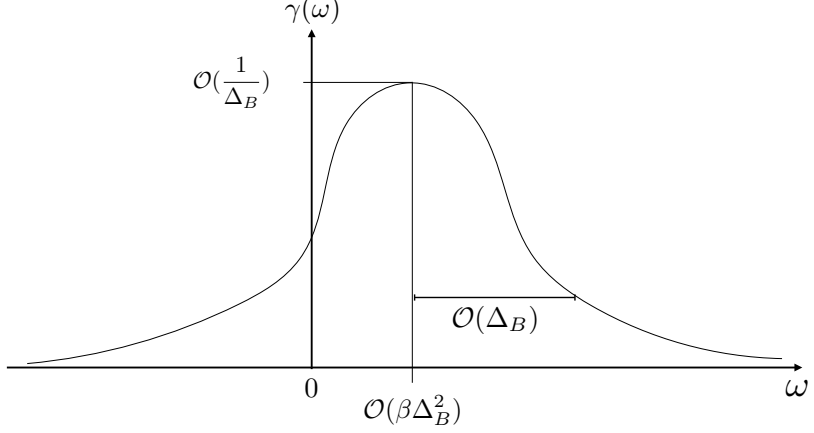


Figure 3. The shape of γ with a tunable parameter Δ_B . Later, for proving convergence with ETH, we can choose Δ_B such that the Gaussian aligns with the ETH transitions $\pm\Delta_{ETH}$.

Next, we compute the finite system size error in the integrand

$$\langle \mathbf{B}^a(t) \mathbf{B}^a \rangle_{\sigma_B} - \langle \mathbf{B}^a(t) \mathbf{B}^a \rangle_{\sigma_{B'}} \quad (2.33)$$

$$= \sum_{\bar{u}} (e^{i\bar{u}t - \beta\bar{u}/2} + e^{-i\bar{u}t + \beta\bar{u}/2}) |f_{\bar{u}}|^2 \frac{\exp(-\beta\bar{u}/2)}{1 + e^{-\beta\bar{u}}} - \int (e^{iut - \beta\bar{u}/2} + e^{-iut + \beta\bar{u}/2}) |f_u|^2 \frac{\exp(-\beta\bar{u}/2)}{1 + e^{-\beta\bar{u}}} du \quad (2.34)$$

$$= \int_{|\bar{u}| \leq \bar{u}_{max}} \left[(e^{i\bar{u}(u)t - \beta\bar{u}(u)/2} + e^{-i\bar{u}(u)t + \beta\bar{u}(u)/2}) - (e^{iut - \beta u/2} + e^{-iut + \beta u/2}) \right] |f_u|^2 \frac{\exp(-\beta u/2)}{1 + e^{-\beta u}} du + \int_{|\bar{u}| > \bar{u}_{max}} (e^{iut - \beta u/2} + e^{-iut + \beta u/2}) |f_u|^2 \frac{\exp(-\beta u/2)}{1 + e^{-\beta u}} du \quad (2.35)$$

$$= \pm \mathcal{O} \left(\frac{(t + \beta)\bar{u}_{max} |a|}{n_B} + \exp\left(-\frac{(\bar{u}_{max} - \beta\Delta_B^2/2)^2}{2\Delta_B^2}\right) \right). \quad (2.36)$$

Together they yield the RHS. \square

Similarly, we can calculate explicitly the functions $\gamma_{aa}(\omega)$, and indeed they satisfy the KMS condition

Proposition II.2.3.

$$\gamma_{ab}(\omega) = \delta_{ab} \frac{1}{\sqrt{2\pi\Delta_B^2}} \exp\left(\frac{-(\omega - \beta\Delta_B^2/2)^2}{2\Delta_B^2}\right) = \gamma_{ba}^*(-\omega) e^{\beta\omega}.$$

In other words, $\gamma_{ab}(\omega)$ has its weight at $\omega \sim [\beta\Delta_B^2 - \Delta_B, \beta\Delta_B^2 + \Delta_B]$ (Fig 3). (Later, we will make it overlap with Δ_{ETH} .)

Proof. Recall the definition (2.7)

$$\gamma_{ab}(\omega) = \int_0^\infty ds e^{i\omega s} \langle \mathbf{B}^{a\dagger}(s) \mathbf{B}^b \rangle_{\sigma_B} + \int_0^\infty ds e^{-i\omega s} \langle \mathbf{B}^{a\dagger}(-s) \mathbf{B}^b \rangle_{\sigma_B} \quad (2.37)$$

$$= \int_{-\infty}^\infty ds e^{i\omega s} \langle \mathbf{B}^{a\dagger}(s) \mathbf{B}^b \rangle_{\sigma_B} \quad (2.38)$$

$$= \delta_{ab} \frac{e^{-\frac{\beta^2\Delta_B^2}{8}}}{\sqrt{2\pi\Delta_B^2}} \exp\left(\frac{-\omega^2}{2\Delta_B^2} + \frac{\beta\omega}{2}\right). \quad (2.39)$$

Complete the square to obtain the advertised result. \square

III. MAIN RESULT I: IMPLEMENTING DAVIES WITH FINITE RESOURCES

Deriving the original Davies' generator requires taking the weak-coupling limit $\lambda \rightarrow 0$, i.e., an infinite run time. In this section, we show that the advertised finitely-resolved Davies' generator approximates iterations of the marginal joint-evolution

$$\mathcal{T}(t)[\rho] := \text{Tr}_B \left[e^{(\mathcal{L}_0^\dagger + \lambda\mathcal{L}_I^\dagger)t} [\rho \otimes \sigma_B] \right]. \quad (3.1)$$

Theorem III.1 (Weak-coupling at finite times.). Assume there are $|a|$ interaction terms in Lindbladian $\sum_a \lambda \mathbf{A}^a \otimes \mathbf{B}^a$. With a quasi-free Fermionic bath, the finitely-resolved Davies' generator at given effective time $\tau = \lambda^2 t$ can be implemented with accuracy ϵ :

$$\forall \rho, \left\| \mathcal{T}(t/\ell)^\ell [\rho] - e^{\bar{\mathcal{L}}^\dagger t} [\rho] \right\|_1 \leq \epsilon, \quad (3.2)$$

for

$$\gamma_{ab}(\omega) = \delta_{ab} \frac{1}{\sqrt{2\pi\Delta_B^2}} \exp\left(\frac{-(\omega - \beta\Delta_B^2/2)^2}{2\Delta_B^2}\right), \quad (3.3)$$

whenever

$$\begin{aligned} \ell &= \theta\left(\frac{|a|^2 \tau^2}{\epsilon \Delta_B^2}\right) && \text{(bath refreshes)} \\ t &= \theta\left(\frac{|a|^2 \tau^2}{\epsilon \Delta_B^2 \bar{\nu}_0}\right) && \text{(total physical runtime)} \\ n_B &= \tilde{\theta}\left(\frac{|a|^2 \tau (\beta \Delta_B^2 + \Delta_B)}{\epsilon \bar{\nu}_0^2}\right) && \text{(size of bath)} \end{aligned}$$

where $\frac{1}{\bar{\nu}_0} = \Omega\left(\frac{|a|\tau}{\epsilon \Delta_B} + \frac{\Delta_B}{|a|}\right)$.

We have phrased the theorem as if we are implementing for a desired effective time τ , and we have chosen the suitable weak-coupling strength λ and resolution $\bar{\nu}_0$. Nevertheless, the approximation holds whenever certain inequalities are satisfied, and see the proof for the complete dependence (Section III A). For example, if one fixes a time t and coupling strength λ , one may infer the appropriate resolution $\bar{\nu}_0$ for which an ϵ approximation holds. This flexibility is the merit of not taking limits. See Section VF for an explicit resource estimate, and Section VG for comments on optimality.

A. Proof of Finitely-resolved Davies' Generator (Theorem III.1)

Proof of Theorem III.1. The proof composes of several simple estimates, and we outline the flow of equations.

$$\begin{aligned} \mathcal{T}_t := \text{Tr}_B \left[e^{(\mathcal{L}_0^\dagger + \lambda \mathcal{L}_I^\dagger)t} [\rho \otimes \sigma_B] \right] &\stackrel{1}{\approx} \text{Tr}_B \left[e^{\mathcal{L}_0^\dagger t} \left(1 + \lambda^2 \int_0^t \int_0^{t_1} \mathcal{L}_I^\dagger(t_1) \mathcal{L}_I^\dagger(t_2) dt_2 dt_1 [\rho \otimes \sigma_B] \right) \right] \\ &\stackrel{2}{\approx} \text{Tr}_{B'} \left[e^{\mathcal{L}_0^\dagger t} \left(1 + \lambda^2 \int_0^t \int_0^{t_1} \mathcal{L}_I^\dagger(t_1) \mathcal{L}_I^\dagger(t_2) dt_2 dt_1 [\rho \otimes \sigma_{B'}] \right) \right] \\ &\stackrel{2.5}{\approx} \text{Tr}_{B'} \left[e^{\mathcal{L}_0^\dagger t} \left(1 + \lambda^2 \int_0^t e^{\mathcal{L}_0^\dagger t_2} \left(\int_{t_2}^t \mathcal{L}_I^\dagger(t_1 - t_2) \mathcal{L}_I^\dagger dt_1 \right) e^{-\mathcal{L}_0^\dagger t_2} dt_2 \right) [\rho \otimes \sigma_{B'}] \right] \\ &\stackrel{3}{\approx} \text{Tr}_{B'} \left[e^{\mathcal{L}_0^\dagger t} \left(1 + \lambda^2 \int_0^t e^{\mathcal{L}_0^\dagger t_2} \left(\int_{t_2}^t \bar{\mathcal{L}}_I^\dagger(t_1 - t_2) \mathcal{L}_I^\dagger dt_1 \right) e^{-\mathcal{L}_0^\dagger t_2} dt_2 \right) [\rho \otimes \sigma_{B'}] \right] \\ &\stackrel{4}{\approx} \text{Tr}_{B'} \left[e^{\mathcal{L}_0^\dagger t} \left(1 + \lambda^2 \int_0^t e^{\mathcal{L}_0^\dagger t_2} \left(\int_0^\infty \bar{\mathcal{L}}_I^\dagger(t') \mathcal{L}_I^\dagger dt_1 \right) e^{-\mathcal{L}_0^\dagger t_2} dt_2 \right) [\rho \otimes \sigma_{B'}] \right] \\ &\stackrel{4.5}{\approx} e^{\mathcal{L}_S^\dagger t + \lambda^2 \bar{K}^\dagger t} [\rho] \\ &\stackrel{5}{\approx} e^{\bar{\mathcal{L}}^\dagger t} [\rho]. \end{aligned}$$

The steps are, in order,

- (1) The interaction picture (Lemma III.3),
- (2) From a finite to an infinite bath ($B \rightarrow B'$),
- (2.5) Rearrangement (3.15),
- (3) Rounding the spectrum of \mathbf{H}_S (Proposition III.3.2),
- (4) A finite-to-infinite time integral (Proposition III.3.3),
- (4.5) Completing the interaction picture (3.18),
- (5) The secular approximation (Lemma III.4).

Let us briefly highlight the intuition for these steps. The idea of weak-coupling, without limit $\lambda \rightarrow \infty$, is really a leading-order approximation in the interaction picture (Step 1); the final form of Lindbladian is the (infinite time) Davies' generator for the rounded Hamiltonian $\bar{\mathbf{H}} = \bar{\nu} \mathbf{H}_\nu$, therefore at some point we approximate $\mathbf{H}_S \rightarrow \bar{\mathbf{H}}_S$ (Step 3); the weak dissipative term in the presence of rapid rotation $\bar{\mathbf{H}}_S$ can be approximated by its time-average. This is the secular approximation (Step 5), with an error depending on the characteristic time scale $\bar{\nu}_0^{-1}$ of Hamiltonian $\bar{\mathbf{H}}_S$.

See below for the accounting for each. Note that (1) interaction picture and (5) secular approximation are only valid for short times, so we have to do a telescoping sum additionally. The total error combines to

$$\|(\mathcal{T}_{t/\ell})^\ell - e^{\bar{\mathcal{L}}^\dagger t}\|_{1-1} \leq \|(\mathcal{T}_{t/\ell})^\ell - e^{i\mathcal{L}_S^\dagger + \lambda^2 \bar{K}^\dagger t}\|_{1-1} + \|e^{i\mathcal{L}_S^\dagger + \lambda^2 \bar{K}^\dagger t} - e^{\bar{\mathcal{L}}^\dagger t}\|_{1-1} \quad (3.4)$$

$$\begin{aligned} &\leq \mathcal{O}\left[\frac{|a|^2 \tau^2}{\Delta_B^2 \ell} + |a| \tau \frac{t}{\ell} \left(\left(\frac{t}{\ell} + \beta\right) \frac{\bar{u}_{max} |a|}{n_B} + \exp\left(-\frac{(\bar{u}_{max} - \beta \Delta_B^2/2)^2}{2\Delta_B^2}\right)\right) \right. \\ &\quad \left. + \frac{|a| \tau}{\Delta_B} \bar{\nu}_0 + \frac{|a| \tau \ell}{\Delta_B t} + \left(\frac{|a|}{\Delta_B} + \bar{\nu}_0\right)^2 \frac{\tau^2}{\bar{\nu}_0 t}\right] \end{aligned} \quad (3.5)$$

where ℓ is the number of refreshes, $\bar{\nu}_0$ is the energy resolution of the final Gibbs state, there are $|a|$ interacting terms, and $\frac{1}{\Delta_B}$ is the characteristic time scale for bath

$$|\langle \mathbf{B}'^{a\dagger}(t) \mathbf{B}'^b \rangle_{B'}| = \mathcal{O}(e^{-\Delta_B^2 t^2/2}). \quad (3.6)$$

The terms in the second and third line, in order, are (1), (2), (3), (4), (5). We simplified the term for (1) since (2) already demands

$$\tau \frac{t}{\ell} |a| \left(\left(\frac{t}{\ell} + \beta\right) \frac{\bar{u}_{max}}{n_B} + \exp\left(-\frac{(\bar{u}_{max} - \beta \Delta_B^2/2)^2}{2\Delta_B^2}\right)\right) \leq \mathcal{O}(\epsilon). \quad (3.7)$$

For a total accuracy ϵ , it suffices to choose

$$\begin{aligned} \ell &= \theta\left(\frac{|a|^2 \tau^2}{\epsilon \Delta_B^2}\right) \\ t &= \theta\left(\frac{|a|^2 \tau^2}{\epsilon \Delta_B^2 \bar{\nu}_0}\right) \\ n_B &= \tilde{\theta}\left(\frac{|a|^2 \tau (\beta \Delta_B^2 + \Delta_B)}{\epsilon \bar{\nu}_0^2}\right) \end{aligned}$$

where

$$\frac{1}{\bar{\nu}_0} = \Omega\left(\frac{|a| \tau}{\epsilon \Delta_B} + \frac{\Delta_B}{|a|}\right),$$

Note that in calculating n_B , we chose that

$$\bar{u}_{max} = \tilde{\theta}(\beta \Delta_B^2 + \Delta_B) \quad (3.8)$$

and $\tilde{\theta}$ suppresses a root-logarithmic dependence (due to the Gaussian decay) on all other parameters $\sqrt{\log(\dots)}$. \square

Here are the error bounds for (1)-(5). The (1) interaction picture and the (5) secular approximation require more work.

1. The interaction picture

We start with the interaction picture

$$\begin{aligned} \text{Tr}_B \left[e^{(\mathcal{L}_0^\dagger + \lambda \mathcal{L}_I^\dagger)t} [\rho \otimes \sigma_B] \right] &= \text{Tr}_B \left[e^{\mathcal{L}_0^\dagger t} \left(1 + \lambda \int_0^t \mathcal{L}_I^\dagger(t_1) dt_1 + \lambda^2 \int_0^t \int_0^{t_1} \mathcal{L}_I^\dagger(t_1) \mathcal{L}_I^\dagger(t_2) dt_2 dt_1 + \dots \right. \right. \\ &\quad \left. \left. + \lambda^m \int_0^t \dots \int_0^{t_{m-1}} \mathcal{L}_I^\dagger(t_1) \dots \mathcal{L}_I^\dagger(t_m) dt_m \dots dt_1 + \dots \right) [\rho \otimes \sigma_B] \right] \end{aligned} \quad (3.9)$$

where $\mathcal{L}_S := -i[\mathbf{H}_S, \cdot]$ denotes the commutator, absorbing the $(-i)$ prefactor. We keep only the second-order term, as the first-order term vanishes and the higher-order terms are subleading in $\tau := \lambda^2 t$.

Fact III.2. If $\text{Tr}_B[\mathbf{B}^a \boldsymbol{\sigma}_B] = 0, \forall a$, then the odd orders vanish, in particular the first order

$$\text{Tr}_B \left[e^{\mathcal{L}_0^\dagger t} \int_0^t \mathcal{L}_I^\dagger(t_1) dt_1 [\boldsymbol{\rho} \otimes \boldsymbol{\sigma}_B] \right] = 0.$$

Lemma III.3 (Davies [14]).

$$\lambda^m \left\| \text{Tr}_B \left[e^{\mathcal{L}_0^\dagger t} \int_0^t \cdots \int_0^{t_{m-1}} \mathcal{L}_I^\dagger(t_1) \cdots \mathcal{L}_I^\dagger(t_m) dt_m \cdots dt_1 [\boldsymbol{\rho} \otimes \boldsymbol{\sigma}_B] \right] \right\|_1 \leq \frac{(c(t)\tau)^{m/2}}{(m/2)!}$$

where

$$c(t) := 4 \int_0^t \sum_{a,b} \|\mathbf{A}^a\| \|\mathbf{A}^b\| |\langle \mathbf{B}^{a\dagger}(t) \mathbf{B}^b \rangle| dt.$$

Proof. Using quasi-freeness, triangle, and Holder's inequality, we obtain a sum over pairings

$$\left\| \text{Tr}_B \left[e^{\mathcal{L}_0^\dagger t} \int_0^t \cdots \int_0^{t_{m-1}} \mathcal{L}_I^\dagger(t_1) \cdots \mathcal{L}_I^\dagger(t_m) dt_m \cdots dt_1 [\boldsymbol{\rho} \otimes \boldsymbol{\sigma}_B] \right] \right\|_1 \quad (3.10)$$

$$\leq \sum_{(\ell_i, r_i)} \int_0^t \cdots \int_0^{t_{m-1}} \prod_i^{m/2} \sum_{a_i, b_i} 2^m \|\mathbf{A}^{a_i}\| \|\mathbf{A}^{b_i}\| |\langle \mathbf{B}^{a_i\dagger}(t_{\ell_i}) \mathbf{B}^{b_i}(t_{r_i}) \rangle| dt_m \cdots dt_1 \quad (3.11)$$

$$= \frac{1}{2^{m/2}(m/2)!} \sum_{\pi \in S_m} \int_0^t \cdots \int_0^{t_{m-1}} \prod_i^{m/2} \sum_{a_i, b_i} 2^m \|\mathbf{A}^{a_i}\| \|\mathbf{A}^{b_i}\| |\langle \mathbf{B}^{a_i\dagger}(t_{\pi(2i)}) \mathbf{B}^{b_i}(t_{\pi(2i-1)}) \rangle| dt_m \cdots dt_1 \quad (3.12)$$

$$= \frac{1}{2^{m/2}(m/2)!} \int_0^t \cdots \int_0^t \prod_i^{m/2} \sum_{a_i, b_i} 2^m \|\mathbf{A}^{a_i}\| \|\mathbf{A}^{b_i}\| |\langle \mathbf{B}^{a_i\dagger}(t_{2i}) \mathbf{B}^{b_i}(t_{2i-1}) \rangle| dt_m \cdots dt_1 \quad (3.13)$$

$$\leq \frac{2^m}{2^{m/2}(m/2)!} \left(t \cdot 2 \int_0^t \sum_{a_i, b_i} \|\mathbf{A}^{a_i}\| \|\mathbf{A}^{b_i}\| |\langle \mathbf{B}^{a_i\dagger}(t) \mathbf{B}^{b_i} \rangle| dt \right)^{m/2}. \quad (3.14)$$

The first equality over-counts the number of pairings by permutation, normalized by the multiplicity. Note that the correlator in absolute value is even in time. The second equality combines the permuted time variables with the time-ordered integral. In the last inequality the integral factorizes, and the factor of 2 comes from a crude estimate. This is the advertised result. \square

The above lemma is at the heart of Davies' derivation of the weak-coupling limit. Crucially, it absorbs half of the t-integral and enables the change of variable $\tau = \lambda^2 t$. However, the higher-order terms behave badly at larger values of τ , and Davies managed to absorb an extra t^ϵ into the correlator. To suppress the higher-order terms at late times, Davies requires the coupling strength $\lambda \rightarrow 0$ to vanish very rapidly. Here, since we are interested in finite values of λ , we must avoid that by keeping τ small. This is why we allow ourselves to refresh the bath. We have not attempted to obtain better control over the higher-order terms, and see Section V G for further discussion on potential improvements.

We move on to massaging the (leading) second-order $\mathcal{O}(\lambda^2)$ term.

2. From a finite to an infinite bath

Next, we replace the finite bath with an infinite bath.

Proposition III.3.1 (Errors from a finite bath).

$$\begin{aligned} \lambda^2 \left| \text{Tr}_B \left[e^{\mathcal{L}_0^\dagger t} \int_0^t \int_0^{t_1} \mathcal{L}_I^\dagger(t_1) \mathcal{L}_I^\dagger(t_2) dt_2 dt_1 \cdot [\boldsymbol{\rho} \otimes \boldsymbol{\sigma}_B] \right] - \text{Tr}_{B'} \left[e^{\mathcal{L}_0^\dagger t} \int_0^t \int_0^{t_1} \mathcal{L}_I^\dagger(t_1) \mathcal{L}_I^\dagger(t_2) dt_2 dt_1 \cdot \boldsymbol{\rho} \otimes \boldsymbol{\sigma}_{B'} \right] \right| \\ \leq \mathcal{O} \left(\tau t \sum_a \|\mathbf{A}^a\|^2 \left(\frac{t \bar{u}_{max} |a|}{n_B} + \exp \left(-\frac{(\bar{u}_{max} - \beta \Delta_B^2/2)^2}{2 \Delta_B^2} \right) \right) \right). \end{aligned}$$

Proof. Expand the commutator

$$\begin{aligned} \text{Tr}_B \left[e^{\mathcal{L}_0^\dagger t} \int_0^t \int_0^{t_1} \mathcal{L}_I^\dagger(t_1) \mathcal{L}_I^\dagger(t_2) dt_2 dt_1 \cdot [\boldsymbol{\rho} \otimes \boldsymbol{\sigma}_B] \right] = \\ \sum_{a,b} \int_0^t \int_0^{t_1} \left([\mathbf{A}^b(t_1), \mathbf{A}^a(t_2) \boldsymbol{\rho}] \cdot \langle \mathbf{B}^b(t_1) \mathbf{B}^a(t_2) \rangle_{\boldsymbol{\sigma}_B} - [\mathbf{A}^b(t_1), \boldsymbol{\rho} \mathbf{A}^a(t_2)] \cdot \langle \mathbf{B}^a(t_2) \mathbf{B}^b(t_1) \rangle_{\boldsymbol{\sigma}_B} \right) dt_2 dt_1, \end{aligned}$$

And recall the finite system size error (Proposition II.2.1) to obtain the advertised result. \square

A great convenience due to an infinite bath is replacing finite time integral to infinite. Rearranging the integration order

$$\lambda^2 \int_0^t \int_0^{t_1} \mathcal{L}_I^\dagger(t_1) \mathcal{L}_I^\dagger(t_2) dt_2 dt_1 = \lambda^2 \int_0^t e^{\mathcal{L}_0^\dagger t_2} \left(\int_{t_2}^t \mathcal{L}_I^\dagger(t_1 - t_2) \mathcal{L}_I^\dagger dt_1 \right) e^{-\mathcal{L}_0^\dagger t_2} dt_2, \quad (3.15)$$

we will soon extend the inner integral to infinite time.

3. Rounding the spectrum

We take a detour on rounding the energy of the system Hamiltonian $\mathbf{H}_S = \bar{\mathbf{H}}_S + \delta\mathbf{H}_S$, with a deviation at most $\|\delta\mathbf{H}_S\| \leq \bar{\nu}_0/2$. The rounded Hamiltonian is a sum over projectors $\bar{\mathbf{H}}_S = \sum_{\bar{\nu}} \bar{\nu} \mathbf{P}_{\bar{\nu}}$ that directly corresponds to the form of Lindbladian.

Technically, we have to round the integrand as the following.

Proposition III.3.2.

$$\begin{aligned} \lambda^2 \left\| \text{Tr}_{B'} \left[\left(\int_0^t \mathcal{L}_I^\dagger(t') \mathcal{L}_I^\dagger dt' - \int_0^t \bar{\mathcal{L}}_I^\dagger(t') \mathcal{L}_I^\dagger dt' \right) \cdot [\rho \otimes \sigma_B] \right] \right\|_1 &\leq 8 \|\delta\mathbf{H}_S\| \cdot \lambda^2 \sum_{a,b} \|\mathbf{A}^a\| \|\mathbf{A}^b\| \int_0^t |\langle \mathbf{B}^a(t') \mathbf{B}^b \rangle| t' dt' \\ &\leq \mathcal{O}\left(\frac{|a| \tau}{t \bar{\nu}_0 \Delta_B}\right) \end{aligned}$$

where $\bar{\mathcal{L}}_I^\dagger(t')[\cdot] := \left[e^{i(\bar{\mathbf{H}}_S + \mathbf{H}_B)t'} H_I e^{-i(\bar{\mathbf{H}}_S + \mathbf{H}_B)t'}, \cdot \right]$.

Note we would do another integral over t .

Proof. Again, expanding the commutator

$$\text{Tr}_B \left[\int_0^{t'} \mathcal{L}_I^\dagger(t') \mathcal{L}_I^\dagger dt' \cdot [\rho \otimes \sigma_B] \right] = \sum_{a,b} \int_0^t \left([\mathbf{A}^b(t'), \mathbf{A}^a \rho] \text{Tr}_B [\mathbf{B}^b(t') \mathbf{B}^a \sigma_B] - [\mathbf{A}^b(t'), \rho \mathbf{A}^a] \text{Tr}_B [\mathbf{B}^a \mathbf{B}^b(t') \sigma_B] \right) dt', \quad (3.16)$$

Rounding \mathcal{L}_I^\dagger amounts to $\|[\mathbf{A}^b(t'), \mathbf{A}^a \rho] - [\mathbf{A}^b(t'), \mathbf{A}^a \rho]\|_1 \leq 2 \|\mathbf{A}^b\| \|\mathbf{A}^a\| \cdot 2 \|\delta\mathbf{H}_S\| t'$, which yields the RHS. \square

4. Infinite time limit

We now extend the inner integral till infinite time.

Proposition III.3.3 (Integral till infinite time.).

$$\begin{aligned} \lambda^2 \left| \text{Tr}_{B'} \left[e^{\mathcal{L}_0^\dagger t} \int_0^t e^{\mathcal{L}_0^\dagger t_2} \left(\int_0^{t-t_2} \bar{\mathcal{L}}_I^\dagger(t') \mathcal{L}_I^\dagger dt' \right) e^{-\mathcal{L}_0^\dagger t_2} dt_2 \right] - \text{Tr}_{B'} \left[e^{\mathcal{L}_0^\dagger t} \int_0^t e^{\mathcal{L}_0^\dagger t_2} \left(\int_0^\infty \bar{\mathcal{L}}_I^\dagger(t') \mathcal{L}_I^\dagger dt' \right) e^{-\mathcal{L}_0^\dagger t_2} dt_2 \right] \right| \\ \leq \lambda^2 \sum_{a,b} 4 \|\mathbf{A}^a\| \|\mathbf{A}^b\| \int_0^t \left(\int_{t_2}^\infty |\langle \mathbf{B}^a(t') \mathbf{B}^b \rangle| dt' \right) dt_2 \\ \leq \mathcal{O}\left(\frac{|a| \tau}{\Delta_B t}\right). \end{aligned}$$

Proof. Expand the commutator and change variable $t - t_2 \rightarrow t_2$ to simplify the integral. Note the above estimate does not depend on $\bar{\mathbf{H}}_S$, which is rounded. \square

Now, the above allows us to compress the dependence on bath into an operator \mathcal{L}^\dagger

$$\text{Tr}_{B'} \left[e^{(\mathcal{L}_0^\dagger + \lambda \mathcal{L}_I^\dagger)t} [\rho \otimes \sigma_{B'}] \right] \approx e^{\mathcal{L}_S^\dagger t} \left(1 + \lambda^2 \int_0^t \bar{K}^\dagger(t_1) dt_1 \right) [\rho] \quad (3.17)$$

$$\approx e^{\mathcal{L}_S^\dagger t + \lambda^2 \bar{K}^\dagger t} [\rho] \quad (3.18)$$

where $\bar{K}^\dagger(t_1) := e^{-\mathcal{L}_S^\dagger t} \bar{K}^\dagger e^{\mathcal{L}_S^\dagger t}$, and

$$\bar{K}^\dagger[\rho] := - \int_0^\infty \text{Tr}_{B'} \left[e^{i(\bar{\mathbf{H}}_S + \mathbf{H}_{B'})t'} H_I e^{-i(\bar{\mathbf{H}}_S + \mathbf{H}_{B'})t'}, [\mathbf{H}_I, \rho \otimes \sigma_{B'}] \right] dt'. \quad (3.19)$$

The second approximation is ‘‘completing’’ the interaction picture, using again that multipoint function factorizes for the infinite system (Lemma III.3).

$$\left\| e^{\mathcal{L}_S^\dagger t} \left(1 + \int_0^t \bar{K}^\dagger(t_1) dt_1 \right) [\rho] - e^{\mathcal{L}_S^\dagger t + \lambda^2 \bar{K}^\dagger t} [\rho] \right\| \leq \mathcal{O}((c_K \tau)^2) \quad (3.20)$$

where

$$\|\bar{K}^\dagger\|_{1-1} \leq c_K = 4 \int_0^\infty \sum_{a,b} \|\mathbf{A}^a\| \|\mathbf{A}^b\| |\langle \mathbf{B}'^a(t') \mathbf{B}'^b \rangle| dt' \leq \mathcal{O}\left(\frac{|a|}{\Delta_B}\right) \quad (3.21)$$

5. The secular approximation

Lemma III.4 (The secular approximation). *For $\mathbf{H}_S = \bar{\mathbf{H}}_S + \delta \mathbf{H}_S$, let $\bar{K}'^\dagger := \bar{K}^\dagger + \delta \mathcal{L}_S^\dagger$ and $\theta := \tau_s \|\bar{K}'^\dagger\|_{1-1}$. Then for $\theta/(\bar{\nu}_0 t_s) \leq \frac{1}{2}$,*

$$\left\| e^{\mathcal{L}_S^\dagger t_s + \lambda^2 \bar{K}^\dagger t_s} - e^{\mathcal{L}_S^\dagger t_s + \lambda^2 \bar{K}_{sec}^\dagger t_s} \right\|_{1-1} \leq \mathcal{O}(1) \cdot \frac{1}{\bar{\nu}_0 t_s} (\theta + \theta^2 e^\theta),$$

where the secular approximation is w.r.t the rounded $\bar{\mathcal{L}}_S^\dagger$

$$\bar{K}_{sec}^\dagger := \lim_{T \rightarrow \infty} \frac{1}{2T} \int_{-T}^T e^{-\bar{\mathcal{L}}_S^\dagger t'} \bar{K}^\dagger e^{\bar{\mathcal{L}}_S^\dagger t'} dt'.$$

Note the exponential e^θ essentially set a time scale $t_s \sim (\lambda^2 \|\bar{K}'^\dagger\|_{1-1})^{-1}$ after which the bound becomes vacuous. Therefore, we would use the bound for short time intervals $t_s = t/\ell_s$, for an ℓ_s such that $\theta = \tau/\ell_s \cdot \|\bar{K}'^\dagger\|_{1-1} = \mathcal{O}(1)$. Note that ℓ_s is different from the number of refreshes ℓ . The total error accumulates to

$$\ell_s \cdot \frac{1}{\bar{\nu}_0 t_s} = \mathcal{O}\left(\frac{\|\bar{K}'^\dagger\|_{1-1}^2 \tau^2}{\bar{\nu}_0 t}\right) = \mathcal{O}\left((\frac{|a|}{\Delta_B} + \bar{\nu}_0)^2 \frac{\tau^2}{\bar{\nu}_0 t}\right). \quad (3.22)$$

Proof. The proof uses a Fourier series (or linear combination of unitaries) argument. In the following we absorb $\bar{K}^\dagger + \delta \mathcal{L}_S^\dagger =: \bar{K}'^\dagger$, and $\bar{K}_{sec}^\dagger + \delta \mathcal{L}_S^\dagger =: \bar{K}_{sec}'^\dagger$. (I) We first illustrate the proof strategy on the linear term in the interaction picture in the eigenbasis of $\bar{\mathcal{L}}_S^\dagger$. Since the Bohr frequencies are integer multiples $n_i \bar{\nu}_0$

$$\left(\int_0^t \bar{K}'^\dagger(t_1) dt_1 - \int_0^t \bar{K}_{sec}'^\dagger(t_1) dt_1 \right)_{ij} = \bar{K}_{ij}'^\dagger \frac{e^{-i(n_i - n_j)\bar{\nu}_0 t} - 1}{-i(n_i - n_j)\bar{\nu}_0} \delta_{n_i \neq n_j}. \quad (3.23)$$

Now, consider the Fourier series for the function

$$f(n) = \frac{e^{-in\bar{\nu}_0 t} - 1}{-in\bar{\nu}_0} \delta_{n \neq 0} = \frac{1}{2\pi} \int_0^{2\pi} \tilde{f}(\theta) e^{in\theta} d\theta, \quad (3.24)$$

which allows us to rewrite (3.23) as a linear combination of time-evolved operators

$$\bar{K}_{ij}'^\dagger \frac{e^{-i(n_i - n_j)\bar{\nu}_0 t} - 1}{-i(n_i - n_j)\bar{\nu}_0} \delta_{n_i \neq n_j} = \frac{1}{2\pi} \bar{K}_{ij}'^\dagger \int_0^{2\pi} \tilde{f}(\theta) e^{i(n_i - n_j)\theta} d\theta \quad (3.25)$$

$$= \frac{1}{2\pi} \int_0^{2\pi} \bar{K}'^\dagger(\bar{\nu}_0 \theta)_{ij} \tilde{f}(\theta) d\theta. \quad (3.26)$$

Therefore, the linear term (in 1-1 norm) can be bounded by

$$\left\| \frac{1}{2\pi} \int_0^{2\pi} \bar{K}'^\dagger(\bar{\nu}_0 \theta) \tilde{f}(\theta) d\theta \right\|_{1-1} \leq \|\bar{K}'^\dagger\|_{1-1} \frac{1}{2\pi} \int_0^{2\pi} |\tilde{f}(\theta)| d\theta \leq \|\bar{K}'^\dagger\|_{1-1} \sqrt{\sum_n |f(n)|^2} \leq \|\bar{K}'^\dagger\|_{1-1} \frac{4}{\bar{\nu}_0} \frac{\pi}{\sqrt{6}}, \quad (3.27)$$

using that Fourier series preserve inner-product, Cauchy-Schwartz, and the identity $\sum_1^\infty 1/n^2 = \pi^2/6$.

(II) For the higher-order terms, consider a telescoping sum

$$\begin{aligned} & \int_0^t \cdots \int_0^{t_{m-1}} \bar{K}'^\dagger(t_1) \cdots \bar{K}'^\dagger(t_m) dt_m \cdots dt_1 - \int_0^t \cdots \int_0^{t_{m-1}} \bar{K}_{sec}'^\dagger \cdots \bar{K}_{sec}'^\dagger dt_m \cdots dt_1 \\ &= \sum_{\ell=1}^m \int_0^t \cdots \int_0^{t_{m-1}} \bar{K}'^\dagger(t_1) \cdots (\bar{K}'^\dagger(t_\ell) - \bar{K}_{sec}'^\dagger) \bar{K}_{sec}'^\dagger \cdots dt_m \cdots dt_1. \end{aligned} \quad (3.28)$$

Since \bar{K}'^\dagger_{sec} are independent of time, we can evaluate the inner integrals

$$\left(\int_0^{t_{\ell-1}} \cdots \int_0^{t_{m-1}} (\bar{K}'^\dagger(t_\ell) - \bar{K}'^\dagger_{sec}) dt_m \cdots dt_\ell \right)_{ij} = \left(\int_0^{t_{\ell-1}} (\bar{K}'^\dagger(s) - \bar{K}'^\dagger_{sec}) \frac{s^{m-\ell}}{(m-\ell)!} ds \right)_{ij} \quad (3.29)$$

$$= \delta_{n_i \neq n_j} \int_0^{t_{\ell-1}} \bar{K}'^\dagger_{ij} e^{-i(n_i - n_j)\bar{\nu}_0 t} \frac{t^{m-\ell}}{(m-\ell)!} dt \quad (3.30)$$

$$= \frac{-e^{-i(n_i - n_j)\bar{\nu}_0 t_{\ell-1}}}{\bar{\nu}_0^{m-\ell+1}} \sum_{q=0}^{m-\ell} \frac{1}{(i(n_i - n_j))^{m-\ell-q+1}} \frac{(\bar{\nu}_0 t_{\ell-1})^q}{q!} \quad (3.31)$$

$$=: \frac{1}{2\pi} \bar{K}'^\dagger_{ij} \int_0^{2\pi} \tilde{f}(\theta) e^{i(n_i - n_j)\theta} d\theta \quad (3.32)$$

where the third equality is the elementary integration by parts formula.

Fact III.5. $\int_0^a e^{x \frac{x^k}{k!}} dx = e^a (-1)^k \sum_{q=0}^k \frac{(-a)^q}{q!}$.

Again, by a Fourier series argument,

$$\left\| \int_0^{t_{\ell-1}} \cdots \int_0^{t_{m-1}} (\bar{K}'^\dagger(t_j) - \bar{K}'^\dagger_{sec}) dt_j \cdots dt_1 \right\|_{1-1} \leq \|\bar{K}'^\dagger\|_{1-1} \left(\frac{1}{2\pi} \int_0^{2\pi} |\tilde{f}(\theta)|^2 d\theta \right)^{1/2} \quad (3.33)$$

$$\leq \|\bar{K}'^\dagger\|_{1-1} \frac{1}{\bar{\nu}_0^{m-\ell+1}} \cdot \sum_{q=0}^{\ell-m} \sqrt{\sum_n^{\infty} \frac{1}{n^{2(m-\ell-q+1)}} \frac{(\bar{\nu}_0 t_{\ell-1})^q}{q!}} \quad (3.34)$$

$$\leq \|\bar{K}'^\dagger\|_{1-1} \frac{1}{\bar{\nu}_0^{m-\ell+1}} \frac{\pi}{\sqrt{6}} \cdot \sum_{q=0}^{\ell-m} \frac{(\bar{\nu}_0 t_{\ell-1})^q}{q!}. \quad (3.35)$$

Completing the remaining integrals, we now have the m -th order bound

$$\begin{aligned} & \left\| \int_0^t \cdots \int_0^{t_{m-1}} \bar{K}'^\dagger(t_1) \cdots \bar{K}'^\dagger(t_m) dt_m \cdots dt_1 - \int_0^t \cdots \int_0^{t_{m-1}} \bar{K}'^\dagger_{sec} \cdots \bar{K}'^\dagger_{sec} dt_m \cdots dt_1 \right\|_{1-1} \\ & \leq \frac{\|\bar{K}'^\dagger\|_{1-1}^m}{\bar{\nu}_0^m} \frac{\pi}{\sqrt{6}} \sum_{\ell=1}^m \sum_{q=\ell-1}^{m-1} \frac{(\bar{\nu}_0 t)^q}{q!} \\ & = \frac{\|\bar{K}'^\dagger\|_{1-1}^m}{\bar{\nu}_0^m} \frac{\pi}{\sqrt{6}} \sum_{q=0}^{m-1} \frac{(q+1)(\bar{\nu}_0 t)^q}{q!}. \end{aligned} \quad (3.36)$$

Finally, rearrange

$$\left\| e^{\mathcal{L}_S^\dagger t + \lambda^2 \bar{K}'^\dagger t} - e^{\mathcal{L}_S^\dagger t + \lambda^2 \mathcal{D} t} \right\|_{1-1} \leq \frac{2\pi}{\sqrt{6}} \sum_{m=1}^{\infty} \frac{(\lambda^2 \|\bar{K}'^\dagger\| t)^m}{(\bar{\nu}_0 t)^m} \sum_{q=0}^{m-1} \frac{(\bar{\nu}_0 t)^q}{(q-1)!} \quad (3.37)$$

$$= \frac{2\pi}{\sqrt{6}} \sum_{q=0}^{\infty} \frac{(\bar{\nu}_0 t)^q}{(q-1)!} \sum_{m=q+1}^{\infty} \frac{(\lambda^2 \|\bar{K}'^\dagger\|_{1-1} t)^m}{(\bar{\nu}_0 t)^m} \quad (3.38)$$

$$\leq \frac{4\pi}{\bar{\nu}_0 t \sqrt{6}} \sum_{q=0}^{\infty} \frac{(\lambda^2 \|\bar{K}'^\dagger\|_{1-1} t)^{q+1}}{(q-1)!} \quad (3.39)$$

$$\leq \frac{4\pi}{\bar{\nu}_0 t \sqrt{6}} \left(\lambda^2 \|\bar{K}'^\dagger\|_{1-1} t + (\lambda^2 \|\bar{K}'^\dagger\|_{1-1} t)^2 e^{\lambda^2 \|\bar{K}'^\dagger\|_{1-1} t} \right), \quad (3.40)$$

where in the second inequality, we sum the geometric series using the assumption $\frac{\lambda^2 \|\bar{K}'^\dagger\|_{1-1} t}{\bar{\nu}_0 t} \leq \frac{1}{2}$, which concludes the proof. \square

Lastly, in this finitely-resolved Lindbladian, it remains to calculate the explicit forms

Fact III.6 ([16]).

$$\lim_{T \rightarrow \infty} \frac{1}{2T} \int_{-T}^T e^{i\bar{\mathcal{L}}_S t'} \bar{K} e^{-i\bar{\mathcal{L}}_S t'} dt' = \mathcal{L}_{LS} + \mathcal{D}$$

where $\mathcal{L}_{LS}, \mathcal{D}$ are as in Theorem III.1.

IV. PRELIMINARIES FOR PROOFS OF FAST CONVERGENCE

We collect the preliminaries for proofs of fast convergence.

A. Modified Log Sobolev Inequality

To keep our discussion self-contained, we instantiate the minimal facts as well as references; this is not intended to be a complete introduction. Recall a (finite-dimensional, unital) von Neumann algebra \mathcal{M} is an algebra with involution and identity

$$\begin{aligned}\forall \mathbf{X}, \mathbf{Y} \in \mathcal{M}, \mathbf{X} + \mathbf{Y} \in \mathcal{M} \\ \forall \mathbf{X}, \mathbf{Y} \in \mathcal{M}, \mathbf{XY} \in \mathcal{M} \\ \forall \mathbf{X} \in \mathcal{M}, \mathbf{X}^* \in \mathcal{M} \\ \forall \lambda \in \mathbb{C}, \lambda \mathbf{I} \in \mathcal{M}.\end{aligned}$$

For an subalgebra $\mathcal{N} \subset \mathcal{M}$, a *conditional expectation* $E_{\mathcal{N}} : B(\mathcal{H}) \rightarrow \mathcal{N}$ is a completely positive unital map that

$$\begin{aligned}\forall \mathbf{a} \in \mathcal{N}, E_{\mathcal{N}}[\mathbf{a}] = \mathbf{a} \\ \forall \mathbf{a}, \mathbf{b} \in \mathcal{N}, E_{\mathcal{N}}[\mathbf{a}\mathbf{X}\mathbf{b}] = \mathbf{a}E[\mathbf{X}]\mathbf{b},\end{aligned}$$

and $E_{\mathcal{N}}^\dagger$ as the adjoint (w.r.t $\text{Tr}[\cdot]$) is a CPTP (channel), i.e.

$$\forall \mathbf{X}, \mathbf{Y} \in \mathcal{B}(\mathcal{H}), \text{Tr}[\mathbf{Y}E_{\mathcal{N}}^\dagger \mathbf{X}] = \text{Tr}[E[\mathbf{Y}]\mathbf{X}]. \quad (4.1)$$

Consider relative entropy for pair of states $\text{Supp}(\boldsymbol{\rho}) \subset \text{Supp}(\boldsymbol{\sigma})$

$$D(\boldsymbol{\rho} || \boldsymbol{\sigma}) = \text{Tr}[\boldsymbol{\rho}(\ln(\boldsymbol{\rho}) - \ln(\boldsymbol{\sigma}))].$$

For Lindbladian $\mathcal{L} : \mathcal{M} \rightarrow \mathcal{M}$, it is said to satisfy *Modified Log Sobolev inequality with constant α* if

$$\alpha D(\boldsymbol{\rho} || E^\dagger[\boldsymbol{\rho}]) \leq -\frac{d}{dt} D(e^{\mathcal{L}^\dagger t}[\boldsymbol{\rho}] || E^\dagger[\boldsymbol{\rho}]) = \text{Tr}[\mathcal{L}^\dagger[\boldsymbol{\rho}](\ln(\boldsymbol{\rho}) - \ln(E^\dagger[\boldsymbol{\rho}]))], \quad (4.2)$$

where E is the projection onto the fixed point algebra of \mathcal{L}

$$\lim_{t \rightarrow \infty} e^{\mathcal{L}^\dagger t} =: E. \quad (4.3)$$

And note that one can choose an arbitrary stationary (or invariant) state $\boldsymbol{\omega}, E^\dagger[\boldsymbol{\omega}] = \boldsymbol{\omega}$ so that [11, Lemma 2]

$$\text{Tr}[\mathcal{L}^\dagger[\boldsymbol{\rho}](\ln(\boldsymbol{\rho}) - \ln(E^\dagger[\boldsymbol{\rho}]))] = \text{Tr}[\mathcal{L}^\dagger[\boldsymbol{\rho}](\ln(\boldsymbol{\rho}) - \ln(\boldsymbol{\omega}))]. \quad (4.4)$$

In other words, an MLSI gives handy bounds on convergence to the stationary state $\boldsymbol{\sigma} = E^\dagger[\boldsymbol{\sigma}]$, measured by relative entropy. It converts to trace distance

$$\left\| e^{\mathcal{L}^\dagger t}[\boldsymbol{\rho}] - \boldsymbol{\sigma} \right\|_1 \leq e^{-\alpha(\mathcal{L})t} \cdot \sqrt{2 \ln(\|\boldsymbol{\sigma}^{-1}\|)} \quad (4.5)$$

through Pinsker's inequality $\|\boldsymbol{\rho} - \boldsymbol{\sigma}\|_1^2 \leq 2D(\boldsymbol{\rho} || \boldsymbol{\sigma})$ and initial relative entropy estimate $D(\boldsymbol{\rho} || \boldsymbol{\sigma}) \leq \ln(\|\boldsymbol{\sigma}^{-1}\|)$.

Often the total Lindbladian has constituents which we understand individually. A recent development called *approximation tensorization* of relative entropy allows us to estimate the *global* MLSI constant from the *local* ones¹⁰.

Fact IV.1 (Approximate Tensorization [35, 36]). *Consider subalgebras $\mathcal{N}_1, \dots, \mathcal{N}_\ell \subset \mathcal{B}(\mathcal{H})$ and the intersection $\mathcal{N} := \cap_i \mathcal{N}_i$. For some conditional expectations $E_{\mathcal{N}} : \mathcal{B}(\mathcal{H}) \rightarrow \mathcal{N}$, $E_i : \mathcal{B}(\mathcal{H}) \rightarrow \mathcal{N}_i$, consider some common invariant state $\boldsymbol{\sigma}$ that $E_{\mathcal{N}}^\dagger[\boldsymbol{\sigma}] = \boldsymbol{\sigma}$, $E_i^\dagger[\boldsymbol{\sigma}] = \boldsymbol{\sigma}$. Then*

$$D(\boldsymbol{\rho} || E^\dagger[\boldsymbol{\rho}]) \leq \frac{2k}{1 - e^2(2 \ln(2) - 1)^{-1}} \frac{1}{m} \sum_{i=1}^m \sum_{s \in S_i} D(\boldsymbol{\rho} || E_s^\dagger[\boldsymbol{\rho}]) \quad (4.6)$$

whenever k satisfies

$$(1 - \epsilon)E_{\mathcal{N}} \leq_{cp} (\Phi^\dagger)^k \leq_{cp} (1 + \epsilon)E_{\mathcal{N}}, \quad (4.7)$$

¹⁰ We thank Cambyse Rouzé for related discussions about [35].

where the inequality denotes completely positive order. Φ^\dagger can be an average of products of conditional expectations corresponding to any regrouping into disjoint subsets $\{1, \dots, \ell\} = S_1 \perp \dots \perp S_m$

$$\Phi^\dagger := \sum_{i=1}^m \frac{1}{2m} \left(\prod_{s \in S_i}^{\rightarrow} E_s + \prod_{s \in S_i}^{\leftarrow} E_s \right). \quad (4.8)$$

The product $\prod_{s \in S_i}^{\rightarrow}$ can take arbitrary order as long as $\prod_{s \in S_i}^{\leftarrow}$ is reversed.

The above is well known to imply global MLSI constants. Note that while we require the completely positive order for Φ^\dagger , we do not need a *complete* MLSI constant [35]. All the MLSI constants discussed in this paper do not consider ancillae.

Corollary IV.1.1 (Global MLSI from local). *In the setting of Fact IV.1,*

$$\alpha(\mathcal{L}) \geq \frac{1 - \epsilon^2(2 \ln(2) - 1)^{-1}}{2k} m \min_i \alpha_i(\mathcal{L}_i).$$

Proof. Following the arguments in [35],

$$\begin{aligned} \sum_{i=1}^{\ell} D(\rho || E_i^\dagger[\rho]) &\leq \sum_{i=1}^{\ell} \frac{1}{\alpha_i} \text{Tr}[\mathcal{L}_i^\dagger[\rho](\ln(\rho) - \ln(\sigma))] \\ &\leq \sum_{i=1}^{\ell} \frac{1}{\min_i \alpha_i} \text{Tr}[\mathcal{L}_i^\dagger[\rho](\ln(\rho) - \ln(\sigma))] \\ &\leq \frac{1}{\min_i \alpha_i} \text{Tr}[\mathcal{L}^\dagger[\rho](\ln(\rho) - \ln(\sigma))]. \end{aligned}$$

First, we use the freedom to choose an arbitrary invariant state (4.4). Lastly, we use that all conditional expectations share some common invariant state. Rearrange to obtain the advertised result. \square

B. Assumptions for the Eigenstate Thermalization Hypothesis and the Density of States

Let us be frank that the calculation will be pretty messy and would be impossible without $\mathcal{O}(\cdot), \Omega(\cdot)$ notations. Meanwhile, this reflects the flexibility of our arguments coming from the parameters in ETH and the density of states. This section collects the assumptions we make as an attempt to strike a balance between concreteness and flexibility.

1. ETH

ETH is a massive subject with various adaptations and loose ends (see, e.g., [2] for a review). Let us give a brief review of the original ETH prescription of Srednicki.

Hypothesis IV.1 (Srednicki's ETH [1]). *Consider a Hamiltonian \mathbf{H} and some suitable observable \mathbf{A} . For energies ν_i, ν_j and their eigenstates $|\psi_i\rangle, |\psi_j\rangle$ of \mathbf{H} ,*

$$A_{ij} = \langle \psi_i | \mathbf{A} | \psi_j \rangle = O_{\mathbf{A}}(\mu) \delta_{ij} + \frac{1}{\sqrt{\dim(\mathbf{H}) \cdot D(\mu)}} f_{\mathbf{A}}(\mu, \omega) r_{ij}$$

where $\mu = (\nu_i + \nu_j)/2$, $\omega = \nu_i - \nu_j$, $D(\cdot)$ is the normalized density of states, $\dim(\mathbf{H}) = \text{Tr}[\mathbf{I}]$ is the dimension of the Hilbert space, and r_{ij} are random variables satisfying $\mathbb{E}[r_{ij}] = 0, \mathbb{E}[r_{ij}^2] = 1$. $O(\mu)$ and $f_{\mathbf{A}}(\mu, \omega)$ are smooth functions of the energies.

The *diagonal* prescriptions, as vague as it is, give a transparent explanation that time-averaging is equal to thermal averaging

$$\bar{\mathbf{A}} := \frac{1}{T} \int_0^T \langle \phi | \mathbf{A}(t) | \phi \rangle dt = \frac{1}{T} \int_0^T \sum_{i,j} c_i^* c_j e^{i(\nu_i - \nu_j)t} \mathbf{A}_{ij} dt \quad (4.9)$$

$$\stackrel{T \rightarrow \infty}{=} \sum_i |O(\nu_i)|^2 \mathbf{A}_{ii} \approx \langle \mathbf{A} \rangle_{\sigma_{\beta}}. \quad (4.10)$$

The last approximation holds if the energies of the test wave function $|\phi\rangle$ and the Gibbs state σ_{β} are both sufficiently narrow. This usually goes by the saying that “even a (generic) eigenstate behaves like a Gibbs state” and has been observed in numerics (see, e.g., [2]) and proven in suitable models [11, 39].

The *off-diagonal* prescriptions explain that the typical fluctuations over time are suppressed by the dimension of the Hilbert space¹¹

$$\frac{1}{T} \int_0^T (\langle \phi | \mathbf{A}(t) | \phi \rangle - \bar{\mathbf{A}})^2 dt = \frac{1}{T} \int_0^T \sum_{i,j} c_i^* c_j e^{i(\nu_i - \nu_j)t} \sum_{k,\ell} c_k^* c_\ell e^{i(\nu_k - \nu_\ell)t} \mathbf{A}_{ij} \mathbf{A}_{k\ell} dt \quad (4.11)$$

$$\stackrel{T \rightarrow \infty}{=} \sum_{i,j} |c_i|^2 |c_j|^2 |\mathbf{A}_{ij}|^2 = \mathcal{O}(e^{-\Omega(n)}). \quad (4.12)$$

The second equality holds under the non-degenerate condition that $\nu_i - \nu_j + \nu_k - \nu_\ell = 0$ is only satisfied with $i = j, k = \ell$ or $i = \ell, k = j$.

However, there remain many unspecified parameters in the original ETH. Much of the subsequent works attempted to justify and specify. We incorporated some of them into our version of ETH.

Hypothesis IV.2 (ETH for this work). *Consider a Hamiltonian \mathbf{H} and a set of k -local Hermitian operators \mathbf{A}^a . We say they satisfy ETH if:*

- It satisfies the original ETH for nearby energies $|\nu_i - \nu_j| \leq \Delta_{ETH}$.
- The random variables for entries i, j and operators \mathbf{A}^a are drawn from independent complex Gaussians $r_{ij}(a) \rightarrow g_{ij}(a)$ (up to the Hermitian constraint).
- The function depends only on the energy difference ω

$$f_{\mathbf{A}}(\mu, \omega) = f_{\omega}, \min_{\omega \leq \Delta_{ETH}} |f_{\omega}| = \theta(\max_{\omega \leq \Delta_{ETH}} |f_{\omega}|) = \theta(\frac{1}{n^{1/d}}).$$

Let us elaborate on the parameters we just filled in. We take the “suitable” observables to be k -local for constant k comparing with the system size $k \ll n$ (i.e., few-body), but not necessarily spatially localized. This is observed numerically (see, e.g., [2]).

As advertised, we explicitly introduce a random matrix theory prescription, which will feature in our proof. Of course, strictly speaking, there is no obvious source of randomness in any given Hamiltonian. Nevertheless, as commonly done in ETH literature [2, 26] (which goes back to Wigner [25]), we *model* the near diagonal band of different operators \mathbf{A}^a as if drawn independently from the complex Gaussian distribution and then *fixed* for the rest of the calculation. We are satisfied if the desired quantities take a universal value for typical samples, i.e., if it *concentrates*.

However, this is a strong requirement¹² that can only be self-consistently imposed in a (small) energy window Δ_{ETH} , and constrained by the time-scale of equilibrium of observable (see, e.g., [26] for further discussions and numerical evidences [40, 41]). Its value remains unsettled (Figure 6), and plausible suggestions are such as [2, 26]

$$\Delta_{ETH} \stackrel{?}{=} \theta(\frac{1}{n^3}), \theta(\frac{1}{n^2}) \quad (4.13)$$

for 1d nearest-neighbor spin systems. Regardless, it does not change the qualitative message of this work and will be kept as the parameter Δ_{ETH} in our calculations. Lastly, we assume the function is only dependent on the energy difference ω , and f_{ω} is pretty flat for $\omega \leq \Delta_{ETH}$, which will greatly simplify the calculations.¹³ Our choice of its numerical value adapts from an ansatz[2, Sec. 4.3]

$$|f_{\omega}|^2 = \begin{cases} \theta(n^{1/d}) & \text{if } \omega = \mathcal{O}(\frac{1}{n^{1/d}}) \\ (“small”) & \text{else.} \end{cases} \quad (4.14)$$

The above is all that we will use to prove thermalization at finite times. For our calculations, we do not need the prescription for the diagonal entries (which has traditionally attracted more discussion); we do not care if the other entries outside the window Δ_{ETH} violate ETH or RMT.

2. The density of states

The density of states is a somewhat flexible parameter that goes into ETH and the random walk on the spectrum.

¹¹ This does not seem to be the best use of RMT.

¹² Technically, our proof only uses RMT within each pair of energies $\bar{\nu}_1, \bar{\nu}_2$, and do not need independence across blocks as we only use a crude union bound.

¹³ When f depends on the energy μ , the convergence rate may depend on temperature. Otherwise, we do not expect qualitative change to the convergence result.

Hypothesis IV.3 (relative ratios of density at the scale Δ_{ETH}). (A) *The spectrum can be treated as continuous that the density $D(\omega)$ is well-defined.* (B) *For any $|\nu - \nu'| \leq \Delta_{ETH}$,*

$$\frac{D(\nu)}{D(\nu')} \leq R(\Delta_{ETH}, \bar{\nu}_0) =: R.$$

The continuum assumptions (A) simplify the notation, and it is reasonable whenever the system size is large. The density ratio R should be thought of as a global constant in the thermodynamics limit. These two assumptions are, in fact, implicit in ETH: when the spectrum exhibits finite-size effects or when the density ratio becomes large, then the ETH ansatz already needs corrections. In addition, the relative ratio of densities plays a role in concentration arguments for quantum expanders. There, if two frequencies ν_1, ν_2 have too disparate density of states, then will we need more flips $|a|$ to ensure a gap. What this practically mean is that we would choose a small enough Δ_{ETH} so that R remain $\mathcal{O}(1)$.

However, the above assumption breaks down near the extreme eigenvalues of any finite-size system. To avoid mundane technical issues, we quickly patch another assumption to focus on the bulk of the spectrum by truncation (Figure 4).

Assumption IV.1 (A truncated spectrum). *The spectrum has a sharp cut-off.*

To justify the sharp artificial cut-off, imagine starting with the original Hamiltonian \mathbf{H}' whose bulk of spectrum, containing all but exponentially rare states, satisfies ETH. Then, we truncate the Hamiltonian $\mathbf{H}' \rightarrow \mathbf{H}$ so that \mathbf{H} lies in the validity of ETH. So long as $\dim(\mathbf{H})/\dim(\mathbf{H}') \rightarrow 1$ in the thermodynamic limit (saying a tiny portion $\sim e^{-\Omega(n)}$ was truncated), the Gibb states (away from the ground state) should be very close. Further, during the run time of Lindbladian (or Metropolis Sampling), a state initialized in the bulk should have very low chances to leave the bulk of the spectrum. In other words, \mathbf{H} can represent \mathbf{H}' for most purposes, but we do not further formalize this part.

Otherwise, if we do not truncate the Hamiltonian, there could be regimes that ETH does not hold, and/or the density of states becomes very low. A state initialized at such energies may be stuck forever. This is not an ETH phenomenon, nor the scope of this work.

We lastly assume a rather generic characterization of the density of the *Gibbs state* (i.e. $D_{\sigma}(\nu) \propto e^{-\beta\nu} D(\nu)$) to give conductance estimates. This should not be confused with the density of states $D(\nu)$.

Assumption IV.2 (The Gibbs distribution with a characteristic scale Δ_{spec}). *We assume the Gibbs state σ satisfies the following: (A) There exists an interval $I_{bulk} = [E_L, E_R]$ that contains more than half of the weight such that for all $\nu \in I_{bulk}$,*

$$D_{\sigma}(\nu) = \theta\left(\frac{1}{\Delta_{spec}}\right).$$

(B) *The tail $I_R = [E_R, \infty]$ is decaying that for all $\nu \in I_R$,*

$$\int_{\nu}^{\infty} D_{\sigma}(\nu') d\nu' = \mathcal{O}\left(\frac{D_{\sigma}(\nu)}{\Delta_{spec}}\right),$$

and similarly for I_L .

These conditions guarantee a gap of $\text{Poly}(R, e^{\beta\Delta_{ETH}}) \cdot \Omega(\Delta_{ETH}^2/\Delta_{spec}^2)$ for the classical random walk on the spectrum with step size $\sim \Delta_{ETH}$ (Appendix B 1). Intuitively, the assumption makes sure the Gibb distribution has “no bottlenecks”(Figure 4).

3. Example: Gaussian density of state

An example that satisfies the above assumptions is a Gaussian density of states, centered at zero, truncated at $\pm \frac{\|\mathbf{H}\|}{2}$.

$$D(\nu) \propto \begin{cases} N_0 \cdot \exp\left(\frac{-\nu^2}{2\Delta_{spec}^2}\right) & \text{if } \nu \in \left[-\frac{\|\mathbf{H}\|}{2}, \frac{\|\mathbf{H}\|}{2}\right] \\ 0 & \text{else.} \end{cases} \quad (4.15)$$

where N_0 is a normalization factor. Let us choose concretely that $\Delta_{spec} = \sqrt{n}$, $\|\mathbf{H}\| = 2n$. Then we can check the relative ratios (Assumption IV.3)

$$\frac{D(\nu)}{D(\nu')} = \exp\left(\frac{\nu^2 - \nu'^2}{2\Delta_{spec}^2}\right) \leq \exp\left(\frac{n\Delta_{ETH} + \Delta_{ETH}^2}{2n}\right) \leq e^{\Delta_{ETH}/2}(1 + o(1)) =: R, \quad (4.16)$$

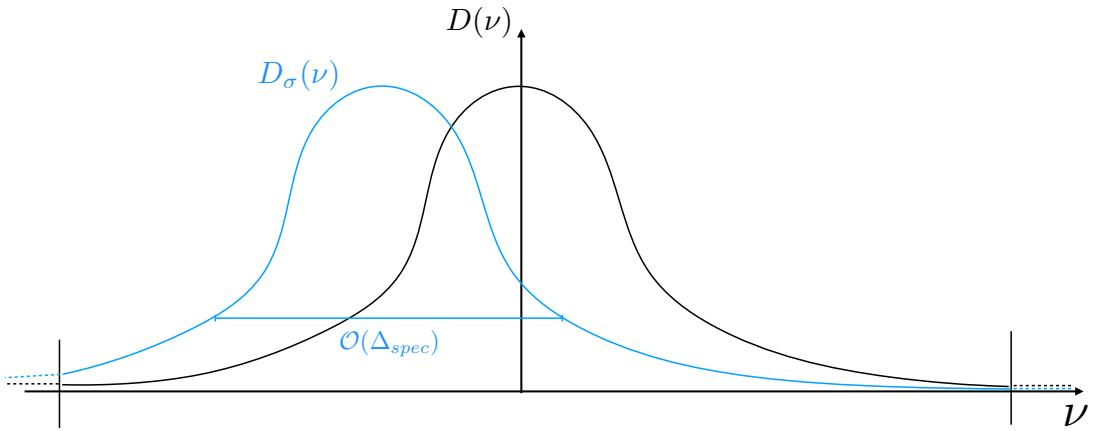


Figure 4. The density of states is truncated such that the continuum limit holds and the relative ratios of density are small, but at the same time not throwing away too many states. The Gibbs state, limited by the same truncation, may be centered at different energies. If we want the gap λ_{RW} of random walk to be large enough, the Gibbs distribution better has no bottlenecks, such as a Gaussian.

which is a constant for any reasonable values of $\Delta_{ETH} \leq \mathcal{O}(1)$. Also, the spectrum remains continuous near the edge

$$D(n) = \Omega\left(\frac{1}{\sqrt{n}} e^{-n/2}\right) \gg \frac{1}{2^n}. \quad (4.17)$$

For Assumption IV.2, we can calculate its Gibbs state, which is a shifted Gaussian

$$D_\sigma(\nu) \propto \begin{cases} N'_0 \cdot \exp\left(\frac{-(\nu + \beta \Delta_{spec}^2)^2}{2\Delta_{spec}^2}\right) \propto \exp\left(\frac{-(\nu + \beta n)^2}{2n}\right) & \text{if } \nu \in [-n, n] \\ 0 & \text{else.} \end{cases} \quad (4.18)$$

where N'_0 is a normalization factor. As long as $\beta < 1$, the tail rapidly decays as required.

The justification for presenting the Gaussian density example is due to central limit theorems for the spectrum of spatially local Hamiltonians [28, Lemma 8]. It was shown that if the Gibbs state has decay of correlation, then the bulk of the Gibbs state is Gaussian (similarly, set $\beta = 0$ for the unbiased spectrum). At a finite system size n , however, the tail (outside of $1 - \mathcal{O}(\frac{1}{\sqrt{n}})$ portion of the weight) may deviate from a Gaussian density. This is partly why we make a somewhat general assumption on the Gibbs distribution (Assumption IV.2).

C. Properties of finite-resolved Davies' generator

This preliminary section simplifies the Lindbladian at hand and prepares ourselves for the proof.

Observation I: the transition between far-apart energies cannot decrease the gap.

ETH only tells us about the matrix element between nearby energies. First, we emphasize that the transitions between far apart energies cannot close the gap as long as each of them satisfies detailed balance.

Fact IV.2 (The gap of sum of Lindbladian [42]). *For a set of σ -detailed balance Lindbladians $\mathcal{L}_s, s \in S$ with a common kernel, the gap is monotone*

$$\text{Gap}\left(\sum_{s \in S} \mathcal{L}_s\right) \geq \text{Gap}\left(\sum_{s \in S' \subset S} \mathcal{L}_s\right).$$

Proof. Since eigenvalues are independent of the basis, do a similarity transformation w.r.t. σ -weighted norm to make it Hermitian. We reduce to the case where each (super-)operator is non-negative and Hermitian, which was proven in [42]. \square

In our settings, the Gibbs state is in the common kernel of each $\mathcal{L}_{\bar{\omega}}$ due to being detailed balance w.r.t. the rounded Gibbs state (Fact II.2). Therefore, we have reduced the problem to showing a gap for the subset of Lindbladians for which ETH holds.

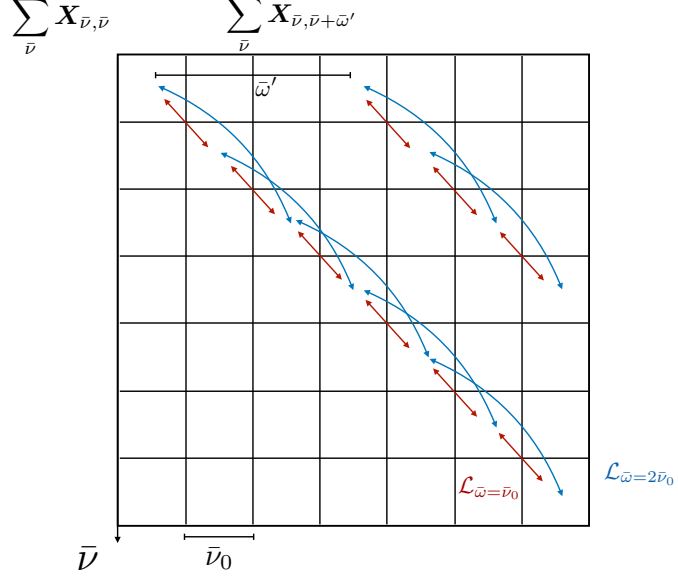


Figure 5. The inputs \mathbf{X} (or ρ) can be dissected into blocks per resolution $\bar{\nu}_0$. The Lindbladians term $\mathcal{L}_{\bar{\omega}}$ hops within sectors (i.e., along the 45-degree slope.) The Gibbs state lies in the diagonal sector where most arguments are devoted, including the classical random walk. The off-diagonal block is simpler to analyze.

$$\mathcal{D}_{\leq \Delta_{ETH}} = \sum_{|\bar{\omega}| \leq \Delta_{ETH}} \sum_a \gamma_a(\bar{\omega}) \left(\mathbf{A}^{a\dagger}(\bar{\omega}) \mathbf{X} \mathbf{A}^a(\bar{\omega}) - \frac{1}{2} \{ \mathbf{A}^{a\dagger}(\bar{\omega}) \mathbf{A}^a(\bar{\omega}), \mathbf{X} \} \right) \quad (4.19)$$

$$= \sum_{0 \leq \bar{\omega} \leq \Delta_{ETH}} \sum_a \left[\gamma_a(\bar{\omega}) \left(\mathbf{A}^{a\dagger}(\bar{\omega}) \mathbf{X} \mathbf{A}^a(\bar{\omega}) - \frac{1}{2} \{ \mathbf{A}^{a\dagger}(\bar{\omega}) \mathbf{A}^a(\bar{\omega}), \mathbf{X} \} \right) + (\bar{\omega} \rightarrow -\bar{\omega}) \right] := \sum_{0 \leq \bar{\omega} \leq \Delta_{ETH}} \mathcal{L}_{\bar{\omega}}. \quad (4.20)$$

Observation II: the Lindbladian splits into the block diagonal and the off-block-diagonal Sectors.

Let us open up the operators

$$\mathbf{A}^a(\bar{\omega}) = \sum_{\bar{\nu}_1 - \bar{\nu}_2 = \bar{\omega}} \mathbf{P}_{\bar{\nu}_2} \mathbf{A}^a \mathbf{P}_{\bar{\nu}_1}. \quad (4.21)$$

The Lindbladian splits into sectors that can be discussed individually [13] (Figure 5). Labeled by $\bar{\omega}'$, any input can be decomposed into

$$\mathbf{X} = \sum_{\bar{\nu}} \sum_{\bar{\nu}'} \mathbf{P}_{\bar{\nu}} \mathbf{X} \mathbf{P}_{\bar{\nu}'} = \sum_{\bar{\omega}'} \sum_{\bar{\nu}} \mathbf{P}_{\bar{\nu}} \mathbf{X} \mathbf{P}_{\bar{\nu}+\bar{\omega}'} =: \sum_{\bar{\omega}'} Q_{\bar{\omega}'}[\mathbf{X}], \quad (4.22)$$

where the Gibbs state lies in the block diagonal sector $Q_{\bar{\omega}'=0}$. Observe that the Lindbladian nicely preserves each sector that $\mathcal{D}Q_{\bar{\omega}'} = Q_{\bar{\omega}'}\mathcal{D}$. The action on the *diagonal blocks* ($\bar{\omega}' = 0$, $\sum_{\bar{\nu}} \mathbf{X}_{\bar{\nu}\bar{\nu}} := \sum_{\bar{\nu}} \mathbf{P}_{\bar{\nu}} \mathbf{X} \mathbf{P}_{\bar{\nu}}$), takes the form

$$\mathcal{L}_{\bar{\omega}} \left[\sum_{\bar{\nu}} \mathbf{X}_{\bar{\nu}\bar{\nu}} \right] = \sum_{\bar{\nu}_1 - \bar{\nu}_2 = \bar{\omega}} \sum_a \left[\frac{\gamma_a(\bar{\omega})}{2} \left(\mathbf{A}_{\bar{\nu}_1 \bar{\nu}_2}^a \mathbf{X} \mathbf{A}_{\bar{\nu}_2 \bar{\nu}_1}^a - \frac{1}{2} \{ \mathbf{A}_{\bar{\nu}_1 \bar{\nu}_2}^a \mathbf{A}_{\bar{\nu}_2 \bar{\nu}_1}^a, \mathbf{X}_{\bar{\nu}_1 \bar{\nu}_1} \} \right) + \frac{\gamma_a(-\bar{\omega})}{2} (\bar{\nu}_1 \leftrightarrow \bar{\nu}_2) \right] \quad (4.23)$$

$$:= \sum_{\bar{\nu}_1 - \bar{\nu}_2 = \bar{\omega}} \mathcal{L}_{\bar{\nu}_1, \bar{\nu}_2}[Q_{\bar{\omega}'=0}[\mathbf{X}]]. \quad (4.24)$$

Note that we fix $\bar{\omega} \geq 0$, i.e. $\bar{\nu}_1 \geq \bar{\nu}_2$. Also, the action on the *off-block-diagonal* inputs, for any $\bar{\omega}'$, is

$$\begin{aligned} \mathcal{L}_{\bar{\omega}} \left[\sum_{\bar{\nu}} \mathbf{X}_{\bar{\nu}, \bar{\nu}+\bar{\omega}'} \right] &= \sum_{\bar{\nu}_1 - \bar{\nu}_2 = \bar{\omega}} \sum_a \left[\frac{\gamma_a(\bar{\omega})}{2} \left(\mathbf{A}_{\bar{\nu}_1 \bar{\nu}_2}^a \mathbf{X} \mathbf{A}_{\bar{\nu}_2+\bar{\omega}', \bar{\nu}_1+\bar{\omega}'}^a - \frac{1}{2} \mathbf{A}_{\bar{\nu}_1 \bar{\nu}_2}^a \mathbf{A}_{\bar{\nu}_2 \bar{\nu}_1}^a \mathbf{X}_{\bar{\nu}_1, \bar{\nu}_1+\bar{\omega}'} - \frac{1}{2} \mathbf{X}_{\bar{\nu}_1, \bar{\nu}_1+\bar{\omega}'} \mathbf{A}_{\bar{\nu}_1+\bar{\omega}', \bar{\nu}_2+\bar{\omega}'}^a \mathbf{A}_{\bar{\nu}_2+\bar{\omega}', \bar{\nu}_1+\bar{\omega}'}^a \right) \right. \\ &\quad \left. + (\bar{\omega} \rightarrow -\bar{\omega}, \bar{\nu}_1 \leftrightarrow \bar{\nu}_2) \right] \end{aligned} \quad (4.25)$$

$$:= \sum_{\bar{\nu}_1 - \bar{\nu}_2 = \bar{\omega}} \mathcal{L}_{\bar{\nu}_1, \bar{\nu}_2, \bar{\omega}'}. \quad (4.26)$$

D. Quantum expanders

Let us briefly review the idea of quantum expanders. Consider a (self-adjoint) channel as an average over set of unitaries

$$\mathcal{N} := \frac{1}{2|a|} \sum_a U_a[\cdot] U_a^\dagger + \frac{1}{2|a|} \sum_a U_a^\dagger[\cdot] U_a, \quad (4.27)$$

then we say it gives *Quantum expander* [31, 34], if¹⁴

$$\lambda_2(\mathcal{N}) \leq \mathcal{O}\left(\frac{1}{\sqrt{|a|}}\right). \quad (4.28)$$

The spectral gap then implies rapid convergence to the maximally mixed state

$$\|\mathcal{N}^\ell[\rho] - \frac{\mathbf{I}}{\text{Tr}[\mathbf{I}]}\|_1 \leq \epsilon, \quad \ell = \frac{\log(1/\epsilon) + 2\log(\text{dim})}{\log(\lambda_2)}. \quad (4.29)$$

For example, i.i.d. unitaries drawn from the Haar measure [31] give quantum expanders, where the RHS is $\frac{\sqrt{2|a|-1}}{|a|}$, with high probability. In general, unitaries giving expanders need not be randomized constructions.

Back to our problem, our convergence results rely on identifying and proving (Section V A) a notion of a quantum expander for Davies' generator, for both the diagonal block (4.24) and the off-diagonal blocks (4.26). In the case of unitary quantum expanders, the constants in $\mathcal{O}(\cdot)$ are absolute. Here, there are extra parameters like the Boltzmann factors (once the common factor $\gamma(-\bar{\omega})$ is divided) as well as the dimensions of subspaces $\mathbf{P}_{\bar{\nu}_1}, \mathbf{P}_{\bar{\nu}_2}$.

Definition IV.3 (Quantum expanders for Lindbladian, with randomness). *We say a set of flips \mathbf{A}^a gives quantum expanders at certain energy scale Δ_{ETH} if for energies $\Delta_{ETH} + \bar{\nu}_2 \geq \bar{\nu}_1 \geq \bar{\nu}_2, \bar{\omega}'$ and with high probability (w.r.t to randomness of \mathbf{A}^a)*

$$\lambda_2(\mathcal{L}_{\bar{\nu}_1, \bar{\nu}_2}) = \left(1 - \mathcal{O}\left(\frac{\text{Poly}(R, e^{\beta\Delta_{ETH}})}{\sqrt{|a|}}\right)\right) \lambda_2(\mathbb{E}\mathcal{L}_{\bar{\nu}_1, \bar{\nu}_2}) \quad (4.30)$$

$$\lambda_1(\mathcal{L}_{\bar{\nu}_1, \bar{\nu}_2, \bar{\omega}'}) = \left(1 - \mathcal{O}\left(\frac{\text{Poly}(R, e^{\beta\Delta_{ETH}})}{\sqrt{|a|}}\right)\right) \lambda_1(\mathbb{E}\mathcal{L}_{\bar{\nu}_1, \bar{\nu}_2, \bar{\omega}'}) . \quad (4.31)$$

Note that the leading eigenvalue on the diagonal block Lindbladian is zero $\lambda_1 = 0$. Since our problem has randomness, the natural object on the RHS is the expectation. If the flips \mathbf{A}^a are not random, as in any given Hamiltonian, one may substitute for an appropriate analog of the RHS. Unfortunately, we do not formalize quantum expanders for the Metropolis setting; this is due to the annoying issues with rounding in QPE and trace-non-preserving.

V. MAIN RESULT II: FINITELY-RESOLVED DAVIES CONVERGENCES TO APPROXIMATE GIBBS STATE

In this section, we show convergence for the finitely-resolved Davies's generator, whose dissipative part takes the form

$$\mathcal{D} = \sum_{\bar{\omega}} \sum_a \gamma(\bar{\omega}) \left(\mathbf{A}^{a\dagger}(\bar{\omega}) \mathbf{X} \mathbf{A}^a(\bar{\omega}) - \frac{1}{2} \{ \mathbf{A}^{a\dagger}(\bar{\omega}) \mathbf{A}^a(\bar{\omega}), \mathbf{X} \} \right), \quad (5.1)$$

for any $\gamma(\bar{\omega})$ (satisfying detailed balance).

In our particular finite time calculation, $\gamma_{ab}(\bar{\omega}) = \delta_{ab}\gamma(\bar{\omega})$ is indeed diagonal. A favorable choice of bath would be (Theorem III.1) such that $\Delta_B = \Delta_{ETH}$ so that $\gamma(\bar{\omega})$ roughly aligns with the transitions of *ETH*

$$\gamma_{ab}(\omega) = \delta_{ab} \frac{1}{\sqrt{2\pi\Delta_{ETH}^2}} \exp\left(\frac{-(\omega - \beta\Delta_{ETH}^2/2)^2}{2\Delta_{ETH}^2}\right). \quad (5.2)$$

Theorem V.1 (Convergence of the finitely-resolved Davies' generator). *For a truncated Hamiltonian \mathbf{H}_S with a well-defined density of states (up to the truncation point), assume its relative ratio of the density of states is R for the*

¹⁴ For the purposes of this work, we focus on the $1/\sqrt{|a|}$ behavior.

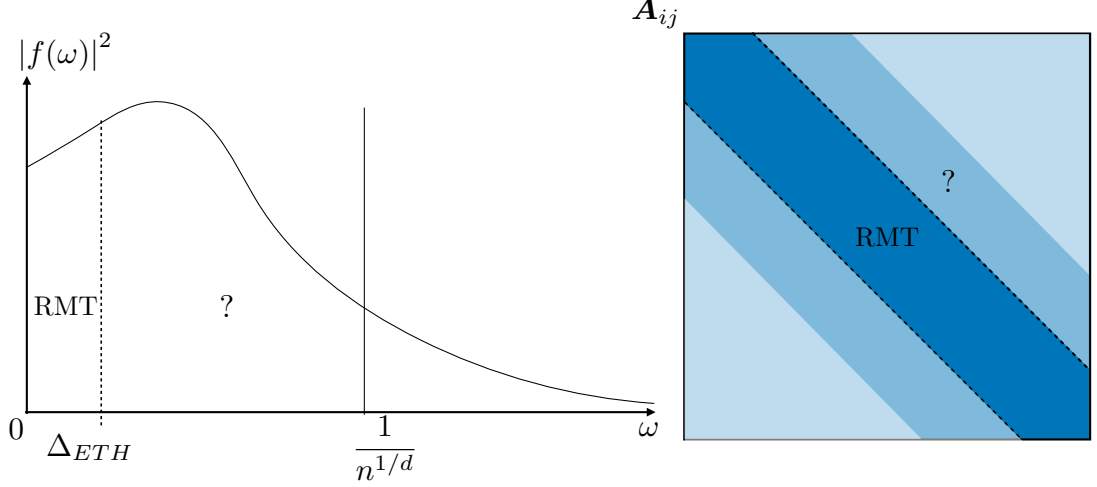


Figure 6. The function f_ω in ETH ansatz is expected to have most weight below scale $1/n^{1/d}$. The scale that random matrix behavior kicks in remains debatable.

energy difference Δ_{ETH} . Assume each \mathbf{A}^a for energy differences below Δ_{ETH} is i.i.d sample from the ETH ansatz, then using flips $|a| = \Omega(R^4 e^{2\beta\Delta_{ETH}})$, and running the finitely-resolved Davies' generator for effective time

$$\tau_\epsilon = \tilde{\Omega} \left(\ln(1/\epsilon) \left(\frac{1}{\alpha_{diag}} + \frac{1}{\lambda_{off}} (n + \beta \|\mathbf{H}_S\|) \right) \right) \text{ ensures } \left\| e^{\mathcal{L}^\dagger t} [\rho] - \bar{\sigma} \right\|_1 \leq \epsilon, \quad (5.3)$$

where $\tilde{\Omega}$ absorbs logarithmic dependence on $n, \beta, \|\mathbf{H}_S\|$ and

$$\alpha_{diag} = \Omega \left(\frac{\lambda_{RW}}{R} \cdot \frac{|a| \Delta_{ETH} \min_{\bar{\omega} \leq \Delta_{ETH}} \gamma(-\bar{\omega}) |f_{\bar{\omega}}|^2}{(n + \beta \|\mathbf{H}_S\|)(n + \beta \Delta_{ETH})} \right) \quad (5.4)$$

$$\lambda_{off} = \Omega \left(\frac{\Delta_{ETH}}{R} \min_{\bar{\omega} \leq \Delta_{ETH}} \gamma(-\bar{\omega}) |f_{\bar{\omega}}|^2 \right) \quad (5.5)$$

$$\bar{\sigma} := \frac{e^{-\beta \bar{\mathbf{H}}_S}}{\text{Tr}[e^{-\beta \bar{\mathbf{H}}_S}]}, \quad (5.6)$$

with energy resolution $\bar{\nu}_0 \leq \mathcal{O}(\Delta_{ETH})$. Also, λ_{RW} is the gap of a 1d classical random walk with the characteristic step size $\sim \Delta_{ETH}$ on the Gibbs distribution.

Lemma V.2. The RMT prescription of ETH can be replaced by that the flips \mathbf{A}^a give Lindbladian Quantum expanders (Definition IV.3).

Proposition V.2.1. If the density of Gibbs state satisfies assumptions in Section IVB 2 (e.g., a Gaussian with variance Δ_{spec}), then $\lambda_{RW} = \Omega(\frac{e^{2\beta\Delta_{ETH}}}{R^2} \frac{\Delta_{ETH}^2}{\Delta_{spec}^2})$.

We see factors of $\text{Poly}(R, e^{\beta\Delta_{ETH}})$ that are potentially worrying. Fortunately, we can choose a small enough $\Delta'_{ETH} < \Delta_{ETH}$ so that $\beta\Delta'_{ETH} = \mathcal{O}(1), R = \mathcal{O}(1)$ (which is polynomial in $1/\beta$ and not exponential!). In the detailed derivations, we have kept the $e^{\beta\Delta_{ETH}}$ factors for completeness.

See Section IVB for ETH, the assumptions on density of states, and the Gibbs state density for gap calculation. For the $\gamma(\omega)$ given by (5.2), $\min_{\bar{\omega}} \gamma(-\bar{\omega}) = \gamma(-\Delta_{ETH}) = \theta(\frac{\exp(\beta^2 \Delta_{ETH}^2/4)}{\Delta_{ETH}})$.

The proof is sketched as follows. In the preliminary section (Section IV C), we have observed that (I) transition between far-apart energies can be removed and (II) the Lindbladian splits into the block diagonal and the off-block-diagonal sectors. Most of the proof is devoted to analyzing the *diagonal blocks* ($\bar{\omega}' = 0, \sum_{\bar{\nu}} \mathbf{X}_{\bar{\nu}\bar{\nu}} := \sum_{\bar{\nu}} \mathbf{P}_{\bar{\nu}} \mathbf{X} \mathbf{P}_{\bar{\nu}}$). There, we first show that the flips \mathbf{A}^a satisfying ETH gives quantum expanders, which convert to local MLSI estimates (Section V A). Second, we use approximate tensorization (Fact IV.1) to lift local MLSI constant to global MLSI constant. This reduces the problem to a 1d *classical* random walk (Section V B), whose gap estimate from conductance calculations is left in Appendix B 1. Lastly, we show the quantum expander condition holds for the *off-block-diagonal* inputs (Section V C). All the above estimates combine in Section V D.

A. Local Gap and MLSI Estimates: ETH Gives Quantum Expanders (block-diagonal Inputs)

Let us estimate the spectral gap for the “local” Lindbladian at nearby energies $\bar{\nu}_1, \bar{\nu}_2$.

Lemma V.3. *In the block diagonal sector $Q_{\bar{\omega}'=0}$ for $\bar{\nu}_1 \neq \bar{\nu}_2$, each term $\mathcal{L}_{\bar{\nu}_1, \bar{\nu}_2}^*$ has stationary states of form*

$$\lim_{t \rightarrow \infty} e^{\mathcal{L}_{\bar{\nu}_1, \bar{\nu}_2}^* t} [Q_{\bar{\omega}'=0}[\rho]] = \sigma_{\bar{\nu}_1, \bar{\nu}_2} \text{Tr}[\mathbf{P}_{\bar{\nu}_2} \rho \mathbf{P}_{\bar{\nu}_2} + \mathbf{P}_{\bar{\nu}_1} \rho \mathbf{P}_{\bar{\nu}_1}] + \sum_{\bar{\nu} \neq \bar{\nu}_1, \bar{\nu}_2} \mathbf{P}_{\bar{\nu}} \rho \mathbf{P}_{\bar{\nu}},$$

where $\sigma_{\bar{\nu}_1, \bar{\nu}_2}$ denotes the local Gibbs state

$$\sigma_{\bar{\nu}_1, \bar{\nu}_2} := \frac{\mathbf{P}_{\bar{\nu}_1} e^{-\beta \bar{\nu}_1} + \mathbf{P}_{\bar{\nu}_2} e^{-\beta \bar{\nu}_2}}{\text{Tr}[\mathbf{P}_{\bar{\nu}_1}] e^{-\beta \bar{\nu}_1} + \text{Tr}[\mathbf{P}_{\bar{\nu}_2}] e^{-\beta \bar{\nu}_2}}.$$

Equivalently in the Heisenberg picture, the conditional expectation gives

$$\lim_{t \rightarrow \infty} e^{\mathcal{L}_{\bar{\nu}_1, \bar{\nu}_2} t} [Q_{\bar{\omega}'=0} \mathbf{X}] := E_{\bar{\nu}_1, \bar{\nu}_2} [Q_{\bar{\omega}'=0} \mathbf{X}] = \text{Tr}[\sigma_{\bar{\nu}_1, \bar{\nu}_2} \mathbf{X}] (\mathbf{P}_{\bar{\nu}_2} + \mathbf{P}_{\bar{\nu}_1}) + \sum_{\bar{\nu} \neq \bar{\nu}_1, \bar{\nu}_2} \mathbf{P}_{\bar{\nu}} \mathbf{X} \mathbf{P}_{\bar{\nu}}. \quad (5.7)$$

Furthermore, with high probability, the gap is at least

$$\lambda_{\text{gap}}(\mathcal{L}_{\bar{\nu}_1, \bar{\nu}_2} Q_{\bar{\omega}'=0}) \geq \Omega\left(\frac{1}{R} |f_{\bar{\omega}}|^2 \bar{\nu}_0 |a| \gamma_a(-\bar{\omega})\right). \quad (5.8)$$

which converts to the MLSI constant

$$\alpha_{\text{MLSI}}(\mathcal{L}_{\bar{\nu}_1, \bar{\nu}_2} Q_{\bar{\omega}'=0}) \geq \Omega\left(\frac{1}{R} \frac{|f_{\bar{\omega}}|^2 \bar{\nu}_0 |a| \gamma_a(-\bar{\omega})}{n + \beta \bar{\omega}}\right). \quad (5.9)$$

The proof relies on analyzing the expectation and the deviation

$$\hat{\mathcal{L}}_{\bar{\nu}_1, \bar{\nu}_2} = (\hat{\mathcal{L}}_{\bar{\nu}_1, \bar{\nu}_2} - \mathbb{E}[\hat{\mathcal{L}}_{\bar{\nu}_1, \bar{\nu}_2}]) + \mathbb{E}[\hat{\mathcal{L}}_{\bar{\nu}_1, \bar{\nu}_2}] \quad (5.10)$$

where the expectation is evaluated over the ETH ansatz (Hypothesis IV.2). Remarkably, this decomposition fits neatly with the RMT prescription: the expectation gives an generator of a *classical* Markov chain in the energy basis, and at large $|a|$, the deviation concentrates with a relative size $\mathcal{O}(\frac{1}{\sqrt{|a|}})$.

1. The Expected Lindbladian

It is more intuitive to further decompose into two Lindbladians

$$\mathbb{E}[\hat{\mathcal{L}}_{\bar{\nu}_1, \bar{\nu}_2}] = \mathbb{E}[\hat{\mathcal{L}}_{\mathbf{G}, \bar{\nu}_1, \bar{\nu}_2}] + \mathbb{E}[\hat{\mathcal{L}}_{\mathbf{D}, \bar{\nu}_1, \bar{\nu}_2}]. \quad (5.11)$$

For the pair of frequency $\bar{\nu}_1, \bar{\nu}_2$, we decompose \mathbf{A} into independent Gaussian matrices $\mathbf{A}_{\bar{\nu}_2 \bar{\nu}_1} = \mathbf{G}_{\bar{\nu}_2 \bar{\nu}_1} + \mathbf{D}_{\bar{\nu}_2 \bar{\nu}_1}$: the coarse-grained part $\mathbf{G}_{\bar{\nu}_2 \bar{\nu}_1}$ has the same variance $V_{\bar{\nu}_1, \bar{\nu}_2}^{\min}$ for all Gaussian entries \mathbf{G}_{ij} and the deviation part $\mathbf{D}_{\bar{\nu}_2 \bar{\nu}_1}$ takes care of the dependence of the refined scales $i \in \bar{\nu}$. In the following analysis we only need to consider $\mathbf{G}_{\bar{\nu}_2 \bar{\nu}_1}$ since $\mathbf{D}_{\bar{\nu}_2 \bar{\nu}_1}$ does not shrink the gap.

Proposition V.3.1. *The eigenvectors and eigenvalues of $\mathbb{E}[\hat{\mathcal{L}}_{\mathbf{G}, \bar{\nu}_1, \bar{\nu}_2}] Q_{\bar{\omega}'=0}$ are*

$$\begin{aligned} & \mathbf{P}_{\bar{\nu}_1} + \mathbf{P}_{\bar{\nu}_2}, \quad \lambda_1 = 0 \\ & \frac{e^{\beta \bar{\omega}}}{\text{Tr}[\mathbf{P}_{\bar{\nu}_1}]} \mathbf{P}_{\bar{\nu}_1} - \frac{1}{\text{Tr}[\mathbf{P}_{\bar{\nu}_2}]} \mathbf{P}_{\bar{\nu}_2}, \quad \lambda_4 = -V \text{Tr}[\mathbf{P}_{\bar{\nu}_2}] \sum_a \gamma_a(\bar{\omega}) - V \text{Tr}[\mathbf{P}_{\bar{\nu}_1}] \sum_a \gamma_a(-\bar{\omega}) \\ & \mathbf{O}_{\bar{\nu}_2}, \text{Tr}[\mathbf{O}_{\bar{\nu}_2}] = 0, \quad \lambda_2 = -V \text{Tr}[\mathbf{P}_{\bar{\nu}_1}] \sum_a \gamma_a(-\bar{\omega}) \\ & \mathbf{O}_{\bar{\nu}_1}, \text{Tr}[\mathbf{O}_{\bar{\nu}_1}] = 0, \quad \lambda_3 = -V \text{Tr}[\mathbf{P}_{\bar{\nu}_2}] \sum_a \gamma_a(\bar{\omega}) \end{aligned}$$

where $V := V_{\bar{\nu}_1, \bar{\nu}_2}^{\min}$.

We see that the second largest eigenvalue is $\lambda_2 = -V \text{Tr}[\mathbf{P}_{\bar{\nu}_1}] \sum_a \gamma_a(-\bar{\omega})$. The proof is based on a simple Gaussian calculation.

Fact V.4. *For complex Gaussian rectangular matrix $d_2 \times d_1$*

$$\mathbb{E}_G[\mathbf{A}_{d_2 d_1}(\mathbf{X}_{d_1}) \mathbf{A}_{d_1 d_2}^\dagger] = \sum_{i_1, i_2} |i_2\rangle \langle i_2| \cdot \mathbf{X}_{i_1 i_1} \cdot \mathbb{E}[\mathbf{A}_{i_1 i_2} \mathbf{A}_{i_2 i_1}^*].$$

In particular, if all entries share the same variance V , then $\mathbb{E}_G[\mathbf{G}_{d_2 d_1}(\mathbf{X}_{d_1}) \mathbf{G}_{d_1 d_2}^\dagger] = V \cdot \text{Tr}_{d_1}[\mathbf{X}_{d_1}] \cdot \mathbf{I}_{d_2}$.

Proof of Proposition V.3.1. Consider the coarse-grained \mathbf{G} component

$$\sum_a \frac{1}{2} \mathbb{E} \left[\gamma(\bar{\omega}) \left(\mathbf{G}_{\bar{\nu}_1 \bar{\nu}_2}^a(\mathbf{X}) \mathbf{G}_{\bar{\nu}_2 \bar{\nu}_1}^a - \frac{1}{2} \{ \mathbf{G}_{\bar{\nu}_1 \bar{\nu}_2}^a \mathbf{G}_{\bar{\nu}_2 \bar{\nu}_1}^a, \mathbf{X}_{\bar{\nu}_1 \bar{\nu}_1} \} \right) + \gamma(-\bar{\omega}) \left(\mathbf{G}_{\bar{\nu}_2 \bar{\nu}_1}^a(\mathbf{X}) \mathbf{G}_{\bar{\nu}_1 \bar{\nu}_2}^a - \frac{1}{2} \{ \mathbf{G}_{\bar{\nu}_2 \bar{\nu}_1}^a \mathbf{G}_{\bar{\nu}_1 \bar{\nu}_2}^a, \mathbf{X}_{\bar{\nu}_2 \bar{\nu}_2} \} \right) \right] \quad (5.12)$$

$$= \sum_a \frac{V}{2} \left[\gamma(\bar{\omega}) \left(\mathbf{P}_{\bar{\nu}_1} \text{Tr}[\mathbf{P}_{\bar{\nu}_2} \mathbf{X} \mathbf{P}_{\bar{\nu}_2}] - \text{Tr}[\mathbf{P}_{\bar{\nu}_2}] \mathbf{P}_{\bar{\nu}_1} \mathbf{X} \mathbf{P}_{\bar{\nu}_1} \right) + \gamma(-\bar{\omega}) \left(\mathbf{P}_{\bar{\nu}_2} \text{Tr}[\mathbf{P}_{\bar{\nu}_1} \mathbf{X} \mathbf{P}_{\bar{\nu}_1}] - \text{Tr}[\mathbf{P}_{\bar{\nu}_1}] \mathbf{P}_{\bar{\nu}_2} \mathbf{X} \mathbf{P}_{\bar{\nu}_2} \right) \right] \quad (5.13)$$

where $V = \mathbb{E}[G_{ij} G_{ij}^*] = V_{\bar{\nu}_1, \bar{\nu}_2}^{\min}$ is the variance of a Gaussian entry. \square

Adding back the deviation \mathbf{D} does not shrink the gap (Fact IV.2). Writing out \mathbf{D} , the bilinear term $A \mathbf{X} D$ vanishes under the expectation

$$\sum_a \frac{1}{2} \mathbb{E} \left[\gamma(\bar{\omega}) \left(\mathbf{D}_{\bar{\nu}_1 \bar{\nu}_2}^a(\mathbf{X}) \mathbf{D}_{\bar{\nu}_2 \bar{\nu}_1}^a - \frac{1}{2} \{ \mathbf{D}_{\bar{\nu}_1 \bar{\nu}_2}^a \mathbf{D}_{\bar{\nu}_2 \bar{\nu}_1}^a, \mathbf{X}_{\bar{\nu}_1 \bar{\nu}_1} \} \right) + \gamma(-\bar{\omega}) \left(\mathbf{D}_{\bar{\nu}_2 \bar{\nu}_1}^a(\mathbf{X}) \mathbf{D}_{\bar{\nu}_1 \bar{\nu}_2}^a - \frac{1}{2} \{ \mathbf{D}_{\bar{\nu}_2 \bar{\nu}_1}^a \mathbf{D}_{\bar{\nu}_1 \bar{\nu}_2}^a, \mathbf{X}_{\bar{\nu}_2 \bar{\nu}_2} \} \right) \right] \quad (5.14)$$

It is indeed another Lindbladian that generates CPTP maps. Formally, we also see it does have the same stationary state due to the coefficient $\gamma(\bar{\omega})$, i.e., it satisfies detailed balance.

2. Concentration around the expectation

Finished with the expectation, we move on to obtain concentration around the expectation. We want to control fluctuations of the second eigenvalue λ_2 through the perturbation theory of eigenvalues. It will be crucial to work with the inner product

$$\langle \mathbf{O}_1, \mathbf{O}_2 \rangle_{\bar{\sigma}} = \text{Tr}[\mathbf{O}_1^\dagger \sqrt{\bar{\sigma}} \mathbf{O}_2 \sqrt{\bar{\sigma}}], \quad (5.15)$$

under which $\mathbb{E}[\mathcal{L}_{\bar{\nu}_1, \bar{\nu}_2}], \mathcal{L}_{\bar{\nu}_1, \bar{\nu}_2}$ are all self-adjoint.

Formally, to be more careful with norms, we should rewrite superoperator as a linear map on a doubled Hilbert space. For each term $\mathcal{L}_{\bar{\nu}_1, \bar{\nu}_2}$,

$$\mathcal{L}_{\bar{\nu}_1, \bar{\nu}_2} \equiv \sum_a \left[\frac{\gamma(\bar{\omega})}{2} \left(\mathbf{A}_{\bar{\nu}_1 \bar{\nu}_2}^a \otimes \mathbf{A}_{\bar{\nu}_1 \bar{\nu}_2}^{*a} - \frac{1}{2} \mathbf{A}_{\bar{\nu}_1 \bar{\nu}_2}^a \mathbf{A}_{\bar{\nu}_2 \bar{\nu}_1}^a \otimes \mathbf{P}_{\bar{\nu}_1} - \frac{1}{2} \mathbf{P}_{\bar{\nu}_1} \otimes \mathbf{A}_{\bar{\nu}_1 \bar{\nu}_2}^{*a} \mathbf{A}_{\bar{\nu}_2 \bar{\nu}_1}^{*a} \right) + \frac{\gamma(-\bar{\omega})}{2} (\bar{\nu}_1 \leftrightarrow \bar{\nu}_2) \right]. \quad (5.16)$$

Note that we use the entry-wise conjugate (not to confuse with transpose $\mathbf{A}^* \neq \mathbf{A}^\dagger$).

Proposition V.4.1. *The deviation $\delta \mathcal{L}_{\bar{\nu}_1, \bar{\nu}_2} := \mathcal{L}_{\bar{\nu}_1, \bar{\nu}_2} - \mathbb{E}[\mathcal{L}_{\bar{\nu}_1, \bar{\nu}_2}]$, with high probability, is at most*

$$\|\delta \mathcal{L}_{\bar{\nu}_1, \bar{\nu}_2}\|_{\infty, \bar{\sigma}} = \mathcal{O} \left(c_{\bar{\nu}_1, \bar{\nu}_2} \cdot e^{\beta(\bar{\nu}_1 - \bar{\nu}_2)} \right),$$

where

$$c_{\bar{\nu}_1, \bar{\nu}_2} := \max_{\bar{\nu}_1, \bar{\nu}_2} (\mathbb{E}|A_{ij}|^2) \cdot \max(\text{Tr}[\mathbf{P}_{\bar{\nu}_1}], \text{Tr}[\mathbf{P}_{\bar{\nu}_2}]) \sqrt{|a|} \gamma(-\bar{\omega})$$

and $\|\cdot\|_{\infty, \bar{\sigma}} := \|\cdot\|_{(2, \bar{\sigma})-(2, \bar{\sigma})}$ is the operator norm w.r.t. the inner product $\langle \cdot, \cdot \rangle_{\bar{\sigma}}$.

The concentration for Gaussian matrices will be useful and see Appendix A for their proofs.

Fact V.5. *For $\mathbf{G}_i, \mathbf{G}'_i$ rectangular matrices with independent complex Gaussian entries,*

$$\mathbb{E} \left\| \sum_i a_i \mathbf{G}_i \otimes \mathbf{G}'_i^* \right\|_p^p \leq (\mathbb{E} \|\mathbf{G}\|_p^p)^2 \cdot (\sum_i a_i^2)^{p/2}.$$

Fact V.6. *For $\mathbf{G}_i, \mathbf{G}'_i$ rectangular matrices with independent complex Gaussian entries,*

$$\mathbb{E} \left\| \sum_i a_i \mathbf{G}_i \mathbf{G}'_i \right\|_p^p \leq \mathbb{E} \|\mathbf{G}_i \mathbf{G}'_i\|_p^p (\sum_i a_i^2)^{p/2}$$

Fact V.7. *For rectangular matrices $\mathbf{G}_{d_2 d_1}$ with i.i.d complex Gaussian entries, with variance $\mathbb{E}[G_{ij} G_{ij}^*] = 2$*

$$\mathbb{E} \|\mathbf{G}\|_p^p \leq \min(d_1, d_2) \mathbb{E} \|\mathbf{G}\|^p \leq \min(d_1, d_2) \cdot \left(\sqrt{\max(d_1, d_2)}^p c_1^p + (c_2 \sqrt{p})^p \right),$$

or $\Pr \left(\|\mathbf{G}\| \geq (\epsilon + c_3) \sqrt{\max(d_1, d_2)} \right) \leq \exp(-\epsilon^2 c_4 \min(d_1, d_2)^2)$, for absolute constants c_1, c_2, c_3, c_4 .

In other words, p can be taken as large as dimension, and they concentrate very sharply. In the end, we should have a union bound in mind over $\text{Poly}(n)$ choices of $\bar{\nu}_1, \bar{\nu}_2$, which is handled by the much stronger concentration. We will simplify the notation by dropping the tails and only saying “with high probability”.

Proof. We will take a standard Gaussian decoupling approach [34]. Control the operator norm by the Schatten p-norm,

$$(\mathbb{E} \|\delta\mathcal{L}_{\bar{\nu}_1, \bar{\nu}_2}\|_{\infty, \bar{\sigma}}^p)^{\frac{1}{p}} \leq (\mathbb{E} \|\delta\mathcal{L}_{\bar{\nu}_1, \bar{\nu}_2}\|_{p, \bar{\sigma}}^p)^{\frac{1}{p}} \quad (5.17)$$

$$\leq (\mathbb{E} \|\delta\mathcal{L}_{\bar{\nu}_1, \bar{\nu}_2} - \delta\mathcal{L}'_{\bar{\nu}_1, \bar{\nu}_2}\|_{p, \bar{\sigma}}^p)^{\frac{1}{p}}, \quad (5.18)$$

where we used convexity conditioned on $\delta\mathcal{L}_{\bar{\nu}_1, \bar{\nu}_2}$ to introduce an identical copy. Recall for any complex Gaussian matrix (entries with possibly different variances) can be decoupled with small constant overhead (from triangle inequality)

$$\mathbf{M} \otimes \mathbf{M}^* - \mathbf{M}' \otimes \mathbf{M}'^* \equiv \frac{(\mathbf{M} + \mathbf{M}')}{\sqrt{2}} \otimes \frac{(\mathbf{M} + \mathbf{M}')^*}{\sqrt{2}} - \frac{(\mathbf{M} + \mathbf{M}')}{\sqrt{2}} \otimes \frac{(\mathbf{M} + \mathbf{M}')^*}{\sqrt{2}} \quad (5.19)$$

$$= \mathbf{M} \otimes \mathbf{M}'^* + \mathbf{M}' \otimes \mathbf{M}^*. \quad (5.20)$$

This implies $\mathcal{L}_{\bar{\nu}_1, \bar{\nu}_2}$ gives quantum expanders

$$\left(\mathbb{E} \|\delta\mathcal{L}_{\bar{\nu}_1, \bar{\nu}_2} - \delta\mathcal{L}'_{\bar{\nu}_1, \bar{\nu}_2}\|_{p, \bar{\sigma}}^p \right)^{\frac{1}{p}} \leq (\mathbb{E} \left\| \sum_a \left[\frac{\gamma(\bar{\omega})}{e^{\beta\bar{\omega}/2}} (\mathbf{A}_{\bar{\nu}_1 \bar{\nu}_2}^a \otimes \mathbf{A}_{\bar{\nu}_1 \bar{\nu}_2}^{a*} + \mathbf{A}_{\bar{\nu}_2 \bar{\nu}_1}^a \otimes \mathbf{A}_{\bar{\nu}_2 \bar{\nu}_1}^{a*}) \right. \right. \quad (5.21)$$

$$\left. \left. - \frac{\gamma(\bar{\omega})}{2} (\mathbf{A}_{\bar{\nu}_1 \bar{\nu}_2}^a \mathbf{A}_{\bar{\nu}_2 \bar{\nu}_1}^{a*} \otimes \mathbf{P}_{\bar{\nu}_1} + \mathbf{P}_{\bar{\nu}_1} \otimes \mathbf{A}_{\bar{\nu}_1 \bar{\nu}_2}^{a*} \mathbf{A}_{\bar{\nu}_2 \bar{\nu}_1}^{a*}) \right] \right\|_p^p)^{\frac{1}{p}} \quad (5.22)$$

$$+ \frac{\gamma(-\bar{\omega})}{2} (\mathbf{A}_{\bar{\nu}_2 \bar{\nu}_1}^a \mathbf{A}_{\bar{\nu}_1 \bar{\nu}_2}^{a*} \otimes \mathbf{P}_{\bar{\nu}_2} + \mathbf{P}_{\bar{\nu}_2} \otimes \mathbf{A}_{\bar{\nu}_2 \bar{\nu}_1}^{a*} \mathbf{A}_{\bar{\nu}_1 \bar{\nu}_2}^{a*}) \right\|_p^p)^{\frac{1}{p}} \quad (5.23)$$

$$= \mathcal{O} \left(V_{\bar{\nu}_1, \bar{\nu}_2}^{\max} \max(\text{Tr}[\mathbf{P}_{\bar{\nu}_1}], \text{Tr}[\mathbf{P}_{\bar{\nu}_2}]) \sqrt{|a| \gamma(\bar{\omega})^2} \right) (= \mathcal{O} \left(\frac{R^2 e^{2\beta\Delta_{ETH}}}{\sqrt{|a|}} \lambda_2(\mathbb{E}[\mathcal{L}_{\bar{\nu}_1, \bar{\nu}_2}]) \right))$$

where a factor 2 cancels out. The inequality uses concentration for sum (Fact V.5, Fact V.6). For each term, we introduce an independent auxiliary matrix that $\mathbf{A} + \mathbf{D} = \mathbf{G}$ with entries $\mathbb{E}[Re(\mathbf{D})_{ij}^2] = \mathbb{E}[Re(\mathbf{A})_{ij}^2] - \max_{ij} \mathbb{E}[Re(\mathbf{A})_{ij}^2]$ and analogously for the imaginary part. Then the expression with \mathbf{A} is now controlled by

$$\mathbb{E} \|\mathbf{A}_1 \otimes \mathbf{A}_2\|_p^p = \mathbb{E} \|\mathbb{E}_{\mathbf{D}_1} \mathbf{G}_1 \otimes \mathbb{E}_{\mathbf{D}_2} \mathbf{G}_2\|_p^p \leq \mathbb{E} \|\mathbf{G}_1 \otimes \mathbf{G}_2\|_p^p \quad (5.24)$$

and analogously for $\mathbb{E} \|\mathbf{A}_1 \mathbf{A}_2\|_p^p$. Then we reduce to Gaussian spectral norm estimates

$$\mathbb{E} \|\mathbf{G} \otimes \mathbf{G}'\|_p^p \leq \mathbb{E} \|\mathbf{G}\|_p^p \cdot \mathbb{E} \|\mathbf{G}'\|_p^p. \quad (5.25)$$

$$\mathbb{E} \|\mathbf{G} \mathbf{G}'\|_p^p \leq N \mathbb{E} \|\mathbf{G}\|_p^p \cdot \mathbb{E} \|\mathbf{G}'\|_p^p. \quad (5.26)$$

Note that p will be large enough ($p = \theta(\min(d_1, d_2))$) to let us drop the dimension N coming from trace. In the last equality, we compare with the second eigenvalue with the expectation to manifest the form of quantum expander, up to a polynomial of Boltzmann factors $e^{\beta\Delta_{ETH}}$ (due to $\gamma(\bar{\omega})/\gamma(-\bar{\omega})$) and density ratios R (due to V_{\max}/V_{\min} and $\text{Tr}[\mathbf{P}_{\bar{\nu}_1}]/\text{Tr}[\mathbf{P}_{\bar{\nu}_2}]$). In other words, the ETH assumption can be replaced by the flips \mathbf{A}^a giving quantum expanders (with a suitable choice of expectation $\mathbb{E}[\mathcal{L}_{\bar{\nu}_1, \bar{\nu}_2}]$). \square

3. Proof of Lemma V.3

We will need simple facts.

Fact V.8 (gap to MLSI (see, e.g., [35, Remark 3.5])). *For primitive Lindbladian \mathcal{L} ,*

$$\frac{\lambda_{\text{gap}}(\mathcal{L})}{\ln(\|\sigma^{-1}\|) + 2} \leq \frac{\alpha_{\text{MLSI}}(\mathcal{L})}{2}$$

where σ is the unique kernel of \mathcal{L} .

This conversion costs a factor of n .

Fact V.9. *For Lindbladian \mathcal{L} , define*

$$(\mathcal{L} \oplus 0)^\dagger[\rho_1 \oplus \rho_2] := \mathcal{L}^\dagger[\rho_1] \oplus 0.$$

Then $\alpha_{\text{MLSI}}(\mathcal{L} \oplus 0) = \alpha_{\text{MLSI}}(\mathcal{L})$.

Proof.

$$D(\rho_1 \oplus \rho_2 \| E^\dagger[\rho_1 \oplus \rho_2]) = \text{Tr} [\rho_1 \oplus \rho_2 (\ln(\rho_1 \oplus \rho_2) - \ln(E^\dagger[\rho_1 \oplus \rho_2]))] \quad (5.27)$$

$$= \text{Tr}[\rho_1 (\ln(\rho_1) - \ln(E^\dagger[\rho_1]))]. \quad (5.28)$$

The first equality simplifies the logarithm by $\ln(\rho_1 \oplus \rho_2) = \ln(\rho_1) \oplus \ln(\rho_2)$. Similarly,

$$\text{Tr}[(\mathcal{L} \oplus 0)^*[\rho_1 \oplus \rho_2] (\ln(\rho_1 \oplus \rho_2) - E^\dagger[\rho_1 \oplus \rho_2])] = \text{Tr}[\mathcal{L}^*[\rho_1] (\ln(\rho_1) - E^\dagger[\rho_1])] \quad (5.29)$$

which concludes the proof. \square

Proof of Lemma V.3. Recall we decomposed into expectation and deviation

$$\hat{\mathcal{L}}_{\bar{\nu}_1, \bar{\nu}_2} = \mathbb{E}[\hat{\mathcal{L}}_{\mathbf{D}, \bar{\nu}_1, \bar{\nu}_2}] + (\hat{\mathcal{L}}_{\bar{\nu}_1, \bar{\nu}_2} - \mathbb{E}[\hat{\mathcal{L}}_{\bar{\nu}_1, \bar{\nu}_2}]) \quad (5.30)$$

$$= \mathbb{E}[\hat{\mathcal{L}}_{\mathbf{G}, \bar{\nu}_1, \bar{\nu}_2}] + (\hat{\mathcal{L}}_{\bar{\nu}_1, \bar{\nu}_2} - \mathbb{E}[\hat{\mathcal{L}}_{\bar{\nu}_1, \bar{\nu}_2}]) + \mathbb{E}[\hat{\mathcal{L}}_{\mathbf{D}, \bar{\nu}_1, \bar{\nu}_2}] \quad (5.31)$$

We may drop $\mathbb{E}[\hat{\mathcal{L}}_{\mathbf{D}, \bar{\nu}_1, \bar{\nu}_2}]$ as it only increase the gap. By gap stability (Fact VII.3),

$$\lambda_{gap}(\mathcal{L}_{\bar{\nu}_1, \bar{\nu}_2} Q_{\bar{\omega}'=0}) \geq \lambda_{gap}(\mathbb{E}[\mathcal{L}_{\mathbf{G}, \bar{\nu}_1, \bar{\nu}_2} Q_{\bar{\omega}'=0}]) - \|\mathcal{L}_{\bar{\nu}_1, \bar{\nu}_2} - \mathbb{E}[\mathcal{L}_{\bar{\nu}_1, \bar{\nu}_2} Q_{\bar{\omega}'=0}]\|_{\infty, \bar{\sigma}} \quad (5.32)$$

$$= \Omega \left(|a| V_{\bar{\nu}_1, \bar{\nu}_2}^{min} \min(\text{Tr}[\mathbf{P}_{\bar{\nu}_1}], \text{Tr}[\mathbf{P}_{\bar{\nu}_2}]) \gamma(-\bar{\omega}) (1 - \mathcal{O}(\frac{R^2 e^{\beta \Delta_{ETH}}}{\sqrt{|a|}})) \right) \quad (5.33)$$

$$= \Omega \left(\frac{|a| \bar{\nu}_0}{R} |f_{\bar{\omega}}|^2 \gamma(-\bar{\omega}) \cdot (1 - \mathcal{O}(\frac{R^2 e^{\beta \Delta_{ETH}}}{\sqrt{|a|}})) \right). \quad (5.34)$$

In the last line we get a factor of density ratio R due to $V_{\bar{\nu}_1, \bar{\nu}_2}^{min} \min(\text{Tr}[\mathbf{P}_{\bar{\nu}_1}], \text{Tr}[\mathbf{P}_{\bar{\nu}_2}])$. This means that it suffices to choose the number of interaction terms

$$|a| = \Omega(R^4 e^{2\beta \Delta_{ETH}}) \quad (5.35)$$

to guarantee the deviation (Proposition V.4.1) does not close the gap from the expectation $\mathbb{E}[\mathcal{L}_{\mathbf{G}, \bar{\nu}_1, \bar{\nu}_2}]$. We convert to MLSI constant (Fact V.8) by a factor of $1/\ln(\|\bar{\sigma}^{-1}\|) = \mathcal{O}(n + \beta \Delta_{ETH})$, which concludes the proof by Fact V.9. \square

B. Local to Global

Now, we have just obtained convergence for $\mathcal{L}_{\bar{\nu}_1, \bar{\nu}_2}$ to a “local” Gibbs state

$$\lim_{t \rightarrow \infty} e^{\mathcal{L}_{\bar{\nu}_1, \bar{\nu}_2} t} [Q_{\bar{\omega}'=0} \mathbf{X}] := E_{\bar{\nu}_1, \bar{\nu}_2} [Q_{\bar{\omega}'=0} \mathbf{X}] = \text{Tr}[\bar{\sigma}_{\bar{\nu}_1, \bar{\nu}_2} \mathbf{X}] (\mathbf{P}_{\bar{\nu}_2} + \mathbf{P}_{\bar{\nu}_1}) + \sum_{\bar{\nu} \neq \bar{\nu}_1, \bar{\nu}_2} \mathbf{P}_{\bar{\nu}} \mathbf{X} \mathbf{P}_{\bar{\nu}}, \quad (5.36)$$

$$\bar{\sigma}_{\bar{\nu}_1, \bar{\nu}_2} := \frac{\mathbf{P}_{\bar{\nu}_1} e^{-\beta \bar{\nu}_1} + \mathbf{P}_{\bar{\nu}_2} e^{-\beta \bar{\nu}_2}}{\text{Tr}[\mathbf{P}_{\bar{\nu}_1}] e^{-\beta \bar{\nu}_1} + \text{Tr}[\mathbf{P}_{\bar{\nu}_2}] e^{-\beta \bar{\nu}_2}}. \quad (5.37)$$

To show global convergence, recall approximate tensorization (Fact IV.1) and let

$$\Phi^* := \frac{1}{m} \sum_{0 < \bar{\omega} \leq \Delta_{ETH}} \left(\prod_{(\bar{\nu}_1, \bar{\nu}_2) \in S(\bar{\omega})} E_{\bar{\nu}_1, \bar{\nu}_2} + \prod_{(\bar{\nu}_1, \bar{\nu}_2) \in S'(\bar{\omega})} E_{\bar{\nu}_1, \bar{\nu}_2} \right) Q_{\bar{\omega}'=0}, \quad (5.38)$$

where $m := 2 \lfloor \frac{\Delta_{ETH}}{\bar{\nu}_0} \rfloor$ is the appropriate normalization, and for each $\bar{\omega}$, we regroup the terms $E_{\bar{\nu}_1, \bar{\nu}_2}$ (with the same difference $\bar{\omega}$) into two sets $S(\bar{\omega})$ and $S'(\bar{\omega})$. Within $S(\bar{\omega})$, we demand terms $E_{\bar{\nu}_1, \bar{\nu}_2}$ to act on disjoint sets

$$\forall (\bar{\nu}_1, \bar{\nu}_2) \neq (\bar{\nu}'_1, \bar{\nu}'_2) \in S(\bar{\omega}), \{\bar{\nu}_1, \bar{\nu}_2\} \cap \{\bar{\nu}'_1, \bar{\nu}'_2\} = \emptyset, \quad (5.39)$$

and similarly for $S'(\bar{\omega})$. This can be assigned greedily (Figure 7); the specific choice does not change the subsequent proofs (up to absolute constants).

Lemma V.10. *In the block-diagonal sector $\bar{\omega}' = 0$,*

$$k = \Omega \left(\max_{\bar{\nu}} |\ln(\text{Tr}[\bar{\sigma}_{\bar{\nu}}])| \cdot \left(1 + \frac{1}{\lambda_{RW}} \right) \right)$$

guarantees completely positive order $(1 - \epsilon) E_{global} \leq (\Phi^*)^k \leq (1 + \epsilon) E_{global}$, where

$$E_{global}[\mathbf{X}] := \text{Tr}[\bar{\sigma} \mathbf{X}] \mathbf{I}$$

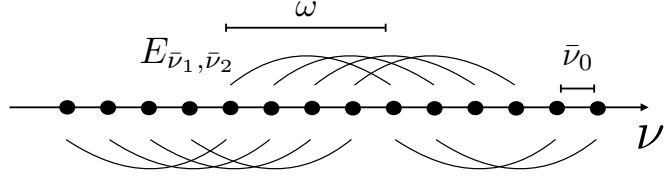


Figure 7. Partition (For each $\bar{\omega}$) of local conditional expectations $E_{\bar{\nu}_1, \bar{\nu}_2}$ into two groups $S(\bar{\omega}), S'(\bar{\omega})$ such that within each group, none of them overlaps.

is the conditional expectation w.r.t the rounded global Gibbs state, and λ_{RW} is the gap of the classical Markov chain associated with Φ^* . This implies

$$\alpha_{MLSI} \left(\sum_{0 < \bar{\omega} \leq \Delta_{ETH}} \sum_{\bar{\nu}_1 - \bar{\nu}_2 = \bar{\omega}} \mathcal{L}_{\bar{\nu}_1, \bar{\nu}_2} Q_{\bar{\omega}'=0} \right) \geq \Omega \left(\frac{m}{k} \min_{0 < \bar{\nu}_1 - \bar{\nu}_2 \leq \bar{\omega}} \alpha_{MLSI} (\mathcal{L}_{\bar{\nu}_1, \bar{\nu}_2} Q_{\bar{\omega}'=0}) \right),$$

with $m := 2 \lfloor \frac{\Delta_{ETH}}{\bar{\nu}_0} \rfloor$.

We will see the map Φ^* is very much a *classical* random walk (with a minor technical difference), whose mixing rate (in terms of the second eigenvalue) determines k .

Proof. Decompose the input operator into $Q_{\bar{\omega}'=0}[\mathbf{X}] = \sum_{\bar{\nu}} C_{\bar{\nu}} \mathbf{P}_{\bar{\nu}} + \mathbf{O}_{\bar{\nu}}$. The action on $\sum_{\bar{\nu}} C_{\bar{\nu}} \mathbf{P}_{\bar{\nu}}$ is equivalent to a classical Markov chain.

$$\Phi^*[\mathbf{P}_{\bar{\nu}}] = \frac{1}{m} \left(\sum_{0 < \bar{\omega} \leq \Delta_{ETH}} E_{\bar{\nu} + \bar{\omega}, \bar{\nu}}[\mathbf{P}_{\bar{\nu}}] + \sum_{0 < \bar{\omega} \leq \Delta_{ETH}} E_{\bar{\nu}, \bar{\nu} - \bar{\omega}}[\mathbf{P}_{\bar{\nu}}] \right), \quad (5.40)$$

where when $\mathbf{P}_{\bar{\nu} + \bar{\omega}}$ exceeds the boundary of the spectrum, we conveniently use the same notation $E_{\bar{\nu} + \bar{\omega}, \bar{\nu}}$ for the identity map. Taking iterations, the input contracts towards the leading eigenvector

$$\Phi^{*k}[\mathbf{P}_{\bar{\nu}}] = \frac{\langle \mathbf{P}_{\bar{\nu}}, \mathbf{I}_{\sigma} \rangle}{\langle \mathbf{I}, \mathbf{I} \rangle_{\sigma}} \cdot \mathbf{I} + \Phi^{*k}[\mathbf{P}_{\bar{\nu}}^{\perp}] \quad (5.41)$$

$$= E_{global}[\mathbf{P}_{\bar{\nu}}] + \sum_{\bar{\nu}'} c_{\bar{\nu}'} \mathbf{P}_{\bar{\nu}'}, \quad (5.42)$$

with a guaranteed rate due to gap (w.r.t to $\sqrt{\langle \cdot, \cdot \rangle_{\sigma}}$)

$$c_{\bar{\nu}'} \sqrt{\text{Tr}[\sigma_{\bar{\nu}'}]} \leq \sqrt{\sum_{\bar{\nu}'} \text{Tr}[\sigma_{\bar{\nu}'}] c_{\bar{\nu}'}^2} \quad (5.43)$$

$$\leq (1 - \lambda_{RW})^k \sqrt{\text{Tr}[\sigma_{\bar{\nu}}]}. \quad (5.44)$$

On the other hand, the action on the traceless parts $\sum_{\bar{\nu}} c_{\bar{\nu}} \mathbf{O}_{\bar{\nu}}$ is simply

$$\Phi^*[\mathbf{O}_{\bar{\nu}}] = \begin{cases} 0 & \text{if both } \bar{\nu} + \bar{\omega}, \bar{\nu} - \bar{\omega} \text{ are valid} \\ \frac{1}{2} \mathbf{O}_{\bar{\nu}} & \text{else.} \end{cases} \quad (5.45)$$

To establish completely positive order, it suffices to show for inputs being a positive operator $\mathbf{K}_{B, \bar{\nu}}$ acting on the subspace $\mathbf{P}_{\bar{\nu}}$ tensored with arbitrary ancilla B .

$$\Phi^{*k}[\mathbf{K}_{B, \bar{\nu}}] = \Phi^{*k}[\mathbf{K}_B \otimes \mathbf{P}_{\bar{\nu}} + \mathbf{O}_{B, \bar{\nu}}] \quad (5.46)$$

$$= \mathbf{K}_B \otimes \sum_{\bar{\nu}'} (\text{Tr}[\sigma_{\bar{\nu}'}] + c_{\bar{\nu}'}) \mathbf{P}_{\bar{\nu}'} + \Phi^{*k}[\mathbf{O}_{B, \bar{\nu}}], \quad (5.47)$$

where we evaluate $E_{\mathcal{N}}[\mathbf{P}_{\bar{\nu}}] = \sum_{\bar{\nu}'} \text{Tr}[\sigma_{\bar{\nu}'}] \mathbf{P}_{\bar{\nu}'}$. To establish completely positive order¹⁵, it suffices to show for every $\bar{\nu}' \neq \bar{\nu}$

$$|c_{\bar{\nu}'}| \leq \epsilon \text{Tr}[\sigma_{\bar{\nu}}], \quad \frac{1}{2^k} + |c_{\bar{\nu}}| \leq \epsilon \text{Tr}[\sigma_{\bar{\nu}}], \quad (5.48)$$

¹⁵ For the second equation, we use that $\Phi^{*k}[\mathbf{O}_{B, \bar{\nu}}] \propto \mathbf{O}_{B, \bar{\nu}}$ and the generalized depolarizing channel is completely positive.

which is possible by demanding

$$k = \Omega \left(\max_{\bar{\nu}} |\ln(\text{Tr}[\sigma_{\bar{\nu}}])| \cdot \left(1 + \frac{1}{\lambda_{RW}} \right) \right). \quad (5.49)$$

We have dropped the $\log(\epsilon)$ dependence since ϵ only needs to be a constant ($\epsilon^2 \leq 2 \ln(2) - 1$); the decay due to $\frac{1}{2^k}$ is absorbed into $\Omega(\cdot)$. \square

1. Calculations for the random walk gap λ_{RW}

Given any Gibbs distribution, the gap λ_{RW} of the classical random walk can be obtained via classical conductance estimates. We will calculate for Gibbs distribution satisfying Assumption IV.2, which includes Gaussians with variance Δ_{spec} .

Proposition V.10.1. *For Gibbs distribution satisfying Assumption IV.2 with the characteristic scale Δ_{spec}^2*

$$\lambda_{RW} = \Omega \left(\frac{\Delta_{ETH}^2 e^{-2\beta\Delta_{ETH}}}{\Delta_{spec}^2 R^2} \right).$$

Intuitively, the Markov chain is a 1d random walk with a characteristic scale being the ratio between the width of distribution $\theta(\Delta_{spec})$ and the hop $\theta(\Delta_{ETH})$. See Appendix B1 for the conductance calculation.

C. Off-block-diagonal Inputs

We now show the off-block-diagonal block gives quantum expanders. The off-block-diagonal inputs $\sum_{\bar{\nu}} \mathbf{P}_{\bar{\nu}+\bar{\omega}'} \mathbf{X} \mathbf{P}_{\bar{\nu}} =: Q_{\bar{\omega}'}[\mathbf{X}]$ has a very much similar story, with the distinction that its local leading eigenvalues are *negative*. We do not need a sophisticated local-to-global estimate. We will see that the off-block-diagonal sectors contract (decohere) faster than the random walk in the diagonal block.

$$\begin{aligned} \mathcal{L}_{\bar{\omega}} \left[\sum_{\bar{\nu}} \mathbf{X}_{\bar{\nu}, \bar{\nu}+\bar{\omega}'} \right] &= \sum_{\bar{\nu}_1 - \bar{\nu}_2 = \bar{\omega}} \mathcal{L}_{\bar{\nu}_1 \bar{\nu}_2, \bar{\omega}'} \\ &= \sum_{\bar{\nu}_1 - \bar{\nu}_2 = \bar{\omega}} \sum_a \left[\frac{\gamma(\bar{\omega})}{2} \left(\mathbf{A}_{\bar{\nu}_1 \bar{\nu}_2}^a \mathbf{X} \mathbf{A}_{\bar{\nu}_2+\bar{\omega}', \bar{\nu}_1+\bar{\omega}'}^a - \frac{1}{2} \mathbf{A}_{\bar{\nu}_1 \bar{\nu}_2}^a \mathbf{A}_{\bar{\nu}_2 \bar{\nu}_1}^a \mathbf{X}_{\bar{\nu}_1, \bar{\nu}_1+\bar{\omega}'} - \frac{1}{2} \mathbf{X}_{\bar{\nu}_1, \bar{\nu}_1+\bar{\omega}'} \mathbf{A}_{\bar{\nu}_1+\bar{\omega}', \bar{\nu}_2+\bar{\omega}'}^a \mathbf{A}_{\bar{\nu}_2+\bar{\omega}', \bar{\nu}_1+\bar{\omega}'}^a \right) \right. \\ &\quad \left. + (\bar{\omega} \rightarrow -\bar{\omega}, \bar{\nu}_1 \leftrightarrow \bar{\nu}_2) \right] \end{aligned} \quad (5.50)$$

Lemma V.11. *For each $\bar{\omega}'$, $0 \leq \bar{\omega} \leq \Delta_{ETH}$, with high probability,*

$$\lambda_{max} \left(\sum_{0 \leq \bar{\omega} \leq \Delta_{ETH}} \sum_{\bar{\nu}_1 - \bar{\nu}_2 = \bar{\omega}} \mathcal{L}_{\bar{\nu}_1 \bar{\nu}_2, \bar{\omega}'} \right) \leq -\Omega \left(\frac{1}{R} \int_0^{\Delta_{ETH}} |a| \gamma(-\omega) |f_{\omega}|^2 d\omega \right)$$

We obtain bounds for the expectation and deviation, with analogous proofs as in Proposition V.3.1, Proposition V.4.1.

Proposition V.11.1. *The expected Lindbladian $\mathbb{E}[\mathcal{L}_{\bar{\nu}_1 \bar{\nu}_2, \bar{\omega}'}]$, acting on $\mathbf{X}_{\bar{\nu}_2, \bar{\nu}_2+\bar{\omega}'} + \mathbf{X}_{\bar{\nu}_1, \bar{\nu}_1+\bar{\omega}'}$ has two clusters of eigenvalue*

$$\begin{aligned} -\frac{|a| \gamma(-\bar{\omega})}{4} (V_{\bar{\nu}_1, \bar{\nu}_2}^{max} \text{Tr}[\mathbf{P}_{\bar{\nu}_1}] + V_{\bar{\nu}_1+\bar{\omega}', \bar{\nu}_2+\bar{\omega}'}^{max} \text{Tr}[\mathbf{P}_{\bar{\nu}_1+\bar{\omega}'}]) &\leq \lambda(P_1 \mathbb{E}[\mathcal{L}_{\bar{\nu}_1 \bar{\nu}_2}] P_1) \leq (\min \leftrightarrow \max) \\ -\frac{|a| \gamma(\bar{\omega})}{4} (V_{\bar{\nu}_1, \bar{\nu}_2}^{max} \text{Tr}[\mathbf{P}_{\bar{\nu}_2}] + V_{\bar{\nu}_1+\bar{\omega}', \bar{\nu}_2+\bar{\omega}'}^{max} \text{Tr}[\mathbf{P}_{\bar{\nu}_2+\bar{\omega}'}]) &\leq \lambda(P_2 \mathbb{E}[\mathcal{L}_{\bar{\nu}_1 \bar{\nu}_2}] P_2) \leq (\min \leftrightarrow \max), \end{aligned}$$

where superoperator $P_i[\cdot] = \mathbf{P}_{\bar{\nu}_i}[\cdot] \mathbf{P}_{\bar{\nu}_i+\bar{\omega}'}$ are the corresponding projectors.

Note that the cross term $\mathbf{A}_{\bar{\nu}_1 \bar{\nu}_2}^a \mathbf{X} \mathbf{A}_{\bar{\nu}_2+\bar{\omega}', \bar{\nu}_1+\bar{\omega}'}^a$ vanishes in expectation, which is why the leading eigenvalue is negative.

Proposition V.11.2. *The deviation $\delta \mathcal{L} := (\mathcal{L}_{\bar{\nu}_1 \bar{\nu}_2, \bar{\omega}'} - \mathbb{E}[\mathcal{L}_{\bar{\nu}_1 \bar{\nu}_2, \bar{\omega}'}])$ is, with high probability, at most*

$$\|\delta \mathcal{L}\|_{\infty, \bar{\sigma}} = \mathcal{O} \left(\sqrt{c_{\bar{\nu}_1, \bar{\nu}_2} c_{\bar{\nu}_1+\bar{\omega}', \bar{\nu}_2+\bar{\omega}'} \cdot e^{\beta \bar{\omega}}} \right) \leq \mathcal{O} \left(\frac{R^2 e^{\beta \Delta_{ETH}}}{\sqrt{|a|}} \lambda_{max}(\mathbb{E} \mathcal{L}) \right)$$

Where $c_{\bar{\nu}_1, \bar{\nu}_2}$ is defined in (5.17). The inequality is arithmetic-geometric as well as estimates due to density variations and Boltzmann factors. We now prove Lemma V.11.

Proof. For each $\mathcal{L}_{\bar{\nu}_1 \bar{\nu}_2, \bar{\omega}'}$, repeat the proof of Lemma V.3. For each $\bar{\omega}$, summing over $\bar{\nu}_1$ yields an operator with global maximal eigenvalue at most as large as (5.51). Note that $V_{\bar{\nu}_1, \bar{\nu}_2}^{max} \text{Tr}[\mathbf{P}_{\bar{\nu}_1}] \lesssim R |f_{\bar{\omega}}|^2 \bar{\nu}_0$ is only dependent on the Bohr frequency $\bar{\nu}_1 - \bar{\nu}_2 = \bar{\omega}$. Sum over $\bar{\omega}$ and pass to an integral to obtain the advertised result. \square

D. Proof of Theorem V.1

Proof. We obtain the global MLSI constant via local gap estimates (Lemma V.3) and approximate tensorization (Lemma V.10)

$$\alpha_{diag} := \alpha(\mathcal{L} \circ Q_{\bar{\omega}'=0}) = \alpha(\mathcal{D} \circ Q_{\bar{\omega}'=0}) \geq \alpha(\mathcal{D}_{\leq \Delta_{ETH}} \circ Q_{\bar{\omega}'=0}) = \alpha \left(\sum_{0 \leq \bar{\omega} \leq \Delta_{ETH}} \sum_{\bar{\nu}_1 - \bar{\nu}_2 = \bar{\omega}} \mathcal{L}_{\bar{\nu}_1, \bar{\nu}_2} \circ Q_{\bar{\omega}'=0}[\cdot] \right) \quad (5.51)$$

$$\geq \alpha \left(\sum_{S_1, S_2} \mathcal{L}_{S_1, S_2} \circ Q_{\bar{\omega}'=0} \right) \quad (5.52)$$

$$\geq \Omega \left(\frac{m}{k} \min_{0 < \bar{\nu}_1 - \bar{\nu}_2 \leq \Delta_{ETH}} \alpha(\mathcal{L}_{\bar{\nu}_1, \bar{\nu}_2}) \right) \quad (5.53)$$

$$\geq \Omega \left(\lambda_{RW} \cdot \frac{|a| \Delta_{ETH} \min_{0 < \bar{\omega} \leq \Delta_{ETH}} \gamma(-\bar{\omega}) |f_{\bar{\omega}}|^2}{(n + \beta \|\mathbf{H}_S\|)(n + \beta \Delta_{ETH})} \right),$$

where we plug in the parameters

$$m = 2 \lfloor \frac{\Delta_{ETH}}{\bar{\nu}_0} \rfloor, \quad (5.54)$$

$$k = \Omega \left(\max_{\bar{\nu}} |\ln(\text{Tr}[\boldsymbol{\sigma}_{\bar{\nu}}])| \cdot \left(1 + \frac{1}{\lambda_{RW}} \right) \right), \quad (5.55)$$

$$\alpha(\mathcal{L}_{\bar{\nu}_1, \bar{\nu}_2} \circ Q_{\bar{\omega}'=0}) \geq \Omega \left(\frac{|a| \bar{\nu}_0 |f_{\bar{\omega}}|^2 \gamma(-\bar{\omega})}{R(n + \beta \Delta_{ETH})} \right). \quad (5.56)$$

We also need enough flips to ensure the deviation is smaller than the expectation

$$|a| = \Omega(R^4 e^{2\beta \Delta_{ETH}}). \quad (5.57)$$

For the off-block-diagonal, the rate is much faster (Lemma V.11)

$$\lambda_{off} := -\lambda_{max} \left(\sum_{0 \leq \bar{\omega} \leq \Delta_{ETH}} \sum_{\bar{\nu}_1 - \bar{\nu}_2 = \bar{\omega}} \mathcal{L}_{\bar{\nu}_1, \bar{\nu}_2, \bar{\omega}'} \right) \geq \Omega \left(\frac{|a| \Delta_{ETH}}{R} \min_{\bar{\omega} \leq \Delta_{ETH}} \gamma(-\bar{\omega}) |f_{\bar{\omega}}|^2 \right). \quad (5.58)$$

Putting everything together,

$$\left\| e^{\bar{\mathcal{L}}^\dagger t} [\boldsymbol{\rho}] - \bar{\boldsymbol{\sigma}} \right\|_1 \leq \left\| e^{\bar{\mathcal{L}}^\dagger t} Q_{\bar{\omega}'=0} [\boldsymbol{\rho}] - \bar{\boldsymbol{\sigma}} \right\|_1 + \left\| e^{\bar{\mathcal{L}}^\dagger t} Q_{\bar{\omega}' \neq 0} [\boldsymbol{\rho}] \right\|_1 \quad (5.59)$$

$$\leq \exp(-\alpha_{diag} \tau) \cdot \sqrt{2 \ln(\|\bar{\boldsymbol{\sigma}}^{-1}\|)} + \exp(-\lambda_{off} \tau) \cdot \left\| \frac{1}{\bar{\boldsymbol{\sigma}}} \right\|_\infty. \quad (5.60)$$

The second inequality uses standard conversions between norms (4.5), (7.61) for the first and second term. This means for ϵ precision, it suffices to evolve for time τ .

$$\tau_\epsilon = \tilde{\Omega} \left(\ln(1/\epsilon) \left(\frac{1}{\alpha_{diag}} + \frac{1}{\lambda_{off}} (n + \beta \|\mathbf{H}_S\|) \right) \right) \text{ ensures } \left\| e^{\bar{\mathcal{L}}^\dagger t} [\boldsymbol{\rho}] - \bar{\boldsymbol{\sigma}} \right\|_1 \leq \epsilon, \quad (5.61)$$

where $\tilde{\Omega}$ absorbs logarithmic dependence on $n, \beta, \|\mathbf{H}_S\|$. This is the advertised result. \square

E. Comments on Non-diagonal $\gamma_{ab}(\bar{\omega})$.

We have focused on Lindbladian with diagonal $\gamma_{ab}(\bar{\omega}) = \delta_{ab} \gamma_{aa}(\bar{\omega})$. For other Lindbladians where $\gamma_{ab} \neq \delta_{ab} \gamma_{ab}$, our proof strategy can be adapted with a quick transformation. For each $\bar{\omega}$, perform a basis transformation to diagonalize $\gamma_{ab} = U_{aa'}^\dagger D_{a'b'} \delta_{a'b'} U_{b'b}$. (Note γ_{ab} is positive-semi-definite.) Then

$$\begin{aligned} \sum_{ab} \gamma_{ab} \mathbf{G}_a^\dagger \otimes \mathbf{G}_b &= \sum_{a'b'ab} U_{aa'}^\dagger D_{a'b'} \delta_{a'b'} U_{b'b} \mathbf{G}_a^\dagger \otimes \mathbf{G}_b \\ &= \sum_{a'b'} D_{a'b'} \delta_{a'b'} \left(\sum_a U_{aa'}^\dagger \mathbf{G}_a^\dagger \right) \otimes \left(\sum_b U_{b'b} \mathbf{G}_b \right) \stackrel{dist}{\sim} \sum_{a'} D_{a'a'} \mathbf{G}_{a'}^\dagger \otimes \mathbf{G}_{a'} \end{aligned} \quad (5.62)$$

in the last line recall that unitary preserves i.i.d Gaussian vectors $U_{b'b}g_b \sim g_b$. This means we only need to replace

$$\sum_a \gamma_a(\bar{\omega}) \rightarrow \|\gamma(\bar{\omega})\|_1 \quad (5.63)$$

$$\sqrt{\sum_a \gamma_a(\bar{\omega})^2} \rightarrow \|\gamma(\bar{\omega})\|_2, \quad (5.64)$$

since 2-norm and 1-norm are preserved by the transformation. For the concentration argument (Section V A), all we require for the bath is that for any constant (more precisely any fixed but potential large constant)

$$\frac{\|\gamma(\bar{\omega})\|_1}{\|\gamma(\bar{\omega})\|_2} \geq \text{Const} \quad (5.65)$$

is possible for large enough number of interaction terms $|a|$.

F. Resource estimates

If we plug in explicit parameters and set

$$\begin{aligned} \Delta_{ETH} &= \theta\left(\frac{1}{n^3}\right) \\ \Delta_{spec} &= \theta(\sqrt{n}) \\ \|\mathbf{H}_S\| &= \theta(n) \\ \min_{\bar{\omega} \leq \Delta_{ETH}} |f_{\bar{\omega}}|^2 &= \theta(n) \\ \beta &\leq \frac{1}{\Delta_{ETH}} \quad (= \theta(n^3)) \end{aligned}$$

Then by Theorem V.1, to be ϵ -close to the fixed point, it suffices to run for effective time

$$\tau = \tilde{\Omega}(\ln(1/\epsilon)n^8(1+\beta)). \quad (5.66)$$

and also the resources (Theorem III.1)

$$\begin{aligned} \ell &= \theta\left(\frac{|a|^2 \tau^2}{\epsilon \Delta_{ETH}^2}\right) = \theta\left(\frac{n^{22}(1+\beta)^2}{\epsilon}\right) && \text{(bath refreshes)} \\ t &= \theta\left(\frac{|a|^2 \tau^2}{\epsilon \Delta_{ETH}^2 \bar{\nu}_0}\right) = \theta\left(\frac{n^{22}(1+\beta)^2}{\epsilon} \left(\frac{\beta}{\epsilon} + n^{11}(1+\beta)\right)\right) && \text{(physical runtime)} \\ n_B &= \tilde{\theta}\left(\frac{|a|^2 \tau \Delta_{ETH}}{\epsilon \bar{\nu}_0^2}\right) = \theta\left(\frac{n^8(1+\beta)}{\epsilon} \left(\frac{\beta}{\epsilon} + n^{11}(1+\beta)\right)^2\right) && \text{(size of bath)} \\ \frac{1}{\bar{\nu}_0} &= \theta\left(\frac{\beta}{\epsilon} + \frac{|a| \tau}{\Delta_{ETH}} + \frac{\Delta_{ETH}}{|a|}\right) && \text{(resolution of Davies' generator).} \end{aligned}$$

Importantly, we see all resource requirements are polynomial.

G. Comments on Optimality

Our convergence results, although depend polynomially in all relevant parameters, honestly speaking, seems awkwardly slow. To find the causes, it is instructive to compare our Lindbladian results (Theorem I.2) with the 1d commuting cases [11]. For a fair comparision, we fix the environment so that $\gamma_{ab}(\bar{\omega})$ is independent of the subsystem size, $\gamma_{ab}(\bar{\omega}) = \mathcal{O}(1)$ for $\bar{\omega} \leq \mathcal{O}(1)$. For our Lindbladians at finite resolution, set the same $\gamma_{ab}(\bar{\omega})$, the characteristic scale of Gibbs state to be $\Delta_{spec}^2 = \theta(n)$, and the flips to be all single site operators $|a| = \theta(n)$,

$$\tau_{comm} = \mathcal{O}(\log(n)) \text{ v.s. } \tau_{ETH} \approx \log(1/\epsilon) \frac{\Delta_{spec}^2}{\Delta_{ETH}^2} \cdot \frac{(n + \beta \|\mathbf{H}_S\|)n}{|a| \int_0^{\Delta_{ETH}} \gamma(-\omega) |f_\omega|^2 d\omega}. \quad (5.67)$$

The classical random walk gap and transition rates are arguably the best we can hope for, and it is the presumed parameters of ETH (Δ_{ETH} , $f_{\bar{\omega}}$) that slow us down; the part of the proof that may be improved is the conversion between norms $(n + \beta \|\mathbf{H}_S\|)n$.

In other words, if we hope our Lindbladian to be as nearly good as the commuting cases, we need (I) a version¹⁶ of ETH that $\Delta'_{ETH} = \mathcal{O}(1)$ and the transition rate f_ω has most weight supported in $\omega = \pm\mathcal{O}(1)$, and (II) better conversions between norms and notions of mixing.

1. Resource costs

In addition to thermalization at the effective time τ , the implementation of Davies's generator (Theorem III.1) uses physical resources (5.67) that scales quadratically with effective time τ^2 . This is rooted in the weak-coupling approximation (Lemma III.3) and the secular approximation (Lemma III.4) that are only provably accurate to the leading order. It is possible that the finitely-resolved Davies' generator can be implemented at a lower resource cost via weak-coupling or other methods(e.g., [24]), but it is not apparent from the current proof strategy. The bath size $\sim \tau^3$ is a potentially loose bound.

VI. QUANTUM METROPOLIS SAMPLING

A. Warmup: Perfect Energy Resolution

If we (unrealistically) assume phase estimation with infinite resolution and the energy spectrum has no degeneracy, Quantum Metropolis iterates the following [3].

- (Step 1) measure the energy via phase estimation

$$|\psi\rangle|0\rangle|0\rangle|0\rangle \rightarrow |\psi_{\nu_1}\rangle|\nu_1\rangle|0\rangle|0\rangle. \quad (6.1)$$

- (Step 2) (randomly) apply an operator \mathbf{A} (a “flip”)

$$|\psi_{\nu_1}\rangle|\nu_1\rangle|0\rangle|0\rangle \rightarrow \sum_{\nu_2} A_{\nu_2\nu_1} |\psi_{\nu_2}\rangle|\nu_1\rangle|0\rangle|0\rangle. \quad (6.2)$$

- (Step 3) estimate the energy, but keep it coherent

$$\sum_{\nu_2} A_{\nu_2\nu_1} |\psi_{\nu_2}\rangle|\nu_1\rangle|0\rangle|0\rangle \rightarrow \sum_{\nu_2} A_{\nu_2\nu_1} |\psi_{\nu_2}\rangle|\nu_1\rangle|\nu_2\rangle|0\rangle. \quad (6.3)$$

To implement the Metropolis weight, apply the following rotation at the 1-bit register

$$\begin{bmatrix} \sqrt{1-f_{21}} & \sqrt{f_{21}} \\ \sqrt{f_{21}} & -\sqrt{1-f_{21}} \end{bmatrix}, \quad f_{21} := \min(1, e^{-\beta(\nu_2-\nu_1)}). \quad (6.4)$$

Then, the state entangles with the 1-bit register

$$\sum_{\nu_2} \sqrt{f_{21}} A_{\nu_2\nu_1} |\psi_{\nu_2}\rangle|\nu_1\rangle|\nu_2\rangle|1\rangle + \sum_{\nu_2} \sqrt{1-f_{21}} A_{\nu_2\nu_1} |\psi_{\nu_2}\rangle|\nu_1\rangle|\nu_2\rangle|0\rangle. \quad (6.5)$$

Now, measure the 1-bit register:

(3-A) If we obtain outcome “1”, this is the *acceptance* instance. This happens with probability weighted by the desired Metropolis factor

$$\Pr(\nu_1 \rightarrow \nu_2) = \sum_a p(a) |A_{\nu_2\nu_1}^a|^2 \cdot \min(1, e^{-\beta(\nu_2-\nu_1)}). \quad (6.6)$$

(3-R) If we obtain outcome “0”, this triggers a *rejection* procedure that attempts to return a state with energy ν_1 . (This may fail to happen, see below (6.25).) Lastly, after either (3-A) or (3-R), initialize the energy registers and go to (Step 1).

Formally, the CPTP map with perfect QPE can be written as the sum of acceptance and rejection moves

$$\mathcal{N} := \mathcal{A} + \mathcal{R}, \quad (6.7)$$

$$\mathcal{A}[\rho] := \sum_{\nu_2\nu_1} \sum_a p(a) \mathbf{P}_{\nu_2} \cdot \mathbf{A}^a (\mathbf{P}_{\nu_1} \rho \mathbf{P}_{\nu_1}) \mathbf{A}^{a\dagger} \cdot \mathbf{P}_{\nu_2} \cdot \min(1, e^{-\beta(\nu_2-\nu_1)}) \quad (6.8)$$

$$\mathcal{R}[\rho] := \sum_{\nu} \mathbf{P}_{\nu} \rho \mathbf{P}_{\nu} (1 - \text{Tr}[\mathcal{A}[\mathbf{P}_{\nu}]]), \quad (6.9)$$

¹⁶ Note that when Δ_{ETH} becomes $\mathcal{O}(1)$, $e^{\beta\Delta_{ETH}}$ grows with inverse temperature β , but remains a constant in the thermodynamic limit.

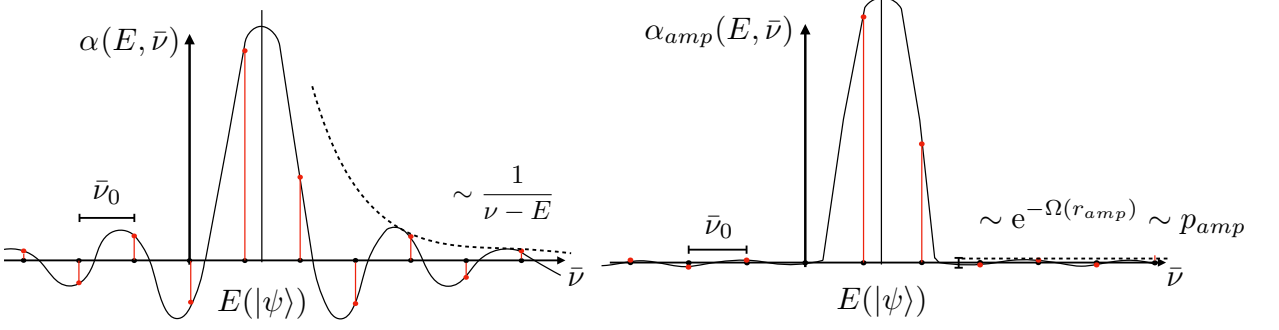


Figure 8. Phase estimation profile at finite times. Fundamentally, the resolution must be inverse runtime. On the left is the original QPE profile. On the right, we improve the $1/(\bar{\nu})$ tail by rounds r_{amp} of amplification so that the outcome lies at either of two registers, with high probability $1 - e^{-\Omega(r_{amp})}$.

and it essentially becomes a classical Markov chain with transition rates (6.6). Markov chains have standard gap estimates (e.g., conductance), and the Metropolis weight $\min(1, e^{-\beta(\nu_2 - \nu_1)})$ guarantees detailed balance and hence the fixed point being the Gibbs state. A natural choice for $p(a)$ is the uniform distribution

$$p(a) = \frac{1}{|a|}. \quad (6.10)$$

B. Explicit CPTN Map with Realistic Phase Estimation

However, phase estimation has a finite resolution inversely proportional to the run time $1/t_{QPE}$. The acceptance instance then compiles to

$$\begin{aligned} \mathcal{A}[\rho] &:= \sum_{\bar{\nu}_2 \bar{\nu}_1} \sum_a p(a) \sum_{upq} S_{\bar{\nu}_2}^{up} \cdot \mathbf{A}^a \left(S_{\bar{\nu}_1}^{p0} \rho S_{\bar{\nu}_1}^{0q} \right) \mathbf{A}^{a\dagger} \cdot S_{\bar{\nu}_2}^{qu} \cdot \min(1, e^{-\beta(\bar{\nu}_2 - \bar{\nu}_1)}) \\ &:= \sum_{\bar{\nu}_2 \bar{\nu}_1} \mathcal{A}_{\bar{\nu}_2 \bar{\nu}_1}[\rho]. \end{aligned} \quad (6.11)$$

Roughly speaking, $S_{\bar{\nu}_1}^{p0} \cdot S_{\bar{\nu}_1}^{0q}$ corresponds to obtaining energy measurement outcome $\bar{\nu}_1$. More carefully,

$$S_{\bar{\nu}}^{up} := M_{\bar{\nu}}^{u\dagger} M_{\bar{\nu}}^p, \quad (6.12)$$

$$M_{\bar{\nu}}^{\bar{\mu}} := \sum_i \alpha(E_i, \bar{\nu} - \bar{\mu}) |\psi_i\rangle \langle \psi_i| \quad (6.13)$$

where $\alpha(E, \bar{\nu})$ is some phase estimation profile (Figure 8). The scripts $M_{\bar{\nu}}^{\bar{\mu}}$ label the measurement value in ancillary register which was traced out in (6.11) by summing over u, p, q . In other words, the full control unitary of a phase estimation subroutine, acting on the input state ρ and the ancillae, would be

$$\Phi := \sum_{\bar{\nu}} \sum_{\bar{\mu}} M_{\bar{\nu}}^{\bar{\mu}} \otimes |\bar{\nu}\rangle \langle \bar{\mu}|. \quad (6.14)$$

In the baby version of QPE, $\alpha(E, \bar{\nu})$ spreads all across the register with a $(\bar{\nu} - E)^{-1}$ decay. An amplified version [43] can restrict the outcome to be supported on only 2 energy registers (but cannot be fewer!), with a small chance of failure p_{amp}

$$p_{amp} = e^{-\Omega(r_{amp})}. \quad (6.15)$$

To be self-contained, we include the full circuit description of the total Complete Positive Trace Non-increasing (CPTN) map $\mathcal{N} := \mathcal{A} + \mathcal{R}$

$$\mathcal{A}[\rho] = \sum_a p(a) \text{Tr}_{anc} \left[\hat{L}^{(a)} \hat{Q}_1^{(a)} \hat{E}[\rho \otimes |0\rangle \langle 0|_{anc}] \right] \quad (6.16)$$

$$\mathcal{R}[\rho] = \sum_a p(a) \text{Tr}_{anc} \left[\sum_{r=0}^{r_{reg}} \sum_{s_1 \dots s_n=0}^1 \hat{P}_1 \left(\sum_s \hat{Q}_s^{(a)} \hat{P}_0 \right)^r \hat{Q}_0^{(a)} \hat{E}[\rho \otimes |0\rangle \langle 0|_{anc}] \right] \quad (6.17)$$

where the hatted operators denote acting by conjugation, e.g., $\hat{L}[\cdot] := \mathbf{L}[\cdot]\mathbf{L}^\dagger$.

$$\mathbf{Q}_s^{(a)} := \sum_{\bar{\nu}_2, \bar{\nu}_1} \mathbf{A}^{a\dagger} \mathbf{M}_{\bar{\nu}_2}^{p_1\dagger} \mathbf{M}_{\bar{\nu}_2}^{p_2} \mathbf{A}^a \otimes |\bar{\nu}_1\rangle \langle \bar{\nu}_1| \otimes |p_1\rangle \langle p_2| \otimes \mathbf{R}^s(\bar{\nu}_1, \bar{\nu}_2), \quad (6.18)$$

$$\mathbf{P}_0 = \sum_{\bar{\nu}_2 \neq \bar{\nu}_1} \mathbf{M}_{\bar{\nu}_2}^{p_1\dagger} \mathbf{M}_{\bar{\nu}_2}^{p_2} \otimes |\bar{\nu}_1\rangle \langle \bar{\nu}_1| \otimes |p_1\rangle \langle p_2| \otimes \mathbf{I}, \quad (6.19)$$

$$\mathbf{P}_1 = \sum_{\bar{\nu}_2 = \bar{\nu}_1} \mathbf{M}_{\bar{\nu}_2}^{p_1\dagger} \mathbf{M}_{\bar{\nu}_2}^{p_2} \otimes |\bar{\nu}_1\rangle \langle \bar{\nu}_1| \otimes |p_1\rangle \langle p_2| \otimes \mathbf{I}, \quad (6.20)$$

where

$$\mathbf{R}^s(\bar{\nu}_1, \bar{\nu}_2) := \mathbf{W}^\dagger(\bar{\nu}_1, \bar{\nu}_2) |s\rangle \langle s| \mathbf{W}(\bar{\nu}_1, \bar{\nu}_2), \quad (6.21)$$

$$\mathbf{W}(\bar{\nu}_1, \bar{\nu}_2) := \begin{bmatrix} \sqrt{1-f_{21}} & \sqrt{f_{21}} \\ \sqrt{f_{21}} & -\sqrt{1-f_{21}} \end{bmatrix}, \quad f_{21} := \min(1, e^{-\beta(\bar{\nu}_2 - \bar{\nu}_1)}). \quad (6.22)$$

And the edge cases

$$\mathbf{E} = \sum_{\bar{\nu}_2, \bar{\nu}_1} \sum_{p_2, p_1} \mathbf{M}_{\bar{\nu}_2}^{p_1\dagger} \mathbf{M}_{\bar{\nu}_2}^{p_2} \otimes |\bar{\nu}_1 \oplus \bar{\nu}_2\rangle \langle \bar{\nu}_1| \otimes |p_1\rangle \langle p_2| \otimes \mathbf{I}, \quad (6.23)$$

$$\mathbf{L} = \sum_{\bar{\nu}_2, \bar{\nu}_1} \sum_{p_2, p_1} \mathbf{M}_{\bar{\nu}_2}^{p_1\dagger} \mathbf{M}_{\bar{\nu}_2}^{p_2} \mathbf{A} \otimes |\bar{\nu}_1\rangle \langle \bar{\nu}_1| \otimes |p_1\rangle \langle p_2| \otimes \mathbf{W}(\bar{\nu}_1, \bar{\nu}_2). \quad (6.24)$$

For our purposes, we will only need the form (6.11) for the acceptance instance. For the rejection step, we keep the abstract form of the rejection instances (6.17) as we will never need it explicitly. Intuitively, if we expand by its first measurement value $\bar{\nu}_1$

$$\mathcal{R} = \sum_{\bar{\nu}_1} \mathcal{R}_{\bar{\nu}_1}, \quad (6.25)$$

the rejection map $\mathcal{R}_{\bar{\nu}_1}$ succeeds when the same measurement value $\bar{\nu}_2 = \bar{\nu}_1$ is obtained (via iterating certain complicated circuit $\sum_s \hat{Q}_s^{(a)} \hat{P}_0$). If this does not happen within some number of rounds r_{rej} , we abort (which makes the Metropolis map \mathcal{N} CPTN instead of CPTP). The probability p_{rej} of such a failure event depends on the circuit $\sum_s \hat{Q}_s^{(a)} \hat{P}_0$ (which depends on the Hamiltonian \mathbf{H}_S). A crude unconditional bound [3, Sec. 3.1] is

$$p_{rej} = \mathcal{O}\left(\frac{1}{r_{rej}}\right), \quad (6.26)$$

whereas we may expect $p_{rej} \sim e^{-\Omega(r_{rej})}$ in practice, but this is hard to show.

The main technical challenge lies in realistic phase estimation: (1) the Metropolis weights (and hence detailed balance) is only approximate and (2) the diagonal blocks (i.e., with similar energies) remain coherent since measurements only distinguish energies far apart.

C. Approximate Detailed Balance.

Our first step towards proving convergence is to make sense of *approximate* detailed balance. The *exact* detailed balance takes a few equivalent forms.

Definition VI.1 (Detailed balance). *For a normalized state $\sigma \geq 0$, we say a self-map \mathcal{E} satisfies σ -detailed balance whenever the equivalent conditions hold*

- $\mathcal{E}[\sqrt{\sigma} \cdot \sqrt{\sigma}] = \sqrt{\sigma} \mathcal{E}^\dagger[\cdot] \sqrt{\sigma}$,
- $\sigma^{-1/4} \mathcal{E}[\sigma^{1/4} \cdot \sigma^{1/4}] \sigma^{-1/4}$ is self-adjoint w.r.t to trace (i.e. H.S. norm),
- \mathcal{E} is self-adjoint w.r.t the σ^{-1} -weighted inner product

$$\text{Tr}[\rho_1^\dagger \frac{1}{\sqrt{\sigma}} \rho_2 \frac{1}{\sqrt{\sigma}}] =: \langle \rho_1, \rho_2 \rangle_{\sigma^{-1}}, \quad (6.27)$$

- \mathcal{E}^\dagger is self-adjoint w.r.t the σ -weighted inner product

$$\text{Tr}[\mathcal{O}_1^\dagger \sqrt{\sigma} \mathcal{O}_2 \sqrt{\sigma}] =: \langle \mathcal{O}_1, \mathcal{O}_2 \rangle_\sigma. \quad (6.28)$$

The interpretation of self-adjointness w.r.t to the weighted norms will be vital in our proofs. Also:

Fact VI.2. *If \mathcal{E} preserves trace and satisfies σ -detailed balance, $\mathcal{E}[\sigma] = \sigma$.*

However, we must allow perturbations from the exact cases above and quantify how they impact the performance: (1) Imperfect QPE means that the Metropolis weights will not be exact, and the channel will have a non-trivial anti-self-adjoint component, w.r.t the inner product $\langle \cdot, \cdot \rangle_{\sigma^{-1}}$

$$\mathcal{N} = \frac{1}{2} \left(\mathcal{N} + \sqrt{\sigma} \mathcal{N}^\dagger \left[\frac{1}{\sqrt{\sigma}} \cdot \frac{1}{\sqrt{\sigma}} \right] \sqrt{\sigma} \right) + \frac{1}{2} \left(\mathcal{N} - \sqrt{\sigma} \mathcal{N}^\dagger \left[\frac{1}{\sqrt{\sigma}} \cdot \frac{1}{\sqrt{\sigma}} \right] \sqrt{\sigma} \right) \quad (6.29)$$

$$=: \mathcal{N}_{H,\sigma} + \mathcal{N}_{A,\sigma}. \quad (6.30)$$

(2) \mathcal{N} is only approximately trace-preserving. The rejection instances must stop at some r_{rej} and come with a failure probability p_{fail} ; the phase estimation step, amplified r_{amp} times, has a small failure probability $e^{-\Omega(r_{QPE})}$.

In the following, we quantify an appropriate notion of “approximate” detailed balance and obtain a bound for the Metropolis CP map \mathcal{N} .¹⁷

Proposition VI.2.1 (Approximate detailed balance). *The Metropolis CP map \mathcal{N} satisfies approximate σ -detailed balance:*

$$\|\mathcal{N}_{A,\sigma}\|_{1-1} \leq \mathcal{O}(\beta r_{rej} \bar{\nu}_0) := \epsilon_{DB}$$

where r_{rej} is the number of rejection iteration.

Right now, it controls how well the fixed point approximates the Gibbs state. (Later, we will need it again for the convergence (7.11).) Observe

$$\|\mathcal{N}[\sigma] - \sigma\|_1 \leq \|\sigma\|_1 \cdot \|\mathcal{N}_{A,\sigma}\|_{1-1} \leq \epsilon_{DB}. \quad (6.31)$$

We first show the fixed point approximates the Gibbs state assuming CPTP.

Fact VI.3 ([3, Sec 4.3]). *Consider a CPTP map \mathcal{E} such that $\|\mathcal{E}[\sigma] - \sigma\|_1 \leq \epsilon_{DB}$, then*

$$\|\sigma_{fix}(\mathcal{E}) - \sigma\|_1 \leq 2\ell \cdot \epsilon_{DB}$$

whenever

$$\eta_1(\mathcal{E}^\ell) := \sup_{\rho_1, \rho_2} \frac{\|\mathcal{E}^\ell[\rho_1 - \rho_2]\|_1}{\|\rho_1 - \rho_2\|_1} \leq \frac{1}{2}.$$

Proof.

$$\|\sigma_{fix}(\mathcal{E}) - \sigma\|_1 = \|\mathcal{E}^\infty[\sigma] - \sigma\|_1 \quad (6.32)$$

$$\leq \|\mathcal{E}^\infty[\sigma] - \mathcal{E}^\ell[\sigma]\|_1 + \|\mathcal{E}^\ell[\sigma] - \sigma\|_1 \quad (6.33)$$

$$\leq \eta_1 \cdot \|\sigma_{fix}(\mathcal{E}) - \sigma\|_1 + \ell \cdot \|\mathcal{E}[\sigma] - \sigma\|_1, \quad (6.34)$$

and rearrange to conclude the proof. \square

When the map is not trace-preserving, we have to tweak the argument.

Proposition VI.3.1. *Consider a CP trace-non-increasing map $\mathcal{N} : \mathcal{N}^\dagger[\mathbf{I}] \leq \mathbf{I}$ with leading eigenstate*

$$\mathcal{N}[\sigma_{fix}] = \lambda \sigma_{fix}, \quad 1 \geq \lambda \geq 0, \quad \sigma \geq 0.$$

Suppose $\|\mathcal{N}[\sigma] - \sigma\|_1 \leq \epsilon_{DB}$, then

$$\|\sigma_{fix} - \sigma\|_1 \leq \frac{2m}{\lambda^m} \cdot (\epsilon_{DB} + 1 - \lambda), \quad (6.35)$$

whenever

$$\eta_1\left(\left(\frac{\mathcal{N}}{\lambda}\right)^m\right) := \sup_{\rho_1, \rho_2} \frac{\left\|\left(\frac{\mathcal{N}}{\lambda}\right)^m [\rho_1 - \rho_2]\right\|_1}{\|\rho_1 - \rho_2\|_1} \leq \frac{1}{2}. \quad (6.36)$$

¹⁷ The related discussion in [3, eq.48, Sec 4.3] has an incomplete proof. Their derivation of $\|\mathcal{E}[\sigma] - \sigma\|_1 \leq \epsilon$ seems to assume an error independent of the matrix entries. The content of our Proposition VI.2.1 is to quantify a notion of approximate detailed balance such that (1) the Gibbs state will be approximately fixed and (2) it does not threaten the convergence.

The bound is only helpful when λ^m is close to 1.

Proof. We first note that the leading eigenstate of a CP map is always positive, with a non-negative eigenvalue. We calculate

$$\|\boldsymbol{\sigma}_{fix} - \boldsymbol{\sigma}\|_1 = \left\| \left(\frac{\mathcal{N}}{\lambda} \right)^\infty [\boldsymbol{\sigma}] - \boldsymbol{\sigma} \right\|_1 \quad (6.37)$$

$$\leq \left\| \left(\frac{\mathcal{N}}{\lambda} \right)^\infty [\boldsymbol{\sigma}] - \left(\frac{\mathcal{N}}{\lambda} \right)^m [\boldsymbol{\sigma}] \right\|_1 + \left\| \left(\frac{\mathcal{N}}{\lambda} \right)^m [\boldsymbol{\sigma}] - \boldsymbol{\sigma} \right\|_1 \quad (6.38)$$

$$\leq \eta_1 \cdot \|\boldsymbol{\sigma}_{fix} - \boldsymbol{\sigma}\|_1 + \left(\sum_{m'=1}^m \left(\frac{\mathcal{N}}{\lambda} \right)^{m'} \right) \cdot \frac{1}{\lambda} (\|\mathcal{N}[\boldsymbol{\sigma}] - \boldsymbol{\sigma}\|_1 + (1 - \lambda) \|\boldsymbol{\sigma}\|_1), \quad (6.39)$$

and rearrange to conclude the proof. \square

For the above proof, approximate detailed balance in superoperator norm (Proposition VI.2.1) is stronger than we need, but it will be crucial to obtain convergence (i.e., obtaining the value of m). To show Proposition VI.2.1, we need the following symmetry of the Metropolis (which resembles the detailed balance condition).

Fact VI.4 ([3, Sec. 4.3]). $\mathcal{R}_{\bar{\nu}_1} = \mathcal{R}_{\bar{\nu}_1}^\dagger, \mathcal{A}_{\bar{\nu}_2 \bar{\nu}_1}^\dagger e^{-\beta \bar{\nu}_1} = \mathcal{A}_{\bar{\nu}_1 \bar{\nu}_2} e^{-\beta \bar{\nu}_2}$.

Fact VI.5 (Polarization identity).

$$\begin{aligned} \mathbf{A}[\cdot] \mathbf{B} &= \frac{1}{4} \sum_{s=\pm 1, \pm i} s \cdot (\mathbf{A} + s \mathbf{B}^\dagger)[\cdot] (\mathbf{A}^\dagger + s^* \mathbf{B}) \\ &:= \frac{1}{4} \sum_{s=\pm 1, \pm i} s \mathbf{E}_s[\cdot] \mathbf{E}_s^\dagger. \end{aligned}$$

Proof. Summing over s selects out the ss^* component, and other powers of s vanish. Or, explicitly, expand

$$(\mathbf{A} + \mathbf{B}^\dagger)[\cdot] (\mathbf{A}^\dagger + \mathbf{B}) - (\mathbf{A} - \mathbf{B}^\dagger)[\cdot] (\mathbf{A}^\dagger - \mathbf{B}) = 2(\mathbf{B}^\dagger[\cdot] \mathbf{A}^\dagger + \mathbf{A}[\cdot] \mathbf{B}) \quad (6.40)$$

$$(\mathbf{A} + i\mathbf{B}^\dagger)[\cdot] (\mathbf{A}^\dagger - i\mathbf{B}) - (\mathbf{A} - i\mathbf{B}^\dagger)[\cdot] (\mathbf{A}^\dagger + i\mathbf{B}) = 2i(\mathbf{B}^\dagger[\cdot] \mathbf{A}^\dagger - \mathbf{A}[\cdot] \mathbf{B}) \quad (6.41)$$

and rearrange to conclude the proof. \square

We now prove approximate detailed balance (Proposition VI.2.1).

Proof of Proposition VI.2.1. Observe that near energy $\bar{\nu}$, $\boldsymbol{\sigma}$ is proportional to identity

$$\mathbf{P}_{\bar{\nu} \pm \omega} \boldsymbol{\sigma} \mathbf{P}_{\bar{\nu} \pm \omega} = \frac{e^{-\beta \bar{\nu}}}{\text{Tr}[e^{-\beta \mathbf{H}}]} \mathbf{P}_{\bar{\nu} \pm \omega} (1 + \delta \mathbf{H}) \mathbf{P}_{\bar{\nu} \pm \omega}, \quad \|\delta \mathbf{H}\| = \mathcal{O}(\beta \omega) \quad (6.42)$$

up to the multiplicative error $\|\delta \mathbf{H}\|$ being roughly the width ω of energy. We begin with decomposing into the acceptance and rejection CP maps $\mathcal{N} = \sum_{\bar{\nu}_2, \bar{\nu}_1} \mathcal{A}_{\bar{\nu}_2 \bar{\nu}_1} + \sum_{\bar{\nu}} \mathcal{R}_{\bar{\nu}}$.

(I) For each $\mathcal{R}_{\bar{\nu}}$ (6.25), we insert local energy projectors

$$\mathcal{R}_{\bar{\nu}}[\cdot] = \mathbf{P}_{\bar{\nu} \pm \omega} \mathcal{R}_{\bar{\nu}} [\mathbf{P}_{\bar{\nu} \pm \bar{\nu}_0} \cdot \mathbf{P}_{\bar{\nu} \pm \bar{\nu}_0}] \mathbf{P}_{\bar{\nu} \pm \omega}, \quad \omega = \mathcal{O}(r_{rej} \bar{\nu}_0). \quad (6.43)$$

Roughly speaking, $\mathcal{R}_{\bar{\nu}}$ makes r_{rej} attempts to reject, each of which introduces an $\bar{\nu}_0$ error that may accumulate [3, Sec. 4.3]. Technically, we have to collect nearby $\mathcal{R}_{\bar{\nu}}$ (per energy ω) into bins $\mathcal{R}_k := \sum_{(k-1)\omega < \bar{\nu} \leq k\omega} \mathcal{R}_{\bar{\nu}}$. Then by inserting projectors and noting that $\boldsymbol{\sigma}$ is diagonal in the energy basis

$$\mathcal{R}_k[\cdot] - \sqrt{\boldsymbol{\sigma}} \mathcal{R}_k^\dagger \left[\frac{1}{\sqrt{\boldsymbol{\sigma}}} \cdot \frac{1}{\sqrt{\boldsymbol{\sigma}}} \right] \sqrt{\boldsymbol{\sigma}} = \mathcal{R}_k[\cdot] - (1 + \delta \mathbf{H}_2) \mathcal{R}_k \left[(1 + \delta \mathbf{H}_1) \cdot (1 + \delta \mathbf{H}_1) \right] (1 + \delta \mathbf{H}_2), \quad (6.44)$$

where $\|\delta \mathbf{H}_1\|, \|\delta \mathbf{H}_2\| = \mathcal{O}(\beta \omega)$. This is looking great because the leading order (with no $\delta \mathbf{H}_i$) cancels; for each term $\mathbf{A} \mathcal{R}_k [\mathbf{B} \cdot \mathbf{C}] \mathbf{D}$ with at least one $\delta \mathbf{H}_i$, expand into a sum over CP maps (Fact VI.5)

$$\mathbf{A} \mathcal{R}_k [\mathbf{B} \cdot \mathbf{C}] \mathbf{D} = \sum_{s', s} s' s \cdot \mathcal{M}'_{\mathbf{A}, \mathbf{D}, k, s'} \circ \mathcal{R}_k \circ \mathcal{M}_{\mathbf{B}, \mathbf{C}, k, s}[\cdot]. \quad (6.45)$$

Then (after triangle inequalities), we use that for CP maps $\|\mathcal{E}\|_{1-1} = \|\mathcal{E}^\dagger[\mathbf{I}]\|_\infty$

$$\left\| \sum_k \mathcal{R}_k[\cdot] - \sqrt{\sigma} \mathcal{R}_k^\dagger \left[\frac{1}{\sqrt{\sigma}} \cdot \frac{1}{\sqrt{\sigma}} \right] \sqrt{\sigma} \right\|_{1-1} \leq \sum_{s',s} \sum_{\mathbf{A},\mathbf{B},\mathbf{C},\mathbf{D}} \left\| \sum_k \mathcal{M}_{\mathbf{B},\mathbf{C},k,s}^\dagger \mathcal{R}_k^\dagger \mathcal{M}_{\mathbf{A},\mathbf{D},k,s'}^\dagger [\mathbf{I}] \right\|_\infty \quad (6.46)$$

$$\leq \mathcal{O}(1) \cdot \sum_{s',s} \sum_{\mathbf{A},\mathbf{B},\mathbf{C},\mathbf{D}} \max_k \left\| \mathcal{M}_{\mathbf{B},\mathbf{C},k,s}^\dagger \mathcal{R}_k^\dagger \mathcal{M}_{\mathbf{A},\mathbf{D},k,s'}^\dagger [\mathbf{I}] \right\|_\infty \quad (6.47)$$

$$\leq \mathcal{O}(\beta r_{rej} \bar{\nu}_0). \quad (6.48)$$

The second inequality is that the range of \mathcal{R}_k overlap with at most $\mathcal{O}(1)$ other \mathcal{R}_k , therefore the spectral norm of the sum can be estimated by the maximum. The last line uses that $\mathcal{M}_{\mathbf{A},\mathbf{D},k,s'}^\dagger[\mathbf{I}] \leq \mathcal{O}(\|\mathbf{A}\|^2 + \|\mathbf{D}\|^2) \cdot \mathbf{I}$ (and similarly for $\mathcal{M}_{\mathbf{B},\mathbf{C},k,s}^\dagger$), and that $\mathcal{R}_k^\dagger[\mathbf{I}] \leq \mathbf{I}$ since \mathcal{R}_k is a CP, trace-non-increasing map.

(II) Similarly, for each $\mathcal{A}_{\bar{\nu}_2 \bar{\nu}_1}$, we insert local energy projectors and expand σ near $\bar{\nu}_1$ and $\bar{\nu}_2$

$$\sqrt{\sigma} \mathcal{A}_{\bar{\nu}_2 \bar{\nu}_1}^\dagger \left[\frac{1}{\sqrt{\sigma}} \cdot \frac{1}{\sqrt{\sigma}} \right] \sqrt{\sigma} = (1 + \delta \mathbf{H}'_1) \mathcal{A}_{\bar{\nu}_1 \bar{\nu}_2} [(1 + \delta \mathbf{H}'_2) \cdot (1 + \delta \mathbf{H}'_2)] (1 + \delta \mathbf{H}'_1) \quad (6.49)$$

for fluctuation of order $\|\delta \mathbf{H}'_1\|, \|\delta \mathbf{H}'_2\| = \mathcal{O}(\beta \bar{\nu}_0)$ (which is smaller than that of the rejection). The Boltzmann factors from σ approximately cancel due to Fact VI.4. Therefore,

pairing up $\mathcal{A}_{\bar{\nu}_2 \bar{\nu}_1}$ with $\mathcal{A}_{\bar{\nu}_1 \bar{\nu}_2}^\dagger$,

$$\begin{aligned} \left\| \sum_{\bar{\nu}_1, \bar{\nu}_2} \mathcal{A}_{\bar{\nu}_1 \bar{\nu}_2} - \sqrt{\sigma} \mathcal{A}_{\bar{\nu}_2 \bar{\nu}_1}^\dagger \left[\frac{1}{\sqrt{\sigma}} \cdot \frac{1}{\sqrt{\sigma}} \right] \sqrt{\sigma} \right\|_{1-1} &\leq \mathcal{O}(1) \sum_{s',s} \sum_{\mathbf{A},\mathbf{B},\mathbf{C},\mathbf{D}} \left\| \sum_{\bar{\nu}_1} \mathcal{M}_{\mathbf{B},\mathbf{C},\bar{\nu}_1,s}^\dagger \sum_{\bar{\nu}_2} \mathcal{A}_{\bar{\nu}_2 \bar{\nu}_1}^\dagger \mathcal{M}_{\mathbf{A},\mathbf{D},\bar{\nu}_2,s'}^\dagger [\mathbf{I}] \right\|_\infty \\ &\leq \mathcal{O}(1) \sum_{s',s} \sum_{\mathbf{A},\mathbf{B},\mathbf{C},\mathbf{D}} \max_{\bar{\nu}_1} \left\| \mathcal{M}_{\mathbf{B},\mathbf{C},\bar{\nu}_1,s}^\dagger \sum_{\bar{\nu}_2} \mathcal{A}_{\bar{\nu}_2 \bar{\nu}_1}^\dagger \mathcal{M}_{\mathbf{A},\mathbf{D},\bar{\nu}_2,s'}^\dagger [\mathbf{I}] \right\|_\infty \\ &\leq \sum_{s',s} \sum_{\mathbf{A},\mathbf{B},\mathbf{C},\mathbf{D}} \mathcal{O}(\|\mathbf{A}\|^2 + \|\mathbf{D}\|^2) \max_{\bar{\nu}_1} \left\| \mathcal{M}_{\mathbf{B},\mathbf{C},\bar{\nu}_1,s}^\dagger \sum_{\bar{\nu}_2} \mathcal{A}_{\bar{\nu}_2 \bar{\nu}_1}^\dagger [\mathbf{I}] \right\|_\infty \\ &\leq \mathcal{O}(\beta \bar{\nu}_0). \end{aligned} \quad (6.50)$$

The second inequality is that for spectral norm it suffices to bound the max over disjoint blocks $\bar{\nu}_1$. The last inequality uses that \mathcal{A} is trace-non-increasing. We conclude the proof by combining the anti-self-adjoint calculations from \mathcal{R} and \mathcal{A} , which are dominated by the former. Note that we did not need the failure probability in the proof but only CPTN. \square

VII. MAIN RESULT III: ETH IMPLIES FAST CONVERGENCE OF QUANTUM METROPOLIS

We now state the main result for Metropolis Sampling.

Theorem VII.1 (ETH implies convergence of Metropolis). *For a truncated Hamiltonian \mathbf{H}_S with a well-defined density of states (up to the truncation point), assume its relative ratio of the density of states is R for the energy difference Δ_{ETH} . Assume each flip \mathbf{A}^a for energy differences below Δ_{ETH} is an i.i.d sample from the ETH ansatz. Then with high probability (w.r.t to the randomness of ETH), running Metropolis sampling for ℓ rounds ensures the output is close to the Gibb state.*

$$\|\mathcal{N}^\ell[\rho] - \sigma\|_1 \leq \epsilon, \quad (7.1)$$

with

$$\ell = \theta \left(e^{\beta \Delta_{ETH}} \frac{R}{\lambda_{RW}} \frac{\ln(1/\epsilon) + n + \beta \|\mathbf{H}_S\|}{\Delta_{ETH} \min_{\bar{\omega} \leq \Delta_{ETH}} |f_{\bar{\omega}}|^2} \right) \quad (Rounds) \quad (7.2)$$

$$|a| = \Omega \left(\frac{R^4}{\lambda_{RW}^2} e^{2\beta \Delta_{ETH}} \right) \quad (choices\ of\ flips) \quad (7.3)$$

$$r_{amp} = \Omega \left(\ln \left(\frac{\ell}{\epsilon} \right) \right) \quad (iterations\ of\ amplification) \quad (7.4)$$

$$t_{QPE} = \theta \left(\frac{1}{\bar{\nu}_0} \right) = \Omega \left(\frac{\beta \ell r_{rej}}{\epsilon} + \left(\beta + \frac{1}{\Delta_{ETH}} \right) \frac{R}{\lambda_{RW}} \right) \quad (run\ time\ per\ QPE). \quad (7.5)$$

$$r_{rej} = \Omega \left(\frac{\ell}{\epsilon} \right) \quad (iterations\ of\ rejection), \quad (7.6)$$

and λ_{RW} is the gap of a 1d classical random walk with characteristic step size $\sim \Delta_{ETH}$ on the spectrum weighted by the Gibbs state. The total time elapsed is the product

$$t_{\text{elapse}} = t_{QPER_{\text{rej}}} r_{\text{amp}} \ell = \Omega \left(\left(\frac{\beta \ell r_{\text{rej}}}{\epsilon} + \left(\beta + \frac{1}{\Delta_{ETH}} \right) \frac{R}{\lambda_{RW}} r_{\text{rej}} \ln \left(\frac{\ell}{\epsilon} \right) \ell \right) \right). \quad (7.7)$$

We keep the variable r_{rej} as in practice $r_{\text{rej}} = \Omega(\ln(\frac{\ell}{\epsilon}))$ may suffice, but we include the unconditional bound as well. Contrasting with Davies' generator, the CP maps are less structured, and hence we use a large number of flips $|a|$ to ensure local fluctuation does not close the global random walk gap. For the random walk gap, we have analog results (with a slightly different transition rate)

Proposition VII.1.1. *If the density of Gibbs state satisfies assumptions in Section IVB2 (e.g., a Gaussian with variance Δ_{spec}), then $\lambda_{RW} = \Omega(\frac{e^{-2\beta\Delta_{ETH}}}{R^2} \frac{\Delta_{ETH}^2}{\Delta_{\text{spec}}^2})$.*

See Section IVB for ETH, the assumptions on the density of states, and the Gibbs state density for gap calculation. See Section VIIE for a resource estimate.

A. Proof Outline

It is instructive to highlight the technical obstacles; our proof is structured to cure them and may hence appear ad-hoc.

1. Convergence with approximate detailed balance

Unlike Davies' generator, the Metropolis CP map does not satisfy exact detailed balance. Formally, if we decompose the Metropolis CPTN map into the self-adjoint and anti-self-adjoint parts, w.r.t to the inner product $\langle \cdot, \cdot \rangle_{\sigma^{-1}}$

$$\mathcal{N} = \frac{1}{2} \left(\mathcal{N} + \sqrt{\sigma} \mathcal{N}^\dagger \left[\frac{1}{\sqrt{\sigma}} \cdot \frac{1}{\sqrt{\sigma}} \right] \sqrt{\sigma} \right) + \frac{1}{2} \left(\mathcal{N} - \sqrt{\sigma} \mathcal{N}^\dagger \left[\frac{1}{\sqrt{\sigma}} \cdot \frac{1}{\sqrt{\sigma}} \right] \sqrt{\sigma} \right) \quad (7.8)$$

$$= \mathcal{N}_{H,\sigma} + \mathcal{N}_{A,\sigma}, \quad (7.9)$$

then the anti-self-adjoint component $\mathcal{N}_A := \mathcal{N}_{A,\sigma}$ will be non-trivial. Our remedy, as advertised, is the notion of approximate detailed balance that quantifies it in an appropriate norm $\|\mathcal{N}_A\|_{1-1} \leq \epsilon_{DB}$. It allows us to study the convergence (in trace distance) via that of the self-adjoint component $\mathcal{N}_H := \mathcal{N}_{H,\sigma}$,

$$\eta_1(\mathcal{N}^\ell) = \sup_{\rho_1, \rho_2} \frac{\|\mathcal{N}^\ell[\rho_1 - \rho_2]\|_1}{\|\rho_1 - \rho_2\|_1} \quad (7.10)$$

$$\leq \sup_{\rho_1, \rho_2} \frac{\|\mathcal{N}_H^\ell[\rho_1 - \rho_2]\|_1}{\|\rho_1 - \rho_2\|_1} + \ell \cdot \|\mathcal{N}_A\|_{1-1}. \quad (7.11)$$

In other words, to show convergence we would need $\ell \cdot \epsilon_{DB} < 1$. Now, since \mathcal{N}_H is self-adjoint w.r.t σ , we further reduce to a gap calculation.

Proposition VII.1.2. *For any CP-trace-non-increasing map \mathcal{N} , suppose $\|\mathcal{N}_A\|_{1-1} \leq \epsilon_{DB}$,*

$$\sup_{\rho_1, \rho_2} \frac{\|\mathcal{N}_H^\ell[\rho_1 - \rho_2]\|_1}{\|\rho_1 - \rho_2\|_1} \leq \lambda_2^\ell(\mathcal{N}_H) \cdot \left\| \frac{1}{\sigma} \right\|_\infty + \mathcal{O}(\ell \cdot \epsilon_{DB}).$$

See Section VII D 1 for the proof. The second term is roughly due to \mathcal{N}_H being not trace-preserving, and it may enlarge the trace by $(1 + \|\mathcal{N}_A\|_{1-1})$.

2. The gap of the trace-non-increasing CP map

Now, the problem is: how to bound the gap of (the self-adjoint component of) a CP, *trace-non-increasing* map $\mathcal{N} := \mathcal{R} + \mathcal{A}$? Even worse, the RMT prescription of ETH only helps for nearby energy transitions in \mathcal{A} ; we have no control over most of the terms in \mathcal{A} and the rejection step \mathcal{R} . In general, the analysis of CP maps has little literature to draw from, but we manage to bound the gap given partial knowledge of the summands.

Proposition VII.1.3. *For any CP trace-non-increasing map $\mathcal{N} = \mathcal{N}_1 + \mathcal{N}_2$, the gap of the σ -self-adjoint component can be controlled by the CP summands*

$$\lambda_2(\mathcal{N}_H) \leq \lambda_2(\mathcal{N}_{1,H}) + \left(1 - \min_{\text{Tr}[\rho]=1} \text{Tr}[\mathcal{N}_1[\rho]]\right) + \left\| \mathcal{N}_{2,A}^\dagger[\mathbf{I}] \right\|_\infty$$

where subscripts σ are omitted (e.g., $\mathcal{N}_H = \mathcal{N}_{H,\sigma}$).

In other words, to obtain the second eigenvalue of the total map, it suffices if we can find some \mathcal{N}_1 with estimates on (1) the second eigenvalue of the self-adjoint component $\mathcal{N}_{1,H}$ and (2) the trace $\text{Tr}[\mathcal{N}_1[\rho]]$ for any input ρ . Also, we should make sure (3) the anti-self-adjoint component $\mathcal{N}_{2,A}$ does not shrink the gap.

For our purposes, we take \mathcal{N}_1 to be the transitions where RMT is valid, but weighted by some factor $0 \leq p(\bar{\nu}_1) \leq 1$

$$\mathcal{N}_1 := \sum_{|\bar{\nu}_1 - \bar{\nu}_2| \leq \Delta_{ETH} - 2\bar{\nu}_0} p(\bar{\nu}_1) \mathcal{A}_{\bar{\nu}_2 \bar{\nu}_1} \quad (7.12)$$

$$\mathcal{N}_2 := \sum_{|\bar{\nu}_1 - \bar{\nu}_2| \leq \Delta_{ETH} - 2\bar{\nu}_0} (1 - p(\bar{\nu}_1)) \mathcal{A}_{\bar{\nu}_2 \bar{\nu}_1} + \sum_{|\bar{\nu}_1 - \bar{\nu}_2| > \Delta_{ETH} - 2\bar{\nu}_0} p(\bar{\nu}_1) \mathcal{A}_{\bar{\nu}_2 \bar{\nu}_1} + \mathcal{R}. \quad (7.13)$$

Indeed, decompose into the expectation and the deviation (and similarly for the self-adjoint component $\mathcal{N}_{1,H}$)

$$\mathcal{N}_1 = (\mathcal{N}_1 - \mathbb{E}\mathcal{N}_1) + \mathbb{E}\mathcal{N}_1, \quad (7.14)$$

then we can estimate (1) the second eigenvalue via that of the expected map (which is classical) and a bound on the deviation. For (2), we can directly calculate the trace of the expected map as a function of input energy $\bar{\nu}_1$, and we choose $p(\bar{\nu}_1)$ accordingly so that each input $\bar{\nu}_1$ has roughly the same trace.

B. Local Properties

It is instructive to first calculate the individual terms in acceptance moves \mathcal{A} . For measured energies before and after the flips,

$$\mathcal{A}_{(\bar{\nu}_2 \bar{\nu}_1)}[\rho] = \sum_a \frac{1}{|a|} \sum_{upq} \left[\mathbf{S}_{\bar{\nu}_2}^{up} \cdot \mathbf{A}^a \left(\mathbf{S}_{\bar{\nu}_1}^{p0} \rho \mathbf{S}_{\bar{\nu}_1}^{0q} \right) \mathbf{A}^{a\dagger} \cdot \mathbf{S}_{\bar{\nu}_2}^{qu} \cdot \min(1, e^{-\beta(\bar{\nu}_2 - \bar{\nu}_1)}) + (\bar{\nu}_2 \leftrightarrow \bar{\nu}_1) \right] \quad (7.15)$$

$$= \sum_a \frac{1}{|a|} \sum_{upq} \left[\mathbf{S}_{\bar{\nu}_2}^{up} \cdot \mathbf{P}_{\bar{\nu}_2} \mathbf{A}^a \mathbf{P}_{\bar{\nu}_1} \left(\mathbf{S}_{\bar{\nu}_1}^{p0} \rho \mathbf{S}_{\bar{\nu}_1}^{0q} \right) \mathbf{P}_{\bar{\nu}_1} \mathbf{A}^{a\dagger} \mathbf{P}_{\bar{\nu}_2} \cdot \mathbf{S}_{\bar{\nu}_2}^{qu} \cdot \min(1, e^{-\beta(\bar{\nu}_2 - \bar{\nu}_1)}) + (\bar{\nu}_2 \leftrightarrow \bar{\nu}_1) \right] \quad (7.16)$$

where subscript $(\bar{\nu}_2 \bar{\nu}_1)$ denotes the symmetry. We inserted projectors $\mathbf{P}_{\bar{\nu}_2} = \mathbf{P}_{\bar{\nu}_2 \pm \bar{\nu}_0}$, which tolerate $\pm \bar{\nu}_0$ rounding errors, to focus on the relevant submatrix $\mathbf{P}_{\bar{\nu}_2} \mathbf{A}^a \mathbf{P}_{\bar{\nu}_1}$. Under ETH, for nearby energies $|\bar{\nu}_2 - \bar{\nu}_1| \leq \Delta_{ETH}$, the entries are model by Gaussian but with slightly different variances. For $i \in \hat{\nu}_2, j \in \hat{\nu}_1$,

$$V_{min,(\bar{\nu}_2 \bar{\nu}_1)} := \min(\mathbb{E}|A_{ij}|^2) \leq \mathbb{E}|A_{ij}|^2 \leq \max(\mathbb{E}|A_{ij}|^2) =: V_{(\bar{\nu}_2 \bar{\nu}_1)}^{max} \quad (7.17)$$

and we treat $(V_{(\bar{\nu}_2 \bar{\nu}_1)}^{min} - V_{(\bar{\nu}_2 \bar{\nu}_1)}^{max})/V_{(\bar{\nu}_2 \bar{\nu}_1)}^{min} = \mathcal{O}(1)$.

1. The expectation

The expectation evaluates to (Fact V.4)

$$\mathbb{E}\mathcal{A}_{(\bar{\nu}_2 \bar{\nu}_1)}[\rho] = \sum_{\nu_1 \in \hat{\nu}_1, \nu_2 \in \hat{\nu}_2} \sum_{upq} \left[\mathbf{S}_{\bar{\nu}_2}^{up} |\nu_2\rangle \langle \nu_2| \mathbf{S}_{\bar{\nu}_2}^{qu} \cdot \langle \nu_1| \mathbf{S}_{\bar{\nu}_1}^{p0} \rho \mathbf{S}_{\bar{\nu}_1}^{0q} |\nu_1\rangle \cdot \mathbb{E}[|A_{\nu_2 \nu_1}|^2] \cdot \min(1, e^{-\beta(\bar{\nu}_2 - \bar{\nu}_1)}) + (\bar{\nu}_2 \leftrightarrow \bar{\nu}_1) \right]. \quad (7.18)$$

In other words, expectation over ETH ensemble $\mathbb{E}\mathcal{A}(\cdot)\mathbf{A}^\dagger$ yields a classical map for transitions between diagonal entries. Note the Kraus operators from phase-estimation preserves energy eigenstates $\mathbf{S}_{\bar{\nu}}^{up} |\nu\rangle \propto |\nu\rangle$.

2. Concentration

Proposition VII.1.4. *With high probability,*

$$\left\| \mathcal{A}_{(\bar{\nu}_2 \bar{\nu}_1)} - \mathbb{E}\mathcal{A}_{(\bar{\nu}_2 \bar{\nu}_1)} \right\|_{\infty, \sigma^{-1}} = \mathcal{O} \left(e^{-\beta|\bar{\nu}_2 - \bar{\nu}_1|/2} \frac{\max(\text{Tr}[\mathbf{P}_{\bar{\nu}_2}], \text{Tr}[\mathbf{P}_{\bar{\nu}_1}]) V_{max,(\bar{\nu}_2 \bar{\nu}_1)}}{\sqrt{|a|}} \right)$$

Proof. Again, by decoupling as in Proposition V.4.1,

$$\begin{aligned}
& (\mathbb{E} \|\mathcal{A}_{(\bar{\nu}_2 \bar{\nu}_1)} - \mathbb{E} \mathcal{A}_{(\bar{\nu}_2 \bar{\nu}_1)}\|_{\infty, \sigma^{-1}}^p)^{1/p} \leq (\mathbb{E} \|\mathcal{A}_{(\bar{\nu}_2 \bar{\nu}_1)} - \mathcal{A}'_{(\bar{\nu}_2 \bar{\nu}_1)}\|_{p, \sigma^{-1}}^p)^{1/p} \\
& \leq 2(\mathbb{E} \left\| \sum_a \frac{1}{|a|} \sum_{upq} \left[\mathbf{S}_{\bar{\nu}_2}^{up} \cdot \mathbf{P}_{\bar{\nu}_2} \mathbf{A}^a \mathbf{P}_{\bar{\nu}_1} \left(\mathbf{S}_{\bar{\nu}_1}^{p0} [\cdot] \mathbf{S}_{\bar{\nu}_1}^{0q} \right) \mathbf{P}_{\bar{\nu}_1} \mathbf{A}'^{a\dagger} \mathbf{P}_{\bar{\nu}_2} \cdot \mathbf{S}_{\bar{\nu}_2}^{qu} \cdot \min(1, e^{-\beta(\bar{\nu}_2 - \bar{\nu}_1)}) + (\bar{\nu}_2 \leftrightarrow \bar{\nu}_1) \right] \right\|_{p, \sigma^{-1}}^p)^{1/p} \\
& \leq \mathcal{O}(1) \cdot (\mathbb{E} \left\| \sum_a \frac{1}{|a|} \left[\mathbf{P}_{\bar{\nu}_2} \mathbf{A}^a \mathbf{P}_{\bar{\nu}_1} [\cdot] \mathbf{P}_{\bar{\nu}_1} \mathbf{A}'^{a\dagger} \mathbf{P}_{\bar{\nu}_2} \cdot \min(1, e^{-\beta(\bar{\nu}_2 - \bar{\nu}_1)}) + (\bar{\nu}_2 \leftrightarrow \bar{\nu}_1) \right] \right\|_{p, \sigma^{-1}}^p)^{1/p} \tag{7.19}
\end{aligned}$$

$$\leq (1 + \mathcal{O}(\beta \bar{\nu}_0)) \cdot \mathcal{O} \left(e^{-\beta|\bar{\nu}_2 - \bar{\nu}_1|} \frac{\max(\text{Tr}[\mathbf{P}_{\bar{\nu}_2}], \text{Tr}[\mathbf{P}_{\bar{\nu}_1}]) V_{\max,(\bar{\nu}_2 \bar{\nu}_1)}}{\sqrt{|a|}} \right) \left(\approx \frac{R^2}{\sqrt{|a|}} \lambda_{\max}(\mathbb{E} \mathcal{A}_{(\bar{\nu}_2 \bar{\nu}_1)}) \right). \tag{7.20}$$

The second inequality decouples with a price of a factor of 2. The third inequality is that the post selected measurements (6.13) has operator norm ≤ 1 , we are summing over $\mathcal{O}(1)$ indices u, p, q . In last inequality we used convexity to throw in \mathbf{D} such that $\mathbf{G}_{\bar{\nu}_2 \bar{\nu}_1} = \mathbf{A}_{\bar{\nu}_2 \bar{\nu}_1} + \mathbf{D}_{\bar{\nu}_2 \bar{\nu}_1}$ has uniform variance $\max(\mathbb{E}|A_{ij}|^2) =: V_{\max,(\bar{\nu}_2 \bar{\nu}_1)}$, and then Gaussian calculations (Fact V.5 and Fact V.7). Note that the Metropolis factors become roughly equal in the norm $\|\cdot\|_{\sigma^{-1}}$, with a subleading $\mathcal{O}(\beta \bar{\nu}_0)$ error (which we drop in the Proposition) due to imperfect phase estimation. Lastly, to emphasize the quantum expander nature, we heuristically compare with the eigenvalue of the expected map, which we do not give a concrete estimate due to the annoying rounding issue from \mathbf{S} . This is the advertised result. \square

C. The Global Gap of the Self-adjoint Component \mathcal{N}_H .

We first prove Proposition VII.1.3.

Proposition (recap). *For a CP trace-non-increasing map $\mathcal{N} = \mathcal{N}_1 + \mathcal{N}_2$, the gap of the self-adjoint component can be controlled by the summands*

$$\lambda_2(\mathcal{N}_H) \leq \lambda_2(\mathcal{N}_{1,H}) + \left(1 - \min_{\text{Tr}[\rho]=1} \text{Tr}[\mathcal{N}_1[\rho]] \right) + \|\mathcal{N}_{2,A}^\dagger[\mathbf{I}]\|_\infty$$

where subscripts σ are omitted (e.g., $\mathcal{N}_H = \mathcal{N}_{H,\sigma}$).

Note that $\|\mathcal{N}_{2,A}^\dagger[\mathbf{I}]\|_\infty \leq \epsilon_{DB}$ can be obtained from the identical proof of Proposition VI.2.1. The proof uses the following.

Fact VII.2 (Russo,Dye). *For CP self-map \mathcal{N} , the spectral radius is bounded by*

$$\forall \lambda, |\lambda(\mathcal{N})| \leq \|\mathcal{N}^\dagger[\mathbf{I}]\|_\infty.$$

Fact VII.3 (Bauer–Fike). *For Hermitian matrix \mathbf{H} perturbed by arbitrary (non-Hermitian) operator \mathbf{O} ,*

$$\delta \lambda_i(\mathbf{H}) \leq \|\mathbf{O}\|.$$

Proof. We start by removing the σ -anti-self-adjoint component by Bauer–Fike theorem. Note eigenvalues are independent of basis, or one may also perform a similarity transformation $\mathcal{N}_H \rightarrow \sigma^{1/4}(\mathcal{N}_H[\sigma^{-1/4} \cdot \sigma^{-1/4}])\sigma^{1/4}$.

$$\lambda_2(\mathcal{N}_H) \leq \lambda_2(\mathcal{N}_{1,H}) + \lambda_1(\mathcal{N}_{2,H}). \tag{7.21}$$

We can massage the second term, which is self-adjoint, by

$$\lambda_1(\mathcal{N}_{2,H}) \leq \|\mathcal{N}_{2,H}[\mathbf{I}]\|_\infty \tag{7.22}$$

$$\leq \|\mathcal{N}_2^\dagger[\mathbf{I}]\|_\infty + \|\mathcal{N}_{2,A}^\dagger[\mathbf{I}]\|_\infty. \tag{7.23}$$

The second is Fact VII.2, and note the dagger $(\cdot)^\dagger$ is w.r.t to trace. The last is the triangle inequality. We conclude the proof by $\mathcal{N}_2 = \mathcal{N} - \mathcal{N}_1$ and \mathcal{N} is trace-non-increasing. \square

1. The choice of $p(\bar{\nu}_1)$

First, let us gain some intuition by calculating the total transition rate for each $\bar{\nu}_1, |\nu_1\rangle$

Proposition VII.3.1 (Probability of acceptance into the ETH window).

$$\sum_{\bar{\nu}_2: |\bar{\nu}_1 - \bar{\nu}_2| \leq \Delta_{ETH} - 2\bar{\nu}_0} \text{Tr} [\mathbb{E} \mathcal{A}_{\bar{\nu}_2 \bar{\nu}_1} [\langle \nu_1 \rangle \langle \nu_1 \rangle]] = \left(1 \pm \mathcal{O}(\beta \bar{\nu}_0 R + \frac{\bar{\nu}_0 R}{\Delta_{ETH}} + p_{amp}) \right) \cdot \Pr(\nu_1 \rightarrow \bar{\nu}_1) \cdot r(\bar{\nu}_1),$$

where

$$r(\bar{\nu}_1) := \sum_{\nu_2 \in \Delta_{ETH}(\bar{\nu}_1)} \mathbb{E}[|A_{\nu_2 \bar{\nu}_1}|^2] \cdot \min(1, e^{-\beta(\nu_2 - \bar{\nu}_1)}).$$

is transitions from $\bar{\nu}_1$ to nearby energies.

The estimates will be handy

$$\Omega \left(\frac{1}{R} \int_0^{\Delta_{ETH}} |f_\omega|^2 e^{-\beta \omega} d\omega \right) \leq r(\bar{\nu}_1) \leq \mathcal{O}(R \int_0^{\Delta_{ETH}} |f_\omega|^2 d\omega). \quad (7.24)$$

In other words, the probability of moving depends on $\bar{\nu}$.

Proof.

$$\sum_{\bar{\nu}_2: |\bar{\nu}_1 - \bar{\nu}_2| \leq \Delta_{ETH} - 2\bar{\nu}_0} \text{Tr} [\mathbb{E} \mathcal{A}_{\bar{\nu}_2 \bar{\nu}_1} [\langle \nu_1 \rangle \langle \nu_1 \rangle]] \quad (7.25)$$

$$= \Pr(\nu_2 \rightarrow \bar{\nu}_2, \nu_1 \rightarrow \bar{\nu}_1) \sum_{\nu_2} \sum_{\bar{\nu}_2: |\bar{\nu}_1 - \bar{\nu}_2| \leq \Delta_{ETH} - 2\bar{\nu}_0} \mathbb{E}[|A_{\nu_2 \nu_1}|^2] \cdot \min(1, e^{-\beta(\bar{\nu}_2 - \bar{\nu}_1)}) \quad (7.26)$$

$$= \Pr(\nu_2 \rightarrow \bar{\nu}_2, \nu_1 \rightarrow \bar{\nu}_1) \sum_{\nu_2} \sum_{\bar{\nu}_2: |\bar{\nu}_1 - \bar{\nu}_2| \leq \Delta_{ETH} - 2\bar{\nu}_0} \mathbb{E}[|A_{\nu_2 \nu_1}|^2] \cdot \min(1, e^{-\beta(\bar{\nu}_2 - \bar{\nu}_1)}) (1 \pm \mathcal{O}(\beta \bar{\nu}_0)) \quad (7.27)$$

$$= \Pr(\nu_1 \rightarrow \bar{\nu}_1) \sum_{\nu_2: |\nu_1 - \nu_2| \leq \Delta_{ETH} \pm \mathcal{O}(\bar{\nu}_0)} \mathbb{E}[|A_{\nu_2 \nu_1}|^2] \cdot \min(1, e^{-\beta(\nu_2 - \bar{\nu}_1)}) (1 \pm \mathcal{O}(\beta \bar{\nu}_0 + p_{amp})) \quad (7.28)$$

$$= \left(1 \pm \mathcal{O}(\beta \bar{\nu}_0 + \frac{\bar{\nu}_0}{\Delta_{ETH}} + p_{amp}) \right) \cdot \Pr(\nu_1 \rightarrow \bar{\nu}_1) \cdot r(\bar{\nu}_1). \quad (7.29)$$

In the first line, we denote

$$\Pr(\nu_2 \rightarrow \bar{\nu}_2, \nu_1 \rightarrow \bar{\nu}_1) = \sum_{upq} \langle \nu_2 | \mathcal{S}_{\bar{\nu}_2}^{up} | \nu_2 \rangle \langle \nu_2 | \mathcal{S}_{\bar{\nu}_2}^{qu} | \nu_2 \rangle \cdot \langle \nu_1 | \mathcal{S}_{\bar{\nu}_1}^{p0} | \nu_1 \rangle \langle \nu_1 | \mathcal{S}_{\bar{\nu}_1}^{0q} | \nu_1 \rangle \quad (7.30)$$

and $\Pr(\nu_1 \rightarrow \bar{\nu}_1) = \sum_{p,q} \langle \nu_1 | \mathcal{S}_{\bar{\nu}_1}^{p0} | \nu_1 \rangle \langle \nu_1 | \mathcal{S}_{\bar{\nu}_1}^{0q} | \nu_1 \rangle$ is the probability of obtaining $\bar{\nu}_1$ from measuring ν_1 . The third line changes $\bar{\nu}_2 \rightarrow \nu_2$, conveniently accounted by the $\pm \mathcal{O}(\cdot)$ notation. In the fourth line we sum over $\bar{\nu}_2$. For any ν_2 , summing over nearby $\bar{\nu}_2$ would simplify $\sum_{\bar{\nu}_2} \Pr(\nu_2 \rightarrow \bar{\nu}_2, \nu_1 \rightarrow \bar{\nu}_1) \rightarrow \Pr(\nu_1 \rightarrow \bar{\nu}_1)$, up to the failure probability of amplification p_{amp} . However, that does not apply when ν_2 is near the edge of spectrum, which can be conveniently accounted by $\mathcal{O}(\bar{\nu}_0)$ error in the summation. Lastly, we shift $\mathbb{E}[|A_{\nu_2 \nu_1}|^2] \rightarrow \mathbb{E}[|A_{\nu_2 \bar{\nu}_1}|^2]$, and when $\bar{\nu}_1$ is near the edge of the spectrum, this introduces error bounded by

$$R \cdot \frac{\bar{\nu}_0 \max_{\omega \leq \Delta_{ETH}} \min(1, e^{-\beta \omega}) |f_\omega|^2}{\int_0^{\Delta_{ETH}} |f_\omega|^2 e^{-\beta \omega} d\omega} = \mathcal{O}(\frac{R \bar{\nu}_0}{\Delta_{ETH}} + R \beta \bar{\nu}_0) \quad (7.31)$$

since we assume the f to be roughly the same across scale $[0, \Delta_{ETH}]$. If $\beta \geq \Delta_{ETH}$, the denominator is roughly f^2/β ; if $\beta \leq \Delta_{ETH}$, the denominator is roughly $\Delta_{ETH} f^2$. This is the advertised result. \square

Right now, the map has quite an uneven probability of moving: near the edge, $r(\bar{\nu}_1)$ has only one direction to move, which is roughly half of that in the bulk of spectrum. This will be cured by the choice

$$p(\bar{\nu}_1) := \frac{\min_{\bar{\nu}_1'} r(\bar{\nu}_1')}{r(\bar{\nu}_1)}, \quad \mathcal{N}_1 := \sum_{|\bar{\nu}_1 - \bar{\nu}_2| \leq \Delta_{ETH} - 2\bar{\nu}_0} p(\bar{\nu}_1) \mathcal{A}_{\bar{\nu}_2 \bar{\nu}_1}. \quad (7.32)$$

This serves to make the expected map has the roughly *the same trace* for different inputs. Lastly, what we need is $\mathbb{E} \mathcal{N}_{1,H}$ instead of $\mathbb{E} \mathcal{N}_1$. Therefore, we repeat Proposition VII.3.1 for the σ -adjoint $\sqrt{\sigma} \mathcal{N}_1^\dagger [\frac{1}{\sqrt{\sigma}} \cdot \frac{1}{\sqrt{\sigma}}] \sqrt{\sigma}$. This incurs an additional $\mathcal{O}(\beta \bar{\nu}_0)$ multiplicative error comes from the Metropolis factor, and thankfully can be absorbed into the same $\pm \mathcal{O}(\cdot)$ notation. The above discussion summarizes to the following.

Corollary VII.3.1. *For any state ρ ,*

$$\text{Tr} [\mathbb{E} \mathcal{N}_{1,H}[\rho]] = \min_{\bar{\nu}_1'} r(\bar{\nu}_1') \left(1 \pm \mathcal{O}(\beta \bar{\nu}_0 R + \frac{\bar{\nu}_0 R}{\Delta_{ETH}} + p_{amp}) \right).$$

Importantly, $\min_{\bar{\nu}_1'} r(\bar{\nu}_1')$ is independent of ρ . Note that $p(\bar{\nu}_1) = \theta(1)$ has uniform sizes across the spectrum. See Proposition VII.4.3 for concentration of trace.

2. The second eigenvalue $\lambda_2(\mathcal{N}_{1,H})$

Now, we calculate the second eigenvalue of the map.

Lemma VII.4. *With high probability,*

$$\lambda_2(\mathcal{N}_{1,H}) \leq \min_{\bar{\nu}'_1} r(\bar{\nu}'_1) \cdot \left(1 - \Omega\left(\frac{e^{-2\beta\Delta_{ETH}}}{R^2} \frac{\Delta_{ETH}^2}{\Delta_{spec}^2}\right) + \mathcal{O}\left(\beta\bar{\nu}_0 R + \frac{\bar{\nu}_0 R}{\Delta_{ETH}} + p_{amp}\right) \right) + \mathcal{O}\left(\frac{R}{\sqrt{|a|}} \int_0^{\Delta_{ETH}} |f_\omega|^2 d\omega\right).$$

As usual, we will decompose into the expectation and the deviation

$$\mathcal{N}_1 = \sum_{|\bar{\nu}_1 - \bar{\nu}_2| \leq \Delta_{ETH} - 2\bar{\nu}_0} p(\bar{\nu}_1) ((\mathcal{A}_{\bar{\nu}_2 \bar{\nu}_1} - \mathbb{E}\mathcal{A}_{\bar{\nu}_2 \bar{\nu}_1}) + \mathbb{E}\mathcal{A}_{\bar{\nu}_2 \bar{\nu}_1}). \quad (7.33)$$

The expectation is a classical positive map between unrounded energies ν , but only approximately preserves the trace. Once we adjust the probability of not moving $\Pr(\nu \rightarrow \nu)$ by T

$$\mathbb{E}[\mathcal{N}_{1,H}] + T = \mathbb{E}[\mathcal{N}'_{1,H}], \quad (7.34)$$

we obtain a map $\mathbb{E}[\mathcal{N}'_1]$ that is a scalar multiple of the stochastic map. Importantly, this map satisfies *exact* detailed balance since we consider the σ -self-adjoint component. The size of the fluctuation of the trace is already calculated in VII.3.1.

Corollary VII.4.1. $\|T\| = \min_{\bar{\nu}'_1} r(\bar{\nu}'_1) \cdot \mathcal{O}\left(\beta\bar{\nu}_0 R + \frac{\bar{\nu}_0 R}{\Delta_{ETH}} + p_{amp}\right)$

Now, $\mathbb{E}[\mathcal{N}_1]'$ is analogous to the one for Davies (Section V B), with the difference that it has small dependence within each rounded energy $\bar{\nu}$. This does not change much for the bottleneck calculation.

Proposition VII.4.1 (Conductance).

$$\lambda_2(\mathbb{E}[\mathcal{N}'_{1,H}]) \leq \min_{\bar{\nu}'_1} r(\bar{\nu}'_1) \cdot \left(1 - \Omega\left(\frac{e^{-2\beta\Delta_{ETH}}}{R^2} \frac{\Delta_{ETH}^2}{\Delta_{spec}^2}\right) \right) + \mathcal{O}(\|T\|).$$

See Section B 1 b for the proof.

For the deviations, we will use crude bound because the fluctuation in trace (which is rooted from finite QPE resolution) already induces vast error in the gap and require a large $|a|$. This marks a difference from Davies' calculation where trace constraints are imposed. Partition the operator and for each partition we bound the spectral norm

Proposition VII.4.2. *With high probability,*

$$\left\| \sum_{|\bar{\nu}_1 - \bar{\nu}_2| \leq \Delta_{ETH} - 2\bar{\nu}_0} p(\bar{\nu}_1) (\mathcal{A}_{\bar{\nu}_2 \bar{\nu}_1} - \mathbb{E}\mathcal{A}_{\bar{\nu}_2 \bar{\nu}_1}) \right\|_{\infty, \sigma^{-1}} \leq \mathcal{O}\left(\frac{R}{\sqrt{|a|}} \int_0^{\Delta_{ETH}} |f_\omega|^2 d\omega\right).$$

Proof. Let $\delta\mathcal{A}_{(\bar{\nu}_1 \bar{\nu}_2)} := \mathcal{A}_{(\bar{\nu}_2 \bar{\nu}_1)} - \mathbb{E}\mathcal{A}_{(\bar{\nu}_2 \bar{\nu}_1)}$. For each $\bar{\omega}$, we regroup into disjoint operators

$$\sum_{|\bar{\nu}_1 - \bar{\nu}_2| \leq \Delta_{ETH} - 2\bar{\nu}_0} \delta\mathcal{A}_{(\bar{\nu}_1 \bar{\nu}_2)} = \sum_{0 \leq \bar{\omega} \leq \Delta_{ETH} - 2\bar{\nu}_0} \left(\sum_{(\bar{\nu}_1, \bar{\nu}_2) \in S_1(\bar{\omega})} \delta\mathcal{A}_{(\bar{\nu}_1 \bar{\nu}_2)} + \cdots + \sum_{(\bar{\nu}_1, \bar{\nu}_2) \in S_k(\bar{\omega})} \delta\mathcal{A}_{(\bar{\nu}_1 \bar{\nu}_2)} \right), \quad (7.35)$$

where we dropped the factor $p(\bar{\nu}_1) \leq 1$ since we are using triangle inequality through out. The reason we did not choose $k = 2$ like in the Lindbladian (5.38), is due to the $\mathcal{O}(\bar{\nu}_0)$ fluctuation from imperfect QPE that smears $\bar{\nu}_1$. Now, since the operator are disjoint, we can take the maximum and recall the concentration we obtained for each $\bar{\nu}_1, \bar{\nu}_2$ (Proposition VII.1.4)

$$\left\| \sum_{(\bar{\nu}_1, \bar{\nu}_2) \in S(\bar{\omega})} \delta\mathcal{A}_{(\bar{\nu}_1 \bar{\nu}_2)} \right\|_{\infty, \sigma^{-1}} = \mathcal{O}\left(\max_{\bar{\nu}_1} \frac{e^{-\beta\bar{\omega}/2}}{\sqrt{|a|}} \max(\text{Tr}[\mathbf{P}_{\bar{\nu}_2}], \text{Tr}[\mathbf{P}_{\bar{\nu}_1}]) V_{\max, (\bar{\nu}_2 \bar{\nu}_1)}\right). \quad (7.36)$$

Plug into the ETH ansatz and drop the Boltzmann factor $e^{-\beta\omega/2}$ to obtain the advertised result. \square

Putting the above together gives Lemma VII.4. Note that Proposition applies to the σ -adjoints of \mathcal{A} , since the (σ) -spectral norm is the same taking (σ) -adjoint.

Lastly, we complete the discussion by obtaining concentration of trace (We have already calculated the expectation).

Proposition VII.4.3. *With high probability,*

$$\sup_{\rho} \left\| (\mathcal{N}_{1,H}^\dagger - \mathbb{E} \mathcal{N}_{1,H}^\dagger)[\rho] \right\|_1 = \mathcal{O} \left(\frac{R}{\sqrt{|a|}} \int_0^{\Delta_{ETH}} |f_\omega|^2 d\omega \right).$$

Proof. For the deviation, it suffices to control the dual

$$\left\| (\mathcal{N}_{1,H}^\dagger - \mathbb{E} \mathcal{N}_{1,H}^\dagger)[I] \right\|_\infty. \quad (7.37)$$

The proof follows a similar argument as in Proposition VII.4.2, but in the last step, we call concentration for $\sum_i a_i \mathbf{G}_i \mathbf{G}_i'$ (Fact V.6) as in Proposition V.4.1. \square

D. Proof of Theorem VII.1

Proof. Denote the leading eigenstate and eigenvalue $\mathcal{N}[\sigma_{fix}] = \lambda \sigma_{fix}$. Then we want a error at most ϵ

$$\left\| \mathcal{N}^\ell[\rho] - \lambda^\ell \sigma \right\|_1 = \left\| \mathcal{N}^\ell[\rho - \sigma_{fix}] \right\|_1 + \lambda^\ell \left\| \sigma_{fix} - \sigma \right\|_1 (\leq \epsilon). \quad (7.38)$$

(1) For the contraction of trace distance, recall (7.11) and Proposition VII.1.2

$$\eta_1(\mathcal{N}^\ell) = \sup_{\rho_1, \rho_2} \frac{\left\| \mathcal{N}^\ell[\rho_1 - \rho_2] \right\|_1}{\left\| \rho_1 - \rho_2 \right\|_1} \leq \sup_{\rho_1, \rho_2} \frac{\left\| \mathcal{N}_{H,\sigma}^\ell[\rho_1 - \rho_2] \right\|_1}{\left\| \rho_1 - \rho_2 \right\|_1} + \ell \cdot \left\| \mathcal{N}_{A,\sigma} \right\|_{1-1}. \quad (7.39)$$

$$\leq \lambda_2^\ell(\mathcal{N}_{H,\sigma}) \cdot \left\| \frac{1}{\sigma} \right\|_\infty + \mathcal{O}(\ell \cdot \epsilon_{DB}). \quad (7.40)$$

Recall Proposition VII.1.3,

$$\lambda_2(\mathcal{N}_H) \leq \lambda_2(\mathcal{N}_{1,H}) + \left(1 - \min_{\text{Tr}[\rho]=1} \text{Tr}[\mathcal{N}_1[\rho]] \right) + \left\| \mathcal{N}_{2,A}^\dagger[I] \right\|_\infty \quad (7.41)$$

$$\begin{aligned} &\leq \min_{\bar{\nu}'_1} r(\bar{\nu}'_1) \cdot \left(1 - \Omega(\lambda_{RW}) + \left(\beta \bar{\nu}_0 R + \frac{\bar{\nu}_0 R}{\Delta_{ETH}} + p_{amp} \right) \right) + \\ &\quad 1 - \min_{\bar{\nu}'_1} r(\bar{\nu}'_1) \left(1 \pm \mathcal{O}(\beta \bar{\nu}_0 R + \frac{\bar{\nu}_0 R}{\Delta_{ETH}} + p_{amp}) \right) + \mathcal{O} \left(\frac{R}{\sqrt{|a|}} \int_0^{\Delta_{ETH}} |f_\omega|^2 d\omega \right) + \mathcal{O}(\epsilon_{DB}). \\ &\leq 1 - \Omega \left[\frac{1}{R} \int_0^{\Delta_{ETH}} |f_\omega|^2 e^{-\beta\omega} d\omega \left(-\mathcal{O}(\beta \bar{\nu}_0 R + \frac{\bar{\nu}_0 R}{\Delta_{ETH}} + p_{amp}) + \lambda_{RW} \right) \right] + \mathcal{O} \left(\epsilon_{DB} + \frac{R}{\sqrt{|a|}} \int_0^{\Delta_{ETH}} |f_\omega|^2 d\omega \right) \\ &= 1 - \Omega \left[\frac{\lambda_{RW}}{R} \int_0^{\Delta_{ETH}} |f_\omega|^2 e^{-\beta\omega} d\omega \right]. \end{aligned} \quad (7.42)$$

The three terms on the RHS are ETH calculations: the gap from Lemma VII.4, the trace from Corollary VII.3.1 and Proposition VII.4.3, and the anti-self-adjoint component from the same calculation for approximate detailed balance (Proposition VI.2.1). The last line is obtained by setting constraints

$$\frac{1}{\bar{\nu}_0} = \Omega \left(\left(\beta + \frac{1}{\Delta_{ETH}} \right) \frac{R}{\lambda_{RW}} \right), \quad (7.43)$$

$$|a| = \Omega \left(\frac{R^4}{\lambda_{RW}^2} e^{2\beta\Delta_{ETH}} \right), \quad (7.44)$$

$$\ell = \theta \left(\frac{\ln(1/\epsilon) + n + \beta \|\mathbf{H}_S\|}{\log(\lambda_2(\mathcal{N}_H))} \right) = \theta \left(\frac{R}{\lambda_{RW}} \frac{\ln(1/\epsilon) + n + \beta \|\mathbf{H}_S\|}{\int_0^{\Delta_{ETH}} e^{-\beta\omega} |f_\omega|^2 d\omega} \right) \quad (7.45)$$

$$(\epsilon_{DB} \lesssim) \beta r_{rej} \bar{\nu}_0 = \mathcal{O} \left(\frac{1}{\ell} \right). \quad (7.46)$$

The above ensures

$$\eta_1(\mathcal{N}^\ell) \leq \frac{\epsilon}{2}. \quad (7.47)$$

(2) To control the distance from the fixed point to Gibbs state, we need the failure probability to be small. Set m (which is similar to the calculation for ℓ , but with $\epsilon = 1/2$) such that the contraction ratio is at most $1/2$

$$m = \theta \left(\frac{R}{\lambda_{RW}} \frac{n + \beta \|\mathbf{H}_S\|}{\int_0^{\Delta_{ETH}} e^{-\beta\omega} |f_\omega|^2 d\omega} \right). \quad (7.48)$$

Then we would need to control

$$\|\boldsymbol{\sigma}_{fix} - \boldsymbol{\sigma}\|_1 \leq \frac{2m}{\lambda^m} \cdot (\epsilon_{DB} + 1 - \lambda) = \mathcal{O}(\epsilon), \quad (7.49)$$

For the last line to hold, it suffices to choose

$$(p_{fail} \leq r_{rej} \cdot p_{amp} + p_{rej} \lesssim) \quad r_{rej} \exp(-\Omega(r_{amp})) + \frac{1}{r_{rej}} = \mathcal{O}\left(\frac{\epsilon}{m}\right), \quad (7.50)$$

$$(\epsilon_{DB} \lesssim) \quad \beta r_{rej} \bar{\nu}_0 = \mathcal{O}\left(\frac{\epsilon}{m}\right) \quad (7.51)$$

which guarantees $\lambda^\ell = 1 - \mathcal{O}(\epsilon)$ since $\lambda \geq 1 - p_{fail}$. Rearrange the terms to obtain

$$r_{amp} = \Omega\left(\ln\left(\frac{m}{\epsilon}\right)\right) \quad (7.52)$$

$$r_{rej} = \Omega\left(\frac{m}{\epsilon}\right) \quad (7.53)$$

$$\bar{\nu}_0 = \mathcal{O}\left(\frac{\epsilon^2}{\beta m^2}\right), \quad (7.54)$$

which is the advertised result. \square

1. Proof of Proposition VII.1.2

Proposition (Recap). *Suppose $\|\mathcal{N}_{A,\boldsymbol{\sigma}}\|_{1-1} \leq \epsilon_{DB}$,*

$$\sup_{\boldsymbol{\rho}_1, \boldsymbol{\rho}_2} \frac{\|\mathcal{N}_{H,\boldsymbol{\sigma}}^\ell[\boldsymbol{\rho}_1 - \boldsymbol{\rho}_2]\|_1}{\|\boldsymbol{\rho}_1 - \boldsymbol{\rho}_2\|_1} \leq \lambda_2^\ell \cdot \left\| \frac{1}{\boldsymbol{\sigma}} \right\|_\infty + \mathcal{O}(\ell \cdot \epsilon_{DB}).$$

Proof. Decompose the input into the leading eigenvector and the orthogonal component

$$\boldsymbol{\rho}_1 - \boldsymbol{\rho}_2 = (\boldsymbol{\rho}_1 - \boldsymbol{\rho}_2)^\perp + \langle \boldsymbol{\rho}_1 - \boldsymbol{\rho}_2, \boldsymbol{\sigma}_{fix} \rangle_{\boldsymbol{\sigma}^{-1},2} \cdot \frac{\boldsymbol{\sigma}_{fix}}{\|\boldsymbol{\sigma}_{fix}\|_{\boldsymbol{\sigma}^{-1},2}^2}. \quad (7.55)$$

Then by triangle inequality,

$$\|\mathcal{N}_H^\ell[\boldsymbol{\rho}_1 - \boldsymbol{\rho}_2]\|_1 \leq \left| \langle \boldsymbol{\rho}_1 - \boldsymbol{\rho}_2, \boldsymbol{\sigma}_{fix} \rangle_{\boldsymbol{\sigma}^{-1},2} \right| \cdot \frac{\text{Tr}[\mathcal{N}_H^\ell[\boldsymbol{\sigma}_{fix}]]}{\|\boldsymbol{\sigma}_{fix}\|_{\boldsymbol{\sigma}^{-1},2}^2} + \|\mathcal{N}_H^\ell[(\boldsymbol{\rho}_1 - \boldsymbol{\rho}_2)^\perp]\|_1 \quad (7.56)$$

where the second inequality is Cauchy-Schwartz. We want to compare with the following

$$\text{Tr}[\mathcal{N}_H^\ell[\boldsymbol{\rho}_1 - \boldsymbol{\rho}_2]] = \langle \boldsymbol{\rho}_1 - \boldsymbol{\rho}_2, \boldsymbol{\sigma}_{fix} \rangle_{\boldsymbol{\sigma}^{-1},2} \cdot \frac{\text{Tr}[\mathcal{N}_H^\ell[\boldsymbol{\sigma}_{fix}]]}{\|\boldsymbol{\sigma}_{fix}\|_{\boldsymbol{\sigma}^{-1},2}^2} + \text{Tr}[\mathcal{N}_H^\ell[(\boldsymbol{\rho}_1 - \boldsymbol{\rho}_2)^\perp]]. \quad (7.57)$$

Hence,

$$\|\mathcal{N}_H^\ell[\boldsymbol{\rho}_1 - \boldsymbol{\rho}_2]\|_1 \leq \left| \text{Tr}[\mathcal{N}_H^\ell[\boldsymbol{\rho}_1 - \boldsymbol{\rho}_2]] \right| + 2 \|\mathcal{N}_H^\ell[(\boldsymbol{\rho}_1 - \boldsymbol{\rho}_2)^\perp]\|_1. \quad (7.58)$$

For the first term, use a telescoping sum

$$\left| \text{Tr}[\mathcal{N}_H^\ell[\boldsymbol{\rho}_1 - \boldsymbol{\rho}_2]] \right| \leq \left| \text{Tr}[\mathcal{N}^\ell[\boldsymbol{\rho}_1 - \boldsymbol{\rho}_2]] \right| + \ell \cdot \|\mathcal{N}_A\|_{1-1} \cdot \|\mathcal{N}_H\|_{1-1}^{\ell-1} \cdot \|\boldsymbol{\rho}_1 - \boldsymbol{\rho}_2\|_1 \quad (7.59)$$

where \mathcal{N} is trace-preserving. For the second term, convert to 2-norm by Cauchy-Schwartz

$$\|\mathcal{N}_H^\ell[(\boldsymbol{\rho}_1 - \boldsymbol{\rho}_2)^\perp]\|_1 \leq \text{Tr}[\boldsymbol{\sigma}] \cdot \|\mathcal{N}_H^\ell[(\boldsymbol{\rho}_1 - \boldsymbol{\rho}_2)^\perp]\|_{\boldsymbol{\sigma}^{-1},2} \leq \lambda_2^\ell \|\boldsymbol{\rho}_1 - \boldsymbol{\rho}_2\|_{\boldsymbol{\sigma}^{-1},2} \quad (7.60)$$

$$\leq \text{Tr}[(\boldsymbol{\rho}_1 - \boldsymbol{\rho}_2)^2 \frac{1}{\boldsymbol{\sigma}}] \leq \|\boldsymbol{\rho}_1 - \boldsymbol{\rho}_2\|_1 \cdot \left\| \frac{1}{\boldsymbol{\sigma}} \right\|_\infty. \quad (7.61)$$

The third inequality is $\text{Tr}[\mathbf{A}\mathbf{B}\mathbf{A}^\dagger\mathbf{B}^\dagger] \leq \text{Tr}[\mathbf{A}\mathbf{A}^\dagger\mathbf{B}^\dagger\mathbf{B}]$, and the fourth uses $\|\boldsymbol{\rho}_1 - \boldsymbol{\rho}_2\| \leq 1$. \square

E. Resource Estimates

For Quantum Metropolis sampling, if we plug in explicit parameters and set

$$\begin{aligned}\Delta_{ETH} &= \theta\left(\frac{1}{n^3}\right) \\ \Delta_{spec} &= \theta(\sqrt{n}) \\ |\mathbf{H}| &= \theta(n) \\ \min_{\bar{\omega} \leq \Delta_{ETH}} |f_{\bar{\omega}}|^2 &= \theta(n) \\ \beta &\leq \frac{1}{\Delta_{ETH}} \quad (= \theta(n^3))\end{aligned}$$

Then by Theorem VII.1,

$$\begin{aligned}\ell &= \theta\left(e^{\beta\Delta_{ETH}} \frac{R}{\lambda_{RW}} \frac{\ln(1/\epsilon) + n + \beta\|\mathbf{H}_S\|}{\Delta_{ETH} \min_{\bar{\omega} \leq \Delta_{ETH}} |f_{\bar{\omega}}|^2}\right) = \theta(n^9 [n(1 + \beta) + \ln(1/\epsilon)]) \quad (\text{Rounds}) \\ |a| &= \Omega\left(\frac{R^4}{\lambda_{RW}^2} e^{2\beta\Delta_{ETH}}\right) = \theta(n^{14}) \quad (\text{choices of flips}) \\ r_{amp} &= \Omega\left(\ln\left(\frac{\ell}{\epsilon}\right)\right) \approx \theta(\ln(n/\epsilon)) \quad (\text{iterations of amplification}) \\ t_{QPE} &= \theta\left(\frac{1}{\bar{\nu}_0}\right) = \Omega\left(\frac{\beta\ell r_{rej}}{\epsilon} + \left(\beta + \frac{1}{\Delta_{ETH}}\right) \frac{R}{\lambda_{RW}}\right) = \Omega\left(\frac{\beta n^{18} [n(1 + \beta) + \ln(1/\epsilon)]^2}{\epsilon^2}\right) \quad (\text{run time per QPE}). \\ r_{rej} &= \Omega\left(\frac{\ell}{\epsilon}\right) = \Omega\left(\frac{n^9 [n(1 + \beta) + \ln(1/\epsilon)]}{\epsilon}\right) \quad (\text{iterations of rejection}),\end{aligned}$$

Therefore, the total elapsed time gives (using the unconditional estimate for r_{rej})

$$t_{elapse} = t_{QPE} r_{rej} r_{amp} \ell = \Omega\left(\frac{\beta n^{36} [n(1 + \beta) + \ln(1/\epsilon)]^4}{\epsilon^3} \ln(n/\epsilon)\right) \approx \Omega\left(\frac{\beta n^{40} (1 + \beta)^4}{\epsilon^3}\right), \quad (7.62)$$

and one should multiply by the cost of simulating $e^{i\mathbf{H}t}$. Also, we need to find $|a| = \theta(n^{14})$ many different “flips” as if drawn independently from the ETH ansatz. One may choose from the 14-local operators ($\binom{n}{14}$ of them), but it is unclear whether they can be truly treated as i.i.d samples.

[1] Mark Srednicki, “The approach to thermal equilibrium in quantized chaotic systems,” *Journal of Physics A: Mathematical and General* **32**, 1163–1175 (1999).

[2] Luca D’Alessio, Yariv Kafri, Anatoli Polkovnikov, and Marcos Rigol, “From quantum chaos and eigenstate thermalization to statistical mechanics and thermodynamics,” *Advances in Physics* **65**, 239–362 (2016).

[3] K. Temme, T. J. Osborne, K. G. Vollbrecht, D. Poulin, and F. Verstraete, “Quantum metropolis sampling,” *Nature* **471**, 87–90 (2011).

[4] Noah Linden, Sandu Popescu, Anthony J Short, and Andreas Winter, “Quantum mechanical evolution towards thermal equilibrium,” *Physical Review E* **79**, 061103 (2009).

[5] Fabio Martinelli, “Lectures on glauber dynamics for discrete spin models,” in *Lectures on probability theory and statistics* (Springer, 1999) pp. 93–191.

[6] Mark Jerrum and Alistair Sinclair, “The markov chain monte carlo method: an approach to approximate counting and integration,” *Approximation Algorithms for NP-hard problems*, PWS Publishing (1996).

[7] Stan Z Li, “Markov random field models in computer vision,” in *European conference on computer vision* (Springer, 1994) pp. 361–370.

[8] Peter Clifford, “Markov random fields in statistics,” *Disorder in physical systems: A volume in honour of John M. Hammersley*, 19–32 (1990).

[9] Philip Resnik and Eric Hardisty, *Gibbs sampling for the uninitiated*, Tech. Rep. (Maryland Univ College Park Inst for Advanced Computer Studies, 2010).

[10] Michael J. Kastoryano and Fernando G. S. L. Brandao, “Quantum gibbs samplers: the commuting case,” (2016), [arXiv:1409.3435 \[quant-ph\]](https://arxiv.org/abs/1409.3435).

[11] Ángela Capel, Cambyses Rouzé, and Daniel Stilck França, “The modified logarithmic sobolev inequality for quantum spin systems: classical and commuting nearest neighbour interactions,” (2021), [arXiv:2009.11817 \[quant-ph\]](https://arxiv.org/abs/2009.11817).

[12] Fernando G. S. L. Brandao and Michael J. Kastoryano, “Finite correlation length implies efficient preparation of quantum thermal states,” (2019), [arXiv:1609.07877 \[quant-ph\]](https://arxiv.org/abs/1609.07877).

[13] Kristan Temme, “Lower bounds to the spectral gap of davies generators,” *Journal of Mathematical Physics* **54**, 122110 (2013).

[14] E. B. Davies, “Markovian master equations,” *Communications in Mathematical Physics* **39**, 91–110 (1974).

[15] E. B. Davies, “Markovian master equations. ii,” *Mathematische Annalen* **219**, 147–158 (1976).

[16] Anton Trushechkin, “Unified gorini-kossakowski-lindblad-sudarshan quantum master equation beyond the secular approximation,” *Physical Review A* **103** (2021), 10.1103/physreva.103.062226.

[17] A.G. REDFIELD, “The theory of relaxation processes* *this work was started while the author was at harvard university, and was then partially supported by joint services contract n5ori-76, project order i.” in *Advances in Magnetic Resonance, Advances in Magnetic and Optical Resonance*, Vol. 1, edited by John S. Waugh (Academic Press, 1965) pp. 1–32.

[18] Angel Rivas, “Refined weak-coupling limit: Coherence, entanglement, and non-markovianity,” *Physical Review A* **95** (2017), 10.1103/physreva.95.042104.

[19] M.-H. Yung and A. Aspuru-Guzik, “A quantum-quantum metropolis algorithm,” *Proceedings of the National Academy of Sciences* **109**, 754–759 (2012).

[20] Fernando GSL Brandao and Krysta M Svore, “Quantum speed-ups for solving semidefinite programs,” in *2017 IEEE 58th Annual Symposium on Foundations of Computer Science (FOCS)* (IEEE, 2017) pp. 415–426.

[21] Mohammad H Amin, Evgeny Andriyash, Jason Rolfe, Bohdan Kulchytskyy, and Roger Melko, “Quantum boltzmann machine,” *Physical Review X* **8**, 021050 (2018).

[22] Eric R Anschuetz and Yudong Cao, “Realizing quantum boltzmann machines through eigenstate thermalization,” arXiv preprint arXiv:1903.01359 (2019).

[23] Patrick Rall, “Faster coherent quantum algorithms for phase, energy, and amplitude estimation,” (2021), arXiv:2103.09717 [quant-ph].

[24] Paweł Wocjan and Kristan Temme, “Szegedy walk unitaries for quantum maps,” (2021), arXiv:2107.07365 [quant-ph].

[25] G. E. Mitchell, A. Richter, and H. A. Weidenmüller, “Random matrices and chaos in nuclear physics: Nuclear reactions,” *Reviews of Modern Physics* **82**, 2845–2901 (2010).

[26] Anatoly Dymarsky, “Bound on eigenstate thermalization from transport,” (2018), arXiv:1804.08626 [cond-mat.stat-mech].

[27] Rahul Nandkishore and David A. Huse, “Many-body localization and thermalization in quantum statistical mechanics,” *Annual Review of Condensed Matter Physics* **6**, 15–38 (2015).

[28] Fernando G. S. L. Brandao and Marcus Cramer, “Equivalence of statistical mechanical ensembles for non-critical quantum systems,” (2015), arXiv:1502.03263 [quant-ph].

[29] David Asher Levin, Yuval Peres, Elizabeth L. Wilmer, James Propp, and David B. Wilson, *Markov chains and mixing times* (American Mathematical Society, 2017).

[30] Anatoly Dymarsky, Nima Lashkari, and Hong Liu, “Subsystem eigenstate thermalization hypothesis,” *Physical Review E* **97** (2018), 10.1103/physreve.97.012140.

[31] M. B. Hastings, “Random unitaries give quantum expanders,” *Physical Review A* **76** (2007), 10.1103/physreva.76.032315.

[32] M. B. Hastings and A. W. Harrow, “Classical and quantum tensor product expanders,” (2008), arXiv:0804.0011 [quant-ph].

[33] Fernando G. S. L. Brandão, Aram W. Harrow, and Michał Horodecki, “Local random quantum circuits are approximate polynomial-designs,” *Communications in Mathematical Physics* **346**, 397–434 (2016).

[34] Gilles Pisier, “Random matrices and subexponential operator spaces,” (2013), arXiv:1212.2053 [math.OA].

[35] Li Gao and Cambyse Rouzé, “Complete entropic inequalities for quantum markov chains,” (2021), arXiv:2102.04146 [quant-ph].

[36] Nicholas LaRacuente, “Quasi-factorization and multiplicative comparison of subalgebra-relative entropy,” (2021), arXiv:1912.00983 [quant-ph].

[37] Joran van Apeldoorn and András Gilyén, “Improvements in quantum sdp-solving with applications,” arXiv preprint arXiv:1804.05058 (2018).

[38] angel Rivas and Susana F. Huelga, “Open quantum systems,” *SpringerBriefs in Physics* (2012), 10.1007/978-3-642-23354-8.

[39] Tomotaka Kuwahara and Keiji Saito, “Eigenstate thermalization from the clustering property of correlation,” *Physical Review Letters* **124** (2020), 10.1103/physrevlett.124.200604.

[40] Jonas Richter, Anatoly Dymarsky, Robin Steinigeweg, and Jochen Gemmer, “Eigenstate thermalization hypothesis beyond standard indicators: Emergence of random-matrix behavior at small frequencies,” *Phys. Rev. E* **102**, 042127 (2020).

[41] Marlon Bremes, Silvia Pappalardi, Mark T. Mitchison, John Goold, and Alessandro Silva, “Out-of-time-order correlations and the fine structure of eigenstate thermalization,” *Physical Review E* **104** (2021), 10.1103/physreve.104.034120.

[42] E. Onorati, O. Buerschaper, M. Kliesch, W. Brown, A. H. Werner, and J. Eisert, “Mixing properties of stochastic quantum hamiltonians,” *Communications in Mathematical Physics* **355**, 905–947 (2017).

[43] Daniel Nagaj, Paweł Wocjan, and Yong Zhang, “Fast amplification of qma,” (2009), arXiv:0904.1549 [quant-ph].

[44] T. Tao, “Topics in random matrix theory,” (2012).

[45] Hyungwon Kim, Tatsuhiko N. Ikeda, and David A. Huse, “Testing whether all eigenstates obey the eigenstate thermalization hypothesis,” *Physical Review E* **90** (2014), 10.1103/physreve.90.052105.

Appendix A: Gaussian Calculations

Fact A.1 (recap.). *For rectangular matrices $\mathbf{G}_{d_2 d_1}$ with i.i.d complex Gaussian entries, with variance $\mathbb{E}[G_{ij}G_{ij}^*] = 2$*

$$\mathbb{E} \|\mathbf{G}\|_p^p \leq \min(d_1, d_2) \mathbb{E} \|\mathbf{G}\|^p \leq \min(d_1, d_2) \cdot \left(\sqrt{\max(d_1, d_2)}^p c_1^p + (c_2 \sqrt{p})^p \right)$$

for absolute constants c_1, c_2 .

Proof. Let us begin with the case $N = d_1 = d_2$ for demonstration. We reproduce a proof in [44, Section 2.3.1] via a simple epsilon net and union bound argument. This strategy worked well here because the concentration is exponential

in dimension $e^{-\Omega(N)}$ that compensates the cardinality of the epsilon net. Consider a $1/2$ maximal net $\Sigma_{1/2}$ on unit sphere $\|x\|_{\ell_2} = 1$, i.e. points in $\Sigma_{1/2}$ are at least $1/2$ apart, but adding any point x must be $1/2$ close to some element in $\Sigma_{1/2}$. First, take the union bound

$$\Pr(\|\mathbf{G}\| \geq \lambda) \leq \Pr(\exists x \in \Sigma_{1/2}, \|Gx\|_{\ell_2} \geq \lambda/2). \quad (\text{A1})$$

In other words, there exists an optimizing y that $\|\mathbf{G}y\|_{\ell_2} = \|\mathbf{G}\|$. We can find a nearby point in the net $x \in \Sigma_{1/2}$ such that $\|x - y\|_{\ell_2} \leq 1/2$, then by the triangle inequality

$$\|\mathbf{G}y\|_{\ell_2} \geq \|\mathbf{G}x\|_{\ell_2} - \|\mathbf{G}(x - y)\|_{\ell_2} \geq \|\mathbf{G}\|/2. \quad (\text{A2})$$

Namely, some point in the epsilon net must be at least half as large as the optimum. Second, we bound the probability of each event by Bernstein's inequality

Fact A.2 (Bernstein's inequality). *For a sum of centered, zero-mean random variables,*

$$\Pr(\sum x_i \geq \epsilon) \leq \exp\left(\frac{-\epsilon^2/2}{v + L\epsilon/3}\right)$$

for $v = \sum \mathbb{E}x_i^2$ and any L such that for all $k > 2$, $\mathbb{E}[x_i^k] \leq \frac{\mathbb{E}[x_i^2]}{2} k! L^{k-2}$.

Hence,

$$\Pr\left(\|\mathbf{G}x\|_{\ell_2} \geq (t+1)\sqrt{2N}\right) = \Pr\left(\sum_{i=1}^{2N} g_i^2 - 2N \geq (t+1)^2 - 1\right) \leq \exp\left(-\frac{4N^2 t^4/2}{2N\mathbb{E}[(g^2 - 1)^2] + 2Nt^2 L/3}\right) \quad (\text{A3})$$

$$\leq \exp\left(-\frac{Nt^4}{2 + 64t^2/3}\right) \quad (\text{A4})$$

$$\leq \begin{cases} \exp(-\frac{Nt^4}{4}) & \text{if } t^2 < 3/32 \\ \exp(-\frac{3}{128}Nt^2) & \text{if } t^2 \geq 3/32 \end{cases} \quad (\text{A5})$$

We used elementary estimates $t'^2 := (t+1)^2 - 1 \geq t^2$, $\mathbb{E}[(g^2 - 1)^2] = 2$, and $L = 64$ for Bernsteins' inequality

$$\mathbb{E}(g^2 - 1)^k \leq \mathbb{E}(g^2 - g'^2)^k \leq 2^k \cdot (2k-1)!! \leq \frac{1}{2} \mathbb{E}(g^2 - 1)^2 k! 4^k \leq \frac{k!}{2} \mathbb{E}(g^2 - 1)^2 64^{k-2}. \quad (\text{A6})$$

Lastly, plugging in the union bound,

$$\Pr\left(\|\mathbf{G}\| \geq (t+1)2\sqrt{2N}\right) \leq 9^N \exp\left(-\frac{3}{128}Nt^2\right) \leq \exp\left(-N\left(\frac{3}{128}t^2 - \ln 36\right)\right) \quad (\text{A7})$$

where the cardinality of $\Sigma_{1/2}$ is at most $(\frac{3}{1/4})^{2N}$ by volumetric argument. Integrating the tail,

$$\mathbb{E}\|\mathbf{G}\|^p \leq \sqrt{N^p} (c_1^p + (c_2 \sqrt{\frac{p}{N}})^p). \quad (\text{A8})$$

At small values of t , the integral gives c_1 . At large enough values of t , the tail is exponential $\sim e^{-Nt^2}$, which gives dependence on p that is suppressed by $1/\sqrt{N}$. When the matrix is rectangular $\mathbf{G}_{d_2 d_1}$ (WLG let $d_1 \geq d_2$ so $t^2 \geq 3/32$) we get

$$\Pr\left(\|\mathbf{G}\| \geq (t+1)2\sqrt{2d_2}\right) \leq 9^{d_1} \exp\left(-\frac{3}{128}d_2 t^2\right), \implies \mathbb{E}\|\mathbf{G}\|^p \leq \sqrt{d_2^p} \left[\left(1 + \sqrt{\frac{d_1}{d_2}}\right)^p c_1^p + (c_2 \sqrt{\frac{p}{d_2}})^p \right]. \quad (\text{A9})$$

This is the advertised result. \square

Fact A.3 (Recap.). *For independent Gaussian matrices $\mathbf{G}_i, \mathbf{G}'_i$ with i.i.d complex Gaussian entries,*

$$\mathbb{E} \left\| \sum_i a_i \mathbf{G}_i \mathbf{G}'_i \right\|_p^p \leq \mathbb{E} \|\mathbf{G}_i \mathbf{G}'_i\|_p^p (\sum_i a_i^2)^{p/2}$$

Proof. Following [34, Theorem 4.4], expand the expected trace

$$\mathbb{E} \left\| \sum_i a_i \mathbf{G}_i \mathbf{G}'_i \right\|_p^p = \sum_{i_p, \dots, i_1} a_{i_p} \cdots a_{i_2}^* a_{i_1} \mathbb{E} \text{Tr} [\mathbf{G}_{i_p}^{\dagger} \mathbf{G}_{i_p}^{\dagger} \cdots \mathbf{G}_{i_2}^{\dagger} \mathbf{G}_{i_2}^{\dagger} \mathbf{G}_{i_1} \mathbf{G}'_{i_1}] \quad (\text{A10})$$

$$= \sum_{i_p, \dots, i_1} a_{i_p} \cdots a_{i_2}^* a_{i_1} \sum_w \phi(w) \mathbb{1}(w \sim i_p, \dots, i_1) \quad (\text{A11})$$

$$\leq \sum_w \phi(w) \sum_{i_p, \dots, i_1} a_{i_p} \cdots a_{i_2}^* a_{i_1} \mathbb{1}(w \sim i_p, \dots, i_1) \quad (\text{A12})$$

$$\leq \sum_w \phi(w) \left(\sum_i a_i a_i^* \right)^{p/2} \quad (\text{A13})$$

$$\leq \mathbb{E} \|\mathbf{G}_1 \mathbf{G}'_1\|_p^p \left(\sum_i a_i^2 \right)^{p/2} \quad (\text{A14})$$

In the second inequality we sum over all wick contraction, each contributing with some positive function $\phi(w)$. For each sequence i_p, \dots, i_1 , we use indicator $\mathbb{1}(w \sim i_p, \dots, i_1)$ to enforce $\mathbf{G}_i (\mathbf{G}'_i)$ only contract with its adjoint $\mathbf{G}_i^{\dagger} (\mathbf{G}'_i^{\dagger})$. Switching the summation in the third, the observation in the fourth is that each pairing w can at most come from $(\sum_i a_i^2)^{p/2}$ different combinations. Note that $a_{i_p} \cdots a_{i_2}^* a_{i_1} \mathbb{1}(w \sim i_p, \dots, i_1)$ are non-negative as enforced by pairing. Lastly, we recombine the contractions back as the moment of one copy $\mathbf{G}_1 \mathbf{G}'_1$. This is the advertised result. \square

Fact A.4. For $\mathbf{G}_i, \mathbf{G}'_i$ i.i.d rectangular matrices with i.i.d complex Gaussian entries,

$$\mathbb{E} \left\| \sum_i a_i \mathbf{G}_i \otimes \mathbf{G}'_i^* \right\|_p^p \leq (\mathbb{E} \|\mathbf{G}\|_p^p)^2 \cdot \left(\sum_i a_i^2 \right)^{p/2}.$$

Proof. Again,

$$\mathbb{E} \left\| \sum_i a_i \mathbf{G}_i \otimes \mathbf{G}'_i^* \right\|_p^p = \sum_{i_p, \dots, i_1} a_{i_p} \cdots a_{i_2}^* a_{i_1} \mathbb{E} \text{Tr} [\mathbf{G}_{i_p}^{\dagger} \cdots \mathbf{G}_{i_2}^{\dagger} \mathbf{G}_{i_1}] \mathbb{E} \text{Tr} [\mathbf{G}_{i_p}^{\dagger} \cdots \mathbf{G}_{i_2}^{\dagger} \mathbf{G}'_{i_1}]^*, \quad (\text{A15})$$

and the rest arguments is analogous, with a different function $\phi(w)$. \square

Appendix B: Conductance Calculation

Our quantum problems reduce to classical Markov chains. Here, we quickly review how to estimate the gap of Markov chains via conductance estimates and later present the calculation needed for the main text. Consider the function of two sets

$$Q(A \rightarrow B) := \sum_{x \in A, y \in B} \pi(x) \Pr(x \rightarrow y), \quad (\text{B1})$$

then the bottleneck ratio is defined by

$$\phi := \min_{\pi(A) \leq 1/2} \frac{Q(A \rightarrow A^c)}{\pi(A)}, \quad (\text{B2})$$

where the RHS can be understood as the chance of leaving set S after a step, divided by its stationary weight. This gives a two-sided estimate of the spectral gap (we will only need the RHS).

Fact B.1 (Cheeger's inequality).

$$1 - 2\phi \leq \lambda_2 \leq 1 - \frac{\phi^2}{2}. \quad (\text{B3})$$

See, e.g., [29] for a textbook introduction.

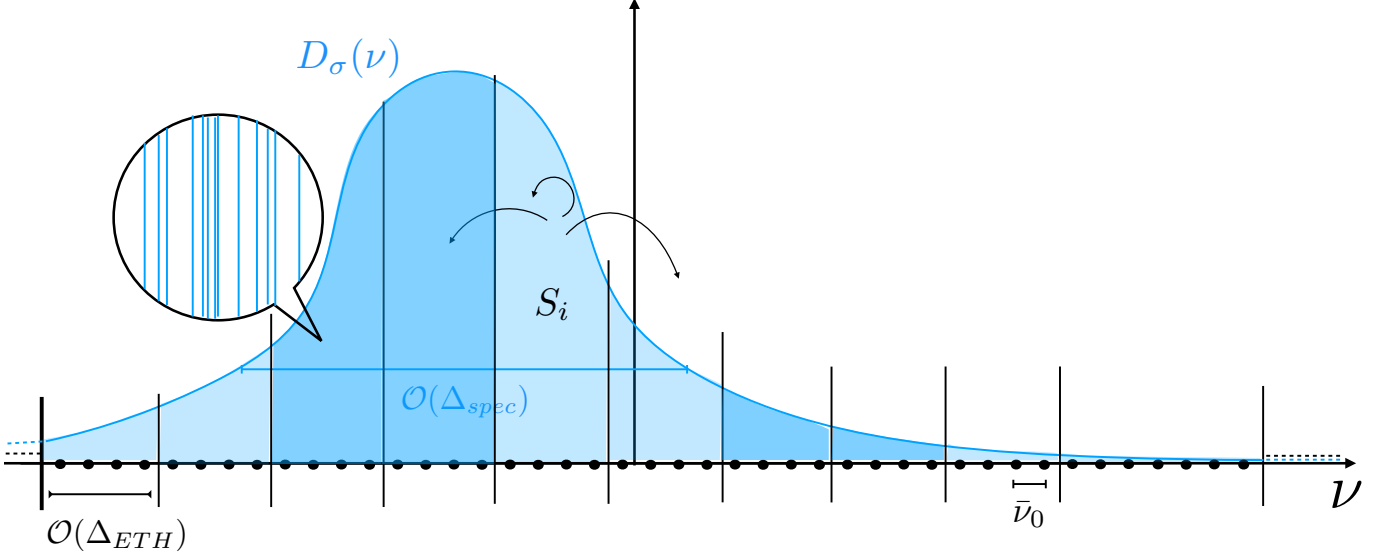


Figure 9. Partition of the spectrum into disjoint sets S_i , each with size Δ_{ETH} . To estimate the bottleneck ratio, for any possible set A , we assign for each S_i a boolean variable b_i whether S_i has more than $3/4$ energies occupied (darker), or not (brighter).

1. The 1d Random Walk with Gaussian Density of state

a. The Markov chain from the Lindbladian

Proposition B.1.1. Suppose the Gibbs state satisfies Assumption IV.2 (e.g., Gaussian distribution with variance Δ_{spec}^2). Consider the Markov chain associated with

$$\Phi^*[\mathbf{P}_{\bar{\nu}}] = \frac{1}{m} \left(\sum_{0 < \bar{\omega} \leq \Delta_{ETH}} E_{\bar{\nu}+\bar{\omega}, \bar{\nu}}[\mathbf{P}_{\bar{\nu}}] + \sum_{0 < \bar{\omega} \leq \Delta_{ETH}} E_{\bar{\nu}, \bar{\nu}-\bar{\omega}}[\mathbf{P}_{\bar{\nu}}] \right).$$

where $E_{\bar{\nu}+\bar{\omega}, \bar{\nu}}$ (or $E_{\bar{\nu}, \bar{\nu}-\bar{\omega}}$) is the identity map if $\bar{\nu} + \bar{\omega}$ (or $\bar{\nu} - \bar{\omega}$) is outside of the spectrum.

Then, the second eigenvalue is at most

$$|\lambda_2| = 1 - \Omega \left(\frac{\Delta_{ETH}^2 e^{-2\beta\Delta_{ETH}}}{\Delta_{spec}^2 R^2} \right). \quad (\text{B4})$$

Note that the scale Δ_{ETH} is the length scale of hops, and this markov chain is characterized entirely by the Gibbs distribution at inverse temperature β and the local density of state (which boils down to the ratio R).

Proof. Let us present the proof¹⁸ by having a Gaussian distribution in mind, but it directly works for distribution satisfying Assumption IV.2. First, let us partition the spectrum by disjoint adjacent sets S_i , with sizes (Figure 9)

$$|S_i| \bar{\nu}_0 = \theta(\Delta_{ETH}), \quad (\text{B5})$$

$$\max_{\bar{\nu}_1 \in S_i, \bar{\nu}_2 \in S_{i+1}} (\bar{\nu}_1 - \bar{\nu}_2) \leq \frac{\Delta_{ETH}}{2}. \quad (\text{B6})$$

To contain the “remainder” sites near the edge, enlarge the last two sets S to trice the size.

We will have to go through the bottleneck ratio estimate. For arbitrary set A , assign a variable b_i for each site S_i (Figure 9) such that

$$\begin{cases} b_i = 1 & \text{if } A \cap S_i \text{ occupies more than } 3/4 \text{ sites of } S_i \\ b_i = 0 & \text{else.} \end{cases} \quad (\text{B7})$$

Let us consider a S_i adjacent to S_{i+1} . Recall that the conditional expectation $E_{\bar{\nu}_1, \bar{\nu}_2}$ sends any local state to the local Gibbs state

$$\sigma_{\bar{\nu}_1, \bar{\nu}_2} := \frac{\mathbf{P}_{\bar{\nu}_1} e^{-\beta \bar{\nu}_1} + \mathbf{P}_{\bar{\nu}_2} e^{-\beta \bar{\nu}_2}}{\text{Tr}[\mathbf{P}_{\bar{\nu}_1}] e^{-\beta \bar{\nu}_1} + \text{Tr}[\mathbf{P}_{\bar{\nu}_2}] e^{-\beta \bar{\nu}_2}}. \quad (\text{B8})$$

¹⁸ Some of the estimates may be adapted from an unpublished note by Charles Xu.

For example, suppose $b_i = 1, b_{i+1} = 0$, then due to the conditional expectations $E_{\bar{\nu}_1, \bar{\nu}_2}$,

$$\frac{Q(A \cap S_i \rightarrow S_{i+1})}{\pi(A \cap S_i)} = \Omega\left(\frac{e^{-\beta \Delta_{ETH}}}{R}\right), \quad (\text{B9})$$

where $e^{-\beta \Delta_{ETH}}/R$ comes from a crude estimate on the ratio $\text{Tr}[\mathbf{P}_{S_{i+1}} \boldsymbol{\sigma}_{\bar{\nu}_1, \bar{\nu}_2}] / \text{Tr}[\mathbf{P}_{S_i} \boldsymbol{\sigma}_{\bar{\nu}_1, \bar{\nu}_2}]$. Similarly, suppose $b_i = 1, b_{i-1} = 0$, then

$$\frac{Q(A \cap S_i \rightarrow S_{i-1})}{\pi(A \cap S_i)} = \Omega\left(\frac{1}{R}\right), \quad (\text{B10})$$

and note the difference from (B9) is whether the energy is increasing ($S_i \rightarrow S_{i+1}$) or decreasing ($S_i \rightarrow S_{i-1}$). Now, decompose A into disjoint sets $A = A_1 + A_2$

$$A_1 := A \cap \{S_i | b_i = 1, \text{ or } b_{i \pm 1} = 1, \}, \quad (\text{B11})$$

$$A_2 := A - A_1. \quad (\text{B12})$$

In other words, A_1 collects those sites S_i with $b_i = 1$, and also the nearest neighbors. This choice ensures that complement A_2 is very ‘conducting’ since its neighbors and itself has 1/4 empty spots (i.e., $b_i = 0$)

$$\frac{Q(A_2 \rightarrow A^c)}{\pi(A_2)} = \Omega(1). \quad (\text{B13})$$

The bottleneck comes from A_1 , and we have to get our hands dirty. We will need the density of states (weighted by Boltzmann factor)

$$D(\omega) = \frac{1}{\sqrt{2\pi \Delta_{spec}^2}} \exp\left(\frac{-(\omega - \beta \Delta_{spec}^2/2)^2}{2\Delta_{spec}^2}\right), \quad (\text{B14})$$

which is a shifted Gaussian $\omega' = \omega - \beta \Delta_{spec}^2/2$. It suffices to consider a contiguous chain $b_L = 0, b_{i+1} = 1, \dots, b_R = 0$ on this density of states, with end points $\omega'_L < \omega'_R$.

Case 1: If

$$\omega'_R \in \left[-\frac{\Delta'_{spec}}{4}, \frac{\Delta_{spec}}{4}\right], \quad (\text{B15})$$

then

$$Q(A_1 \rightarrow A^c) = \Omega\left(\frac{e^{-\beta \Delta_{ETH}}}{R} \text{Tr}[\mathbf{P}_{S_R} \boldsymbol{\sigma}] + \text{Tr}[\mathbf{P}_{S_L} \boldsymbol{\sigma}]\right) \quad (\text{B16})$$

$$= \Omega\left(\frac{e^{-\beta \Delta_{ETH}}}{R} \frac{\Delta_{ETH}}{\Delta_{spec}}\right), \quad (\text{B17})$$

where we used that $\text{Tr}[\mathbf{P}_{S_R} \boldsymbol{\sigma}] = \theta(\Delta_{ETH} \cdot \frac{1}{\Delta_{spec}})$ and (B9). The computation is identical for $\omega'_L \in \left[-\frac{\Delta'_{spec}}{4}, \frac{\Delta_{spec}}{4}\right]$, but without the Boltzmann factor.

Case 2: If

$$\omega'_L, \omega'_R \in \left[-\frac{\Delta'_{spec}}{4}, \frac{\Delta_{spec}}{4}\right]^c, \quad (\text{B18})$$

WLG let us consider $\omega'_R \leq -\frac{\Delta'_{spec}}{4}$, then

$$Q(A_1 \rightarrow A^c) = \Omega\left(\text{Tr}[\mathbf{P}_{S_R} \boldsymbol{\sigma}] \cdot \frac{e^{-\beta \Delta_{ETH}}}{R}\right) \quad (\text{B19})$$

$$= \Omega\left(\frac{\Delta_{ETH}}{\Delta_{spec}} \exp\left(\frac{-\omega'^2_R}{2\Delta_{spec}^2}\right) \cdot \frac{e^{-\beta \Delta_{ETH}}}{R}\right), \quad (\text{B20})$$

but A_1 is weighted on a Gaussian tail

$$\pi(A_1) = \mathcal{O}\left(\int_{-\infty}^{\omega'_R} \frac{1}{\Delta_{spec}} \exp\left(\frac{-\omega'^2}{2\Delta_{spec}^2}\right) d\omega'\right) \quad (\text{B21})$$

$$= \mathcal{O}\left(\frac{\Delta_{spec}}{\omega'_R} \exp\left(\frac{-\omega'^2_R}{2\Delta_{spec}^2}\right)\right). \quad (\text{B22})$$

which means

$$\frac{Q(A_1 \rightarrow A^c)}{\pi(A_1)} = \Omega\left(\frac{\Delta_{ETH}\omega'_R}{\Delta_{spec}^2} \frac{e^{-\beta\Delta_{ETH}}}{R}\right) \quad (\text{B23})$$

$$= \Omega\left(\frac{\Delta_{ETH}}{\Delta_{spec}} \frac{e^{-\beta\Delta_{ETH}}}{R}\right). \quad (\text{B24})$$

Combining the estimates for A_2 , and disjoint subsets $A_1^{(j)}$ of A_1 (from case 1 or 2),

$$\frac{Q((A_2 + \sum_j A_1^{(j)}) \rightarrow A^c)}{\pi(A_2 + \sum_j A_1^{(j)})} = \frac{Q(A_2 \rightarrow A^c) + \sum_j Q(A_1^{(j)} \rightarrow A^c)}{\pi(A_2) + \sum_j \pi(A_1^{(j)})} = \Omega\left(\frac{\Delta_{ETH}}{\Delta_{spec}} \frac{e^{-\beta\Delta_{ETH}}}{R}\right), \quad (\text{B25})$$

which converts to eigenvalue estimate by Fact B.1. More generally, the above derivation is analogous for the ‘‘Gaussian-like’’ Gibbs distribution satisfying Assumption IV.2, which feeds into the arguments in Case 1 and Case 2. \square

b. The Markov chain from Metropolis sampling

Proposition B.1.2. *For the Markov chain from taking expectation of Metropolis (T added so that $M^\dagger[\mathbf{I}] \propto \mathbf{I}$)*

$$M := \frac{1}{2} \left(\sum_{|\bar{\nu}_1 - \bar{\nu}_2| \leq \Delta_{ETH} - 2\bar{\nu}_0} p(\bar{\nu}_1) \mathbb{E} \mathcal{A}_{\bar{\nu}_2 \bar{\nu}_1} + (\sigma\text{-adjoint}) \right) + T,$$

, and the Gibbs state satisfying Assumption IV.2 (e.g., Gaussian distribution with variance Δ_{spec}^2), then the second eigenvalue is at most

$$\lambda_2 = \min_{\bar{\nu}'_1} r(\bar{\nu}'_1) \left(1 - \Omega\left(\frac{e^{-2\beta\Delta_{ETH}}}{R^2} \frac{\Delta_{ETH}^2}{\Delta_{spec}^2}\right) \right) + \mathcal{O}(\|T\|). \quad (\text{B26})$$

Proof. The proof is analogous to the case from Lindbladians (Proposition B.1.1), but with an extra Boltzmann factor and density ratio (This was accounted by $\gamma(-\omega)$, with is not present after using approximate tensorization). First, we rescale M

$$M' := \frac{1}{\text{Tr}[M]} M. \quad (\text{B27})$$

Let us calculate the key expressions for M' , presented in the same notations. The transition rates from S_i to S_{i+1} reads

$$\frac{Q(S_i \rightarrow S_{i+1})}{\pi(S_i)} = \frac{1}{\text{Tr}[M]} \theta \left(\min_{\nu_1 \in S_i} \sum_{\nu_2 \in S_{i+1}} \exp\left(-S\left(\frac{\nu_2 + \nu_1}{2}\right)\right) |f(\nu_2 - \nu_1)|^2 \right) \min(1, e^{-\beta(\bar{\nu}_2 - \bar{\nu}_1)}) \quad (\text{B28})$$

$$= \frac{1}{\text{Tr}[M]} \Omega\left(\frac{e^{-\beta\Delta_{ETH}}}{R} \int_0^{\Delta_{ETH}} |f_\omega|^2 d\omega\right) = \Omega\left(\frac{e^{-\beta\Delta_{ETH}}}{R}\right), \quad (\text{B29})$$

where $\Omega(\cdot)$ suppresses the density ratios $1/R$. In the last line, we plugged in

$$\text{Tr}[M] = \min_{\bar{\nu}'_1} r(\bar{\nu}'_1) \pm \mathcal{O}(\|T\|) \quad (\text{B30})$$

and evaluate (B29) by

$$\frac{\int_0^{\Delta_{ETH}} |f_\omega|^2 d\omega}{\int_0^{\Delta_{ETH}} e^{-\beta\omega} |f_\omega|^2 d\omega} \leq 1. \quad (\text{B31})$$

Now, this becomes very much the Lindbladian case up to factor $e^{-\beta\Delta_{ETH}}$, and the rest of the proof follows. \square

Appendix C: Numerical tests of expander properties

We exactly diagonalize ¹⁹ a chaotic spin chain

$$\mathbf{H} = g \sum_{i=1}^L \boldsymbol{\sigma}_i^x + h \sum_{i=1}^L \boldsymbol{\sigma}_i^z + J \sum_{i=1}^L \boldsymbol{\sigma}_i^z \boldsymbol{\sigma}_{i+1}^z \quad (\text{C1})$$

up to $L = 12$ qubits with periodic boundary condition $L + 1 \sim 1$. This is intended for a quick sanity check, and we expect to carry out a larger scale numerics in a follow-up work. At parameter $g = 0.9045, h = 0.8090, J = 1$, this model is presumably robustly chaotic [45] and numerically tested to satisfy the traditional ETH, i.e., most eigenstates give thermal expectations [45].

We wish to check the expander properties from the prediction of ETH in the sense that

$$\lambda_2(\mathcal{L}_{\bar{\nu}_1, \bar{\nu}_2}) = \left(1 - \mathcal{O}\left(\frac{1}{\sqrt{|a|}}\right)\right) \lambda_2(\mathbb{E}\mathcal{L}_{\bar{\nu}_1, \bar{\nu}_2}) = -\Omega\left(|a| \cdot |f(\bar{\omega})|^2 \bar{\nu}_0\right), \quad (\text{C2})$$

$$\lambda_1(\mathcal{L}_{\bar{\nu}_1, \bar{\nu}_2, \bar{\omega}'}) = \left(1 - \mathcal{O}\left(\frac{1}{\sqrt{|a|}}\right)\right) \lambda_1(\mathbb{E}\mathcal{L}_{\bar{\nu}_1, \bar{\nu}_2, \bar{\omega}'}) = -\Omega\left(|a| \cdot |f(\bar{\omega})|^2 \bar{\nu}_0\right), \quad (\text{C3})$$

where we set $\gamma(\bar{\omega}) = \text{const}$. The two equalities are the two checkable quantities we focus on: the scaling of the gap and the deviation from expectation.

1. The gap of the Lindbladian

At large $|a|$, we want to check whether the eigenvalues scale linearly with the number of flips $|a|$

$$\lambda_2(\mathcal{L}_{\bar{\nu}_1, \bar{\nu}_2}) \stackrel{?}{=} -\Omega\left(|a| \cdot |f(\bar{\omega})|^2 \bar{\nu}_0\right), \quad (\text{C4})$$

$$\lambda_1(\mathcal{L}_{\bar{\nu}_1, \bar{\nu}_2, \bar{\omega}'}) \stackrel{?}{=} -\Omega\left(|a| \cdot |f(\bar{\omega})|^2 \bar{\nu}_0\right). \quad (\text{C5})$$

This is, after all, what we need for the proof (to feed into approximate tensorization). Indeed, we observe a roughly linear trend for the diagonal inputs (Figure 10) and for the off-block-diagonal inputs (Figure 11).

2. The deviation

Next, we check something stronger than we need for the proof as a more refined probe to RMT: whether the Lindbladian is close to the “expectation”.

$$\|\mathcal{L}_{\bar{\nu}_1, \bar{\nu}_2} - \hat{\mathbb{E}}\mathcal{L}_{\bar{\nu}_1, \bar{\nu}_2}\| \stackrel{?}{=} \mathcal{O}\left(\frac{1}{\sqrt{|a|}} \lambda_2(\hat{\mathbb{E}}\mathcal{L}_{\bar{\nu}_1, \bar{\nu}_2})\right) \quad (\text{C6})$$

$$\|\mathcal{L}_{\bar{\nu}_1, \bar{\nu}_2, \bar{\omega}'} - \hat{\mathbb{E}}\mathcal{L}_{\bar{\nu}_1, \bar{\nu}_2, \bar{\omega}'}\| \stackrel{?}{=} \mathcal{O}\left(\frac{1}{\sqrt{|a|}} \lambda_1(\hat{\mathbb{E}}\mathcal{L}_{\bar{\nu}_1, \bar{\nu}_2, \bar{\omega}'})\right). \quad (\text{C7})$$

Note that numerically, we do not have access to the idealized expectation, and we just manually drop all the cross-terms that supposedly have zero-mean, denoted by $\hat{\mathbb{E}}$

$$\hat{\mathbb{E}}\mathcal{L}_{\bar{\nu}_1, \bar{\nu}_2}[\mathbf{X}] := \sum_a \left[\frac{\gamma_a(\bar{\omega})}{2} \left(\mathbf{A}_{\nu_1 \nu_2}^a \mathbf{X} \mathbf{A}_{\nu_2 \nu_1}^a - \frac{1}{2} \{ \mathbf{A}_{\nu_1 \nu_2}^a \mathbf{A}_{\nu_2 \nu_1}^a, \mathbf{X}_{\nu_1 \nu_1} \} \right) + \frac{\gamma_a(-\bar{\omega})}{2} (\nu_1 \leftrightarrow \nu_2) \right] \quad (\text{C8})$$

where $\mathbf{A}_{\nu_1 \nu_2} := |\nu_1\rangle \langle \nu_1| \mathbf{A}_{\bar{\nu}_1 \bar{\nu}_2} |\nu_2\rangle \langle \nu_2|$ ²⁰. Indeed, we observe that the deviation scales slower than the eigenvalues (Figure 12).

¹⁹ The jupyter notebook code is available at https://github.com/Shawnger/ETH_expander.

²⁰ In other words, the energies are disentangled by taking $\hat{\mathbb{E}}$; this also resembles the original Davies’ generator at infinite time (1.2)

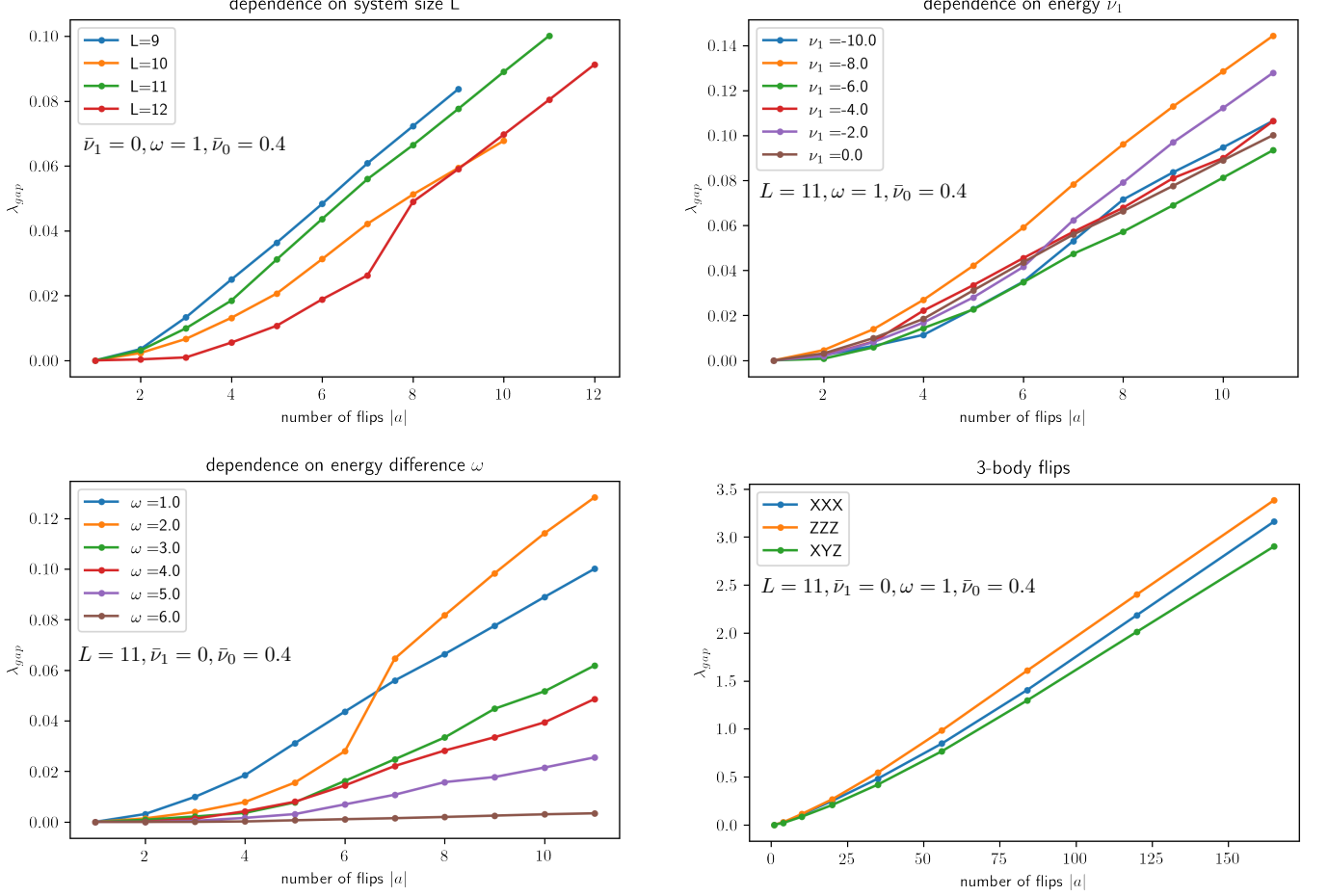


Figure 10. The gap of the Lindbladian $\lambda_{gap}(\mathcal{L}_{\bar{\nu}_1, \bar{\nu}_2})$ for block-diagonal inputs at $\bar{\nu}_1 = [\nu_1, \nu_1 + \bar{\nu}_0], \bar{\nu}_2 = [\nu_1 + \omega, \nu_1 + \omega + \bar{\nu}_0]$, for ranges of parameters and flips σ_i^x . (a) The dependence on the system size L . (b) The dependence on energy $\bar{\nu}_1$. (c) The dependence on the energy difference ω . (d) 3-body flips for $\sigma_i^x \sigma_j^x \sigma_k^x$, $\sigma_i^z \sigma_j^z \sigma_k^z$, $\sigma_i^x \sigma_j^y \sigma_k^z$.

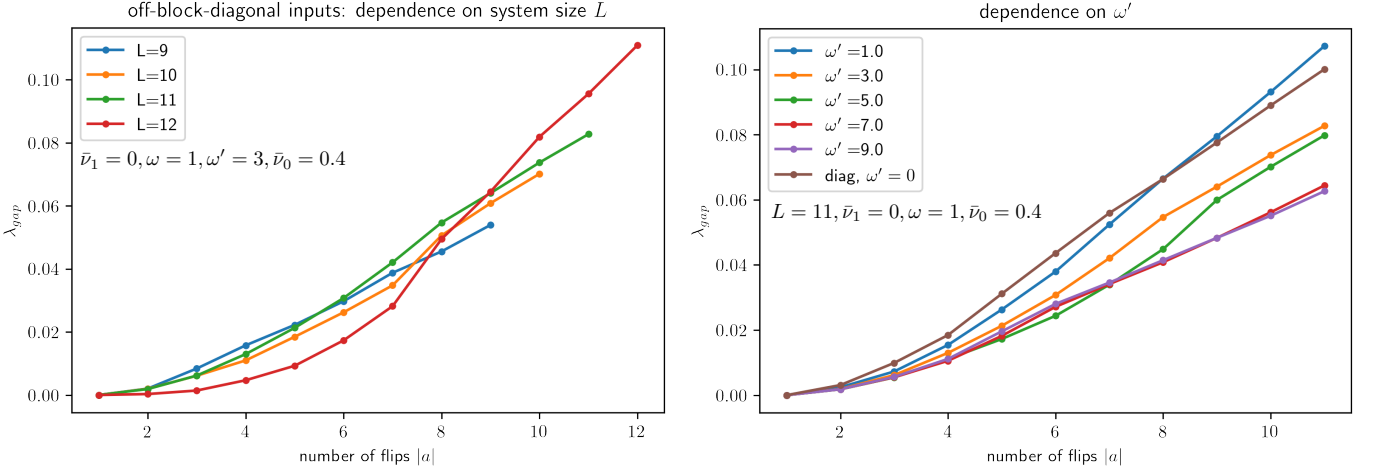


Figure 11. The gap of the Lindbladian $\lambda_{gap}(\mathcal{L}_{\bar{\nu}_1, \bar{\nu}_2, \omega'})$ for off-block-diagonal inputs at $\bar{\nu}_1 = [\nu_1, \nu_1 + \bar{\nu}_0], \bar{\nu}_2 = [\nu_1 + \omega, \nu_1 + \omega + \bar{\nu}_0], \bar{\nu}'_1 = [\nu_1 + \omega', \nu_1 + \bar{\nu}_0 + \omega'], \bar{\nu}'_2 = [\nu_1 + \omega + \omega', \nu_1 + \omega + \bar{\nu}_0 + \omega']$, for ranges of parameters and flips σ_i^x . (a) The dependence on the system size L . (b) The dependence on the energy difference ω' . Indeed, for a wide range of ω' , the gap is within a ratio of ~ 2 from each other.

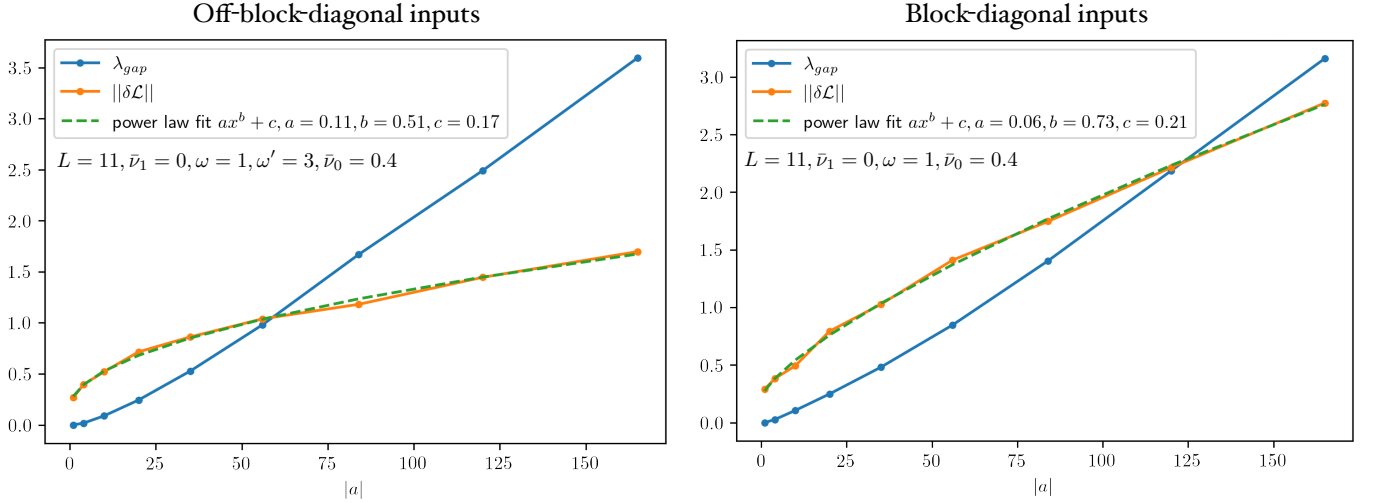


Figure 12. The deviation from the expectation for block-diagonal inputs $\|\mathcal{L}_{\bar{\nu}_1, \bar{\nu}_2} - \hat{\mathbb{E}}[\mathcal{L}_{\bar{\nu}_1, \bar{\nu}_2}]\|$ and off-block-diagonal inputs $\|\mathcal{L}_{\bar{\nu}_1, \bar{\nu}_2, \omega'} - \hat{\mathbb{E}}[\mathcal{L}_{\bar{\nu}_1, \bar{\nu}_2, \omega'}]\|$. The flips are 3-body $\sigma_i^x \sigma_j^x \sigma_k^x$, and the energy windows are parameterized by $\bar{\nu}_1 = [\nu_1, \nu_1 + \bar{\nu}_0]$, $\bar{\nu}_2 = [\nu_1 + \omega, \nu_1 + \omega + \bar{\nu}_0]$, $\bar{\nu}'_1 = [\nu_1 + \omega', \nu_1 + \bar{\nu}_0 + \omega']$, $\bar{\nu}'_2 = [\nu_1 + \omega + \omega', \nu_1 + \omega + \bar{\nu}_0 + \omega']$. For both, we see the deviation scales slower than the gap.